University of Veterinary Medicine Budapest

Doctoral School of Veterinary Sciences,
Aladár Aujeszky Doctoral Program of Theoretical Veterinary Sciences

Modification of the Innate Immune Response using Low Molecular Weight Substances and its Effect on Different Tumor Types

Ph.D. thesis

Dominik Gulyás

2024

Supervisors:

Márta Lőrincz, D.V.M., Ph.D., Habil.
Department of Microbiology and Infectious Diseases, University of Veterinary Medicine Budapest

.....
Márta Lőrincz

Béla Dénes, D.V.M., CSc., Dr. Habil., Titular Professor
Department of Microbiology and Infectious Diseases, University of Veterinary Medicine Budapest

.....
Béla Dénes

Consultant:

Anna Valkó, D.V.M., Ph.D.
Department of Microbiology and Infectious Diseases, University of Veterinary Medicine Budapest

Made in 8 copies. This is the …. copy.

.....
Dominik Gulyás

Table of contents

Summary 7
1. Introduction 8
1.1. Neoantigens. 9
1.2. The role of the immune system. 9
1.2.1. Damage Associated Molecular Patterns (DAMPs) 11
1.2.2. Toll-like receptors (TLRs) 11
1.2.3. Retinoic Acid-Inducible Gene I (RIG-I) and RIG-like receptors 13
1.2.4. Dendritic Cells (DCs) 14
1.2.5. Effector T cells (Teff), regulatory T cells (Treg), and natural killer (NK) cells 16
1.3. Tumor Immunotherapies 17
1.3.1. Therapeutic procedures using immune checkpoint inhibitors (ICIs) 20
1.3.2. Chimeric antigen receptor (CAR) T cell therapy 22
1.3.3. Dendritic cell-based therapies 23
1.3.4. Cytokine therapies 23
1.3.5. mRNA vaccines 24
1.3.6. *In situ* vaccination 24
1.4. Low molecular weight substances and treatment combinations 25
1.4.1. OX40 and Anti-OX40 (Treg inhibitor) 26
1.4.2. Cytosine-Phosphorothioate-Guanine (CpG) (PAMP/DAMP) 28
1.4.3. CpG and Anti-OX40 28
1.4.4. Retinoic Acid-Inducible Gene I (RIG-I) agonists (PAMP/DAMP and Treg inhibitor) 29
1.4.4.1. Influenza A Virus RNA 29
1.4.4.2. Porcine Parvovirus Type 1 DNA 31
1.4.4.3. Viral RNA and DNA purified in our laboratory 32
1.5. IL10, IL6, and IFNγ 32
1.6. Tumor models 34
1.6.1. The MB49 cell line 34
1.6.2. The Renca CRL-2947 cell line 35
2. Aims 37
3. Materials and Methods 38
3.1. The fundamental framework of the investigations 38
3.2. Cancer Cell Lines 38
3.3. Mice 39
3.4. Therapeutic Agents 40
3.5. The purification protocol of nucleic acids produced in our own laboratory 40
3.6. Humane endpoints 41

3.7. Pre-Experiments on cell culture 41
3.8. Postmortem Data Collection 42
3.9. Statistical analysis 43
3.10. Dosages and Course of Treatment 43
4. Results 46
4.1. First experiment – MB49 46
4.1.1. Assessment of survival times 46
4.1.2. Primary tumor growth and appearance 47
4.1.3. Metastatic events 48
4.2. Second experiment – Renca I 49
4.2.1. Assessment of survival times 49
4.2.2. Primary tumor growth and appearance 50
4.2.3. Metastatic events 50
4.3. Third experiment – Renca II. 51
4.3.1. Assessment of survival times 52
4.3.2. Primary tumor growth and appearance 53
4.3.3. Metastatic events 55
5. Discussion 58
5.1. Investigation on the MB49 cell line 59
5.2. Investigation on the Renca CRL-2947 cell line I. 60
5.3. Investigation on the Renca CRL-2947 cell line II. 61
5.4. Conclusions 64
6. Novel Scientific Findings 66
7. Reference List 67
8. Scientific publications 85
8.1. Original Full-Length Publications in Peer-Reviewed Journals with Assigned Impact Factors 85
8.2. Oral Conference Presentations 85
8.3. Poster Conference Presentations 86
9. Appendices 87
10. Acknowledgements 90

List of Figures

Figure 1.: TLR stimulation in cancer 12
Figure 2.: The pathway of IFN induction, triggered by the interaction between RIG-I and viral RNA 14
Figure 3.: Dendritic cell-induced CD4+ T-cell (Th) formation and functions, and cytotoxic T-cell (Tc) activation in tumor cell killing....16
Figure 4.: Immunosuppressive Impact of Tumors 18
Figure 5.: Monoclonal Antibodies Targeting PD-1, PD-L1 (A) and CTLA-4 (B) 21
Figure 6.: Illustration of T Cell Modification Using Chimeric Antigen Receptors 22
Figure 7.: The three distinct mechanisms of action of the low molecular weight compounds we employed may potentially facilitate the induction of anti-tumor immune responses. 26
Figure 8.: Binding of OX40 receptor and their ligands initiates a signaling cascade that leads to CD4+ T (Th), regulatory T (Treg) activation and CD8+ T (Tc) expansion....27
Figure 9.: RIG-I activation by genomic panhandle structures of Influenza A virus (IAV) and other negative-strand RNA viruses. 31
Figure 10.: Three types of interactions between Thelper 1-mediated release of interleukin-10, interleukin-12, and interferon-gamma during parasitic infections 34
Figure 11.: The experimental timeline (First experiment – MB49)....47
Figure 12.: Primary tumor morphology (Second experiment – Renca I.)....50
Figure 13.: Histological assessments (Second experiment – Renca I.)....51
Figure 14.: The experimental timeline (Third experiment – Renca II.)....53
Figure 15.: Primary tumor morphology (Third experiment – Renca II.)....54
Figure 16.: Histological assessments I. (Third experiment – Renca II.)....55
Figure 17.: Histological assessments II. (Third experiment – Renca II.)....57

List of Tables

Table 1.: The parameters of the series of experiments. 43
Table 2.: Mean tumor diameter (MTD) of primary tumors (First experiment – MB49)....48
Table 3.: Histopathological assessments (First experiment – MB49) 49
Table 4.: Histopathological assessments (Second experiment – Renca I.) 51
Table 5.: Histopathological assessments (Third experiment – Renca II.) 56
Table 6.: Meticulous evaluation of antitumor interventions deployed across a series of three trials. 64

List of Abbreviations

3p-hpRNA – 5’ Triphosphate Hairpin RNA

APC – Antigen Presenting Cell

ATCC – American Type Culture Collection

B cell – B lymphocyte

BATF – Basic Leucine Zipper ATF-Like Transcription Factor

BC – Bladder Cancer

CAR – Chimeric Antigen Receptor

CARD – Caspase Active Recruitment Domain

CD – Cluster of Differentiation

CO_2 – Carbon-Dioxide

CpG – Cytosine-phosphorothioate-Guanine

CTLA-4 – Cytotoxic T Lymphocyte-Associated Protein 4

DAMP – Damage Associated Molecular Pattern

DC – Dendritic Cell

DNA – Deoxyribonucleic Acid

dsRNA – Double-stranded Ribonucleic Acid

ELISA – Enzyme-Linked Immunosorbent Assay

FBS – Fetal Bovine Serum

FOXP3 – Forkhead Box P3

GM-CSF – Granulocyte-Macrophage Colony-Stimulating Factor

IAV – Influenza A Virus

IFN – Interferon

IL – Interleukin

IL-6R – Interleukin-6 Receptor

IRF – Interferon Regulatory Factor

ISG – Interferon Stimulated Gene

IV – Influenza Virus

JAK – Janus Kinase

Kbp – Kilo-base pair

LGP2 – Laboratory of Genetics and Physiology 2

LPS – LipoPolySaccharide

MAVS – Mitochondrial AntiViral-Signaling

MDA5 – Melanoma Differentiation-Associated 5

MHC – Major Histocompatibility Complex

MIBC – Muscle-Invasive Bladder Cancer

mRNA – Messenger Ribonucleic Acid

MTD – Mean Tumor Diameter

NF-κB – Nuclear Factor Kappa-light-chain-enhancer of activated B cells

NK – Natural Killer

NMIBC – Non-Muscle-Invasive Bladder Cancer

NS – Non-Structural protein

ODN – Oligodeoxynucleotide

OMM – Oral Malignant Melanoma

ORF – Open Reading Frame

OSA – Spontaneously occurring Osteosarcoma

OX40L – OX40 Ligand

PAMP – Pathogen-Associated Molecular Pattern

PBS- Phosphate-Buffered Saline

PD-1 – Programmed cell Death protein 1

PD-L1 – Programmed cell Death Ligand-1

PGE – Prostaglandin E

PLGA – Poly[Lactic-co-Glycolic Acid]

PPV – Porcine ParvoVirus

PRR – Pattern Recognition Receptor

RCC – Renal Cell Carcinoma

RIG-I – Retinoic Acid-Inducible Gene I

RLR – RIG-I-Like Receptor

RNA – Ribonucleic Acid

RT – Room Temperature

SLR – Stem-Loop RNA

ssRNA – Single-stranded Ribonucleic Acid

STAT – Signal Transducer and Activator of Transcription

TAA – Tumor Associated Antigen
TB – Trypan Blue
Tc – Cytotoxic T lymphocyte
T cell – T lymphocyte
TCR – T Cell Receptor
Teff – Effector T lymphocyte
TGF – Transforming growth factor
Th – Helper T lymphocyte
TLR – Toll-Like Receptor
TNF – Tumor Necrosis Factor
TNFR – Tumor Necrosis Factor Receptor
Treg – Regulatory T lymphocyte
VP – Viral (capsid) Protein

Summary

Cancer presents in multifarious forms and remains a paramount contributor to global mortality. Unfortunately, existing local and systemic interventions for diverse neoplasms exhibit suboptimal efficacy. A longstanding acknowledgment endures regarding the immune system's potential to combat nascent tumors. However, the presence of immunosuppressive factors, as expressed by malignant cells, may obscure the host's capacity to eradicate established neoplasms, thereby disrupting the equilibrium between regulatory and effector immune constituents. Consequently, concurrent with conventional modalities, immunotherapeutic strategies have flourished in recent years, yielding promising outcomes in the field of oncology. Central to immunotherapy is the innate capacity of the organism to elicit an anti-tumor response through deliberate immunostimulation.

Our primary objective encompassed scrutinizing the therapeutic efficacy of *in situ* vaccination in murine models afflicted with two distinct tumor phenotypes, hitherto unexplored in analogous therapeutic paradigms. The envisioned mechanism of action of the low molecular weight compounds under investigation – that we have vaccinated directly into the tumor – suggests a promising avenue for therapeutic tumor ablation, owing to their facilitation of immune response directed towards cellular pathways. These entities offer potential advantages compared to conventional chemotherapeutic agents, due to their purported specificity, and compared to targeted immunotherapies, due to their purported cost-effectiveness.

In our experiments, we utilized 132 mice (C57BL6/N or BALB/c). Over the span of four years, we conducted three large-scale experiments employing two types of tumor cell lines (MB49, Renca CRL-2947) and six different treatment combinations (CpG + anti-OX40, LPS + anti-OX40, CpG + 3p-hpRNA, 3p-hpRNA, IV-RNA + anti-OX40, PPV1-DNA + anti-OX40).

One of the treatment combinations mentioned above (LPS + anti-OX40) yielded clearly negative results. We believe that the highly aggressive nature of the tumor did not allow sufficient time for a humoral immune response to develop. Another combination (PPV1-DNA + anti-OX40) produced mixed results. We suggest that increasing treatment concentrations or fragmenting the DNA genome might enhance the treatment's efficacy. The remaining four treatments (CpG + anti-OX40, CpG + 3p-hpRNA, 3p-hpRNA, IV-RNA + anti-OX40) showed promising results, although there is potential for further improvement. Enhancements could be achieved by increasing treatment concentrations, the number and frequency of treatments, or using agents that slow down the absorption of components.

1. Introduction

In contemporary times, mortality attributable to cancer stands as the secondary principal cause of death subsequent to cardiovascular ailments (Bloom et al., 2019). Various methodologies are extensively used to manage diverse neoplasms, encompassing localized modalities such as surgical excision or radiation therapy alongside systemic interventions like cytotoxic agents. Nevertheless, these conventional therapeutic methods are beset by manifold shortcomings in terms of both efficacy and cost-effectiveness considerations. In spontaneous malignancies, the host immune system orchestrates a repertoire of natural innate defenses to impede the proliferation of neoplastic cells. Nonetheless, through a phenomenon recognized as immune evasion, an evolving tumor possesses the capacity to incapacitate extant T lymphocytes (or T cells), thereby facilitating unhindered cellular replication and proliferation. Over the past two decades, the evolution of immunotherapeutic methodologies has profoundly influenced the landscape of oncological interventions, increasingly integrated in conjunction with conventional therapeutic methods (e.g., surgery or radiation therapy) (Palumbo et al., 2013; Emens and Middleton 2015).

Consequently, the immune system is progressively acknowledged as a pivotal contributor in the anticancer armamentarium (Wages et al., 2018). The 2018 Nobel Prize in Physiology or Medicine attribution to James P. Allison and Tasuku Honjo for their groundbreaking advancements in modern immunotherapeutic strategies exemplifies this paradigm shift. The 2011 Nobel Prize also recognized the meticulous exploration of the innate immune system, notably dendritic cells, underscoring its intricate involvement in antitumor immunity, surpassing the classical understanding of the adaptive immune response. T lymphocytes with the capability to recognize tumor-specific antigens populate the microenvironment of the neoplastic lesion; however, the established tumor engenders an immunosuppressive milieu, leading to the attenuation of T cell functionality (Staveley-O'Carroll et al., 1998; Sotomayor et al., 1999). Through immunotherapeutic interventions, the immune system is invigorated, enabling tumor eradication. Notably, this approach not only elicits a potent antitumor response at the primary tumor site but also exhibits efficacy against distant metastases disseminated throughout the body (Luo et al., 2019). Presently, many of immunotherapeutic modalities are available, delineated comprehensively in Section "*1.3. Tumor Immunotherapies"* In recent years, the utilization of diverse immunotherapeutic interventions has demonstrated efficacy in managing numerous malignancies, including advanced melanoma, lung carcinoma, gastric adenocarcinoma, and renal cell carcinoma. This success can be attributed to their capacity to elicit a durable antitumor immune response (Hodi et al., 2010; Topalian Suzanne L. et al., 2012; Kyi and Postow 2016; Spranger 2016).

1.1. Neoantigens

Tumor neoantigens, representing novel protein entities (pathogen-associated molecular pattern, PAMP) absent in physiologically normal human tissues, are pivotal in eliciting tumor-specific T cell-mediated responses. Due to their non-concordance with the host's germline, these neoantigens are deemed optimal targets for therapeutic intervention, leveraging the immune system's inherent ability to discern self from non-self (Jiang et al., 2019). Recent findings have elucidated that the T cell-mediated immune response is activated in response to these neoantigens, precipitated by deoxyribonucleic acid (DNA) damage events within the organism. The discernment and targeting of these neoantigens have emerged as pivotal determinants driving the clinical efficacy of T cell checkpoint blockade and adoptive T cell therapy modalities employed in immunotherapeutic protocols (Schumacher et al., 2019). Multiple immunotherapeutic strategies target these neoantigens, focusing on tailoring interventions to the unique antigenic profile of individual tumors. Nonetheless, recent advancements have showcased a broader spectrum of neoantigen-targeting approaches, specifically targeting recurrent mutations prevalent across various malignancies. This latter approach is oriented towards intercepting key proteins vital for malignant proliferation, thereby promising a more universally applicable therapeutic strategy across diverse patient cohorts (Pearlman et al., 2021).

1.2. The role of the immune system

The process of immune activation initiates upon the release of tumor-associated antigens (TAAs) by neoplastic cells, commonly expressed on tumor cell surfaces. Antigen-presenting cells (APCs), aptly named, present these TAAs via major histocompatibility complexes (MHC), notably MHCI and MCHII, facilitating T cell recognition of TAAs. (Charles A Janeway et al., 2001). T cell activation ensues upon receipt of diverse co-stimulatory signals, including CD (cluster of differentiation) 80 and CD86 ligands, alongside the CD28 antigen (Linsley and Ledbetter 1993; Laidlaw et al., 2016; O'Neill and Cao 2019). Members of the tumor necrosis factor receptor (TNFR) superfamily play pivotal roles as co-stimulators in initiating immune responses (Alves Costa Silva et al., 2020). These activated T cells differentiate into effector T cells (Teffs), comprising cytotoxic CD8+ T cells (Tc) and helper $CD4^+$ T cells (Th). Activated $CD8^+$ T cells target altered cells presenting recognized TAAs, inducing apoptosis through cytotoxic molecules such as tumor necrosis factor α (TNFα) and interferon γ (IFNγ) (Wajant et al., 2003). Conversely, effector $CD4^+$ T cells are instrumental in fostering long-term memory $CD8^+$ T cells (Bourgeois et al., 2002; Janssen et al., 2003; Zloza et al., 2012; Laidlaw et al., 2016) and augmenting dendritic cell MHC expression, thereby enhancing $CD8^+$ T cell activation and persistence (Thaiss et al., 2011; Laidlaw et al., 2016). $CD4^+$ T cells can further

delineate into type 1 helper (Th1) and type 2 helper (Th2) cells, producing cytokines like IFNγ, interleukin (IL)-2, TNF-β (Th1), and IL-4, IL-5, IL-10, and IL-13 (Th2), modulating cell-mediated and humoral immune processes, respectively (Constant and Bottomly 1997; Romagnani 1999). Activating these innate immune-signaling pathways alongside immunomodulatory cytokines facilitates efficient neoplastic cell eradication. However, alongside TAAs, tumor cells release immunosuppressive cytokines such as transforming growth factor-β (TGF-β) and IL-10, endowed with potent anti-inflammatory properties, potentially impeding immune responses. TGF-β, a multifaceted cytokine, serves as a regulatory checkpoint for immune cells traversing barrier tissues, playing a crucial role in maintaining tissue integrity and preventing undue damage under homeostatic conditions. It facilitates the maintenance of tolerance to environmental antigens by aiding autoreactive T cells (Li and Flavell 2008; Tauriello et al., 2022). Specifically, TGF-β directly fosters the expansion of regulatory T cells (Tregs). The genesis of Tregs is initiated when naïve $CD4^+$ T cells encounter TGF-β, triggering the expression of Forkhead box P3 (FOXP3), a pivotal regulator in regulatory T cell (Treg) differentiation (Li and Flavell 2008; Tauriello et al., 2022). Furthermore, TGF-β exerts a downregulatory effect on the generation and function of effector T cells, natural killer (NK) cells, and antigen-presenting cells (Li and Flavell 2008). In the context of a healthy individual, TGF-β assumes a critical role in tumor suppression by inducing apoptosis in unestablished neoplastic cells and mitigating inflammatory damage. However, upon circumvention of this regulatory pathway by a tumor, the immunosuppressive attributes of TGF-β are exploited, facilitating untrammeled tumor proliferation (Batlle and Massagué 2019). Similar to TGF-β, interleukin-10 (IL-10) manifests both beneficial and inhibitory influences on cancer progression, contingent upon the contextual milieu in which it operates (Gonzalez-Garza et al., 2020). Notably, IL-10 production is markedly induced upon programmed cell death protein (PD-1) activation in immune cells (Said et al., 2010). The principal role of IL-10 is to mitigate potential collateral damage to neighboring healthy cells during infection, thereby averting the escalation of inflammation to detrimental levels (Trinchieri 2007; Li and Flavell 2008). During the initial phases of carcinogenesis, this entails dampening tumor-associated inflammation. However, in advanced stages, tumor cells exploit the immunosuppressive capacity of IL-10 to incapacitate natural killer and T cells, curtailing antigen-presenting cells ability to orchestrate heightened production of pro-inflammatory cytokines such as interleukin-12 (IL-12) (Trinchieri 2007; Dennis et al., 2013; Gonzalez-Garza et al., 2020).

1.2.1. Damage Associated Molecular Patterns (DAMPs)

In numerous tissues, the encounter with spontaneous malignancy, succeeded by the proliferation of aberrant cells, prompts a pivotal response from the immune system, relying predominantly on releasing damage-associated molecular patterns (DAMPs). DAMPs, elicited in response to stress and cellular death, are fundamental contributors to sterile inflammation. The recognition of DAMPs augments the fortification of protective mechanisms within the innate immune system (Hernandez et al., 2016). Notably, phagocytic cells, including macrophages and neutrophil granulocytes, play a significant role in responding to DAMPs. These cells bind to DAMPs, engulfing and digesting abnormal cells, thereby eliminating cancerous cells from the body. Macrophages, in particular, are indispensable for tissue homeostasis, effectively modulating unwanted processes such as angiogenesis and metastasis (DeNardo and Ruffell 2019). Central to the understanding of the processes above is the recognition of DAMPs, facilitated by pattern recognition receptors (PRRs), notably toll-like receptors (TLRs) (Kaur et al., 2022). Initially characterized in the context of innate immune responses against microbial pathogens, TLRs have since been recognized for their crucial role in bridging innate and adaptive immunity. They exhibit multifaceted functions in inflammation, autoimmune diseases, and cancer (Yang et al., 2022). Appreciation of the stimulatory potential of TLRs and the development of Toll-like receptor (TLR)-targeted therapeutic strategies for cancer have yielded promising outcomes in regulating tumor microenvironment and the induction of tumoricidal phenotypes.

1.2.2. Toll-like receptors (TLRs)

Structurally, TLRs are type I transmembrane glycoproteins (Rakoff-Nahoum and Medzhitov 2009), exhibiting evolutionarily conserved features across plants and vertebrates (Loiarro et al., 2010). Since their discovery in 1966, thirteen functional homologs of TLRs have been identified in humans and mice, with both species conserving TLR9 and TLR11 (Kawai and Akira 2010; Patidar et al., 2018; Anwar et al., 2019). Toll-like receptors (TLRs) are indispensable components of the innate immune system, pivotal in detecting and responding to pathogenic threats by initiating intracellular signaling cascades. This culminates in orchestrating an immune response to eradicate pathogens and infected cells (Kawai and Akira 2010). TLRs are ubiquitously expressed across various immune cell types, encompassing B-lymphocytes (or B cells), macrophages, dendritic cells, neutrophils, mast cells, and non-immune cells such as endothelial and epithelial cells, adipocytes, and cardiomyocytes. The recognition of TLRs by these diverse cell populations triggers a downstream signaling pathway (Takeuchi and Akira 2010), mediated notably by myeloid differentiation factor 88 (MyD88) and the toll-interleukin-1 receptor domain (TIR), ultimately resulting in the activation of nuclear

factor kappa-light-chain-enhancer (NF-κB) in activated B cells. This activation event subsequently facilitates the transcription of pro-inflammatory cytokines, including but not limited to tumor necrosis factor-alpha (TNF-α), IL-1, and IL-6 (Takeda and Akira 2004). Recent investigations have unveiled the expression of TLRs within tumor cell populations, encompassing tumor stem cells, alongside stromal constituents like cancer-associated fibroblasts, tumor-associated macrophages, myeloid-derived suppressor cells (MDSCs), regulatory T cells, and adipocytes. The involvement of TLRs in the modulation of tumor growth is complex, as evidenced by their dual capacity to exert both inhibitory and promotional effects on tumorigenesis (**Figure 1**) (Chang 2010; Bayraktar et al., 2019; Chen et al., 2019).

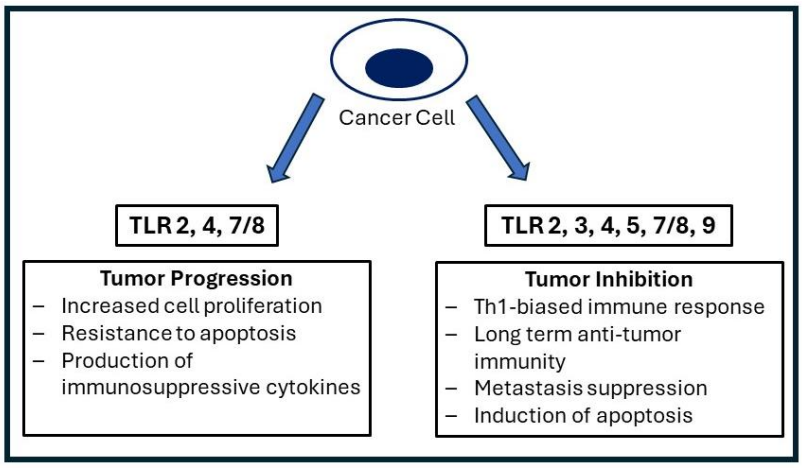

Figure 1: *Toll-like receptor (TLR) stimulation in cancer (based on Urban-Wojciuk et al., 2019).*

The exploitation of TLRs is a cornerstone in current anti-tumor therapeutic strategies, eliciting profound enhancements in innate and adaptive immune responses, ultimately culminating in the induction of apoptosis in neoantigen-expressing tumor cells (Kanzler et al., 2007). Notably, a significant challenge confronting TLR-mediated therapies lies in their inherent inability to discriminate between self and non-self, instead responding robustly to a spectrum of “danger signals”, encompassing both exogenous and endogenous ligands (Khan et al., 2016). TLR ligands can be categorized into three principal groups: natural exogenous ligands, commonly known as pathogen-associated molecular patterns (PAMPs); natural endogenous ligands, referred to as damage-associated molecular patterns; and a third category comprising synthetically engineered agents. PAMPs primarily originate from microbial elements present in bacteria, fungi, parasites, and viruses (Kanzler et al., 2007; Khajeh Alizadeh Attar et al., 2018; Bayraktar et al., 2019). TLRs detect these PAMPs as indicators of invading pathogens, triggering direct activation of the innate immune system while concurrently orchestrating an indirect stimulation of the adaptive immunity, thus affording invaluable protection against pathogenic threats (Satoh and Akira 2016). As previously alluded, DAMPs arise in response to various forms of cellular stress and demise, serving as principal contributors to sterile inflammation (Hernandez et al., 2016).

1.2.3. Retinoic Acid-Inducible Gene I (RIG-I) and RIG-like receptors

Retinoic acid-inducible gene I, or RIG-I, denotes an RNA helicase renowned for detecting viral single- and double-stranded RNA. Positioned within the pantheon of PRRs, RIG-I belongs to the RIG-like helicases group, sharing a close lineage with the most common PRRs, the Toll-like receptors. Within the RIG-I-like receptor family (RLR), RIG-I stands alongside melanoma differentiation-associated 5 (MDA5) and Laboratory of Genetics and Physiology 2 (LGP2) as the fundamental constituents (Offermanns and Rosenthal 2008). Extensive investigations have centered on RLRs, particularly in the realm of antiviral immune signaling, given their adeptness in binding to an assorted array of 5' uncapped triphosphate single- or double-stranded RNA, derived from both viral and host origins (Kato et al., 2008; Rehwinkel and Gack 2020). Notably, RIG-I exhibits a proclivity towards binding shorter single-stranded RNA and approximately 1 kilo-base pair (kbp) double-stranded RNA. At the same time, MDA5 has been implicated in interferon production contingent upon approximately 2 kbp double-stranded RNA (Kato et al., 2008). Both receptors, however, harbor a caspase activation and recruitment domain (CARD), which, upon RNA binding, becomes exposed to instigate signaling cascades. In contrast, LGP2 binds to double-stranded RNA and is postulated to transregulate other RLRs in the presence of interferons, owing to its inherent lack of a CARD domain. Interferons modulate the expression of all three RLRs, albeit RIG-I exhibits a constitutive presence in most tissues at low levels (Saito et al., 2007). Upon RNA binding facilitated by a lysine-63 polyubiquitin chain, the exposed CARD domain on RIG-I orchestrates the recruitment of mitochondrial antiviral-signaling proteins (MAVS), thereby attracting an array of downstream effectors to initiate the activation of interferon regulatory factors (IRF) 3 and 7 (Zeng et al., 2010). Subsequently, IRF3 and IRF7, acting as transcription factors, translocate into the cellular nucleus, thereby instigating the production of type I and III interferons. A comprehensive depiction of this intricate signaling pathway is provided in **Figure 2** (Borg 2019).

A readily accessible synthetic influenza sequence, denoted as 5’ triphosphate hairpin RNA (3p-hpRNA), serves as a commercially available ligand for RIG-I, thereby facilitating the transcriptional induction of type I interferons (IFNs). The presence of 5' triphosphate caps precludes recognition by melanoma differentiation-associated gene 5 (MDA5), thereby ensuring selective binding of this ligand exclusively to RIG-I among the three members of the RIG-I-like receptor family (Berke and Modis 2012).

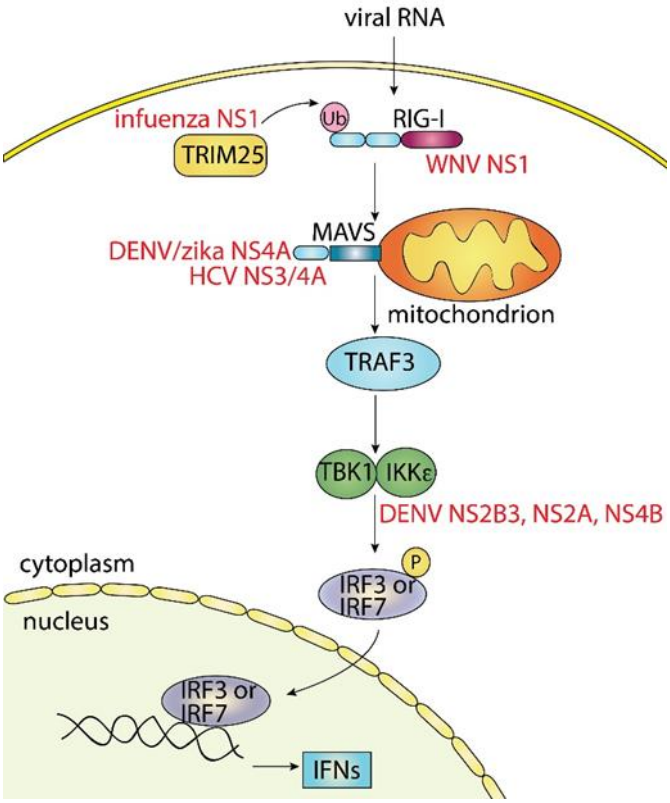

Figure 2: *The pathway of IFN induction is triggered by the interaction between RIG-I and viral RNA.: Upon RIG-I recognition of RNA, the recruitment of MAVS (Mitochondrial antiviral-signaling protein) ensues, facilitating the assembly of a signaling complex comprising TRAF (TNF receptor-associated factor) 3, TBK (TANK-binding kinase) 1, and IKK (I-kappa-B kinase) ε. This intricate cascade culminates in the subsequent activation of IRF (Interferon Regulatory Factor) 3 or IRF7. Ultimately, the engagement of these transcription factors with nuclear DNA prompts the initiation of interferon production, thereby orchestrating an effective antiviral response (Borg 2019).*
Further abbreviations in the figure: NS (non-structural protein); WNV (West Nile Virus); TRIM25 (Tripartite Motif Containing 25); Ub (Ubiquitin); DENV (Dengue Virus); ZIKV (Zika Virus); HCV (Hepatitis C Virus); P (Phosphor).

1.2.4. Dendritic Cells (DCs)

Dendritic cells (DCs) were initially discerned within the epidermis and were named Langerhans cells. They are now widely recognized as a fundamental constituent of the lymphohematopoietic system, serving as sentinels for the immune system. DCs inhabit the interstitium of most organs, albeit in scant quantities within the brain, a characteristic contributing to the well-documented phenomenon of immune privilege. Initiating immune responses, DCs capture small amounts of antigens, subsequently presenting them to antigen-specific T cells, thus initiating their maturation. This process typically unfolds in three phases while concurrently fostering the generation of lymphokine-secreting helper T cells and effector Tc, which subsequently migrate to tumor cells. Only DCs activate memory cells and naïve T

cells among APCs, thus earning the epithet of professional APCs (Nizar et al., 2009). Concerning their role in antitumor immunity, dendritic cells can capture antigens from dying tumor cells and present them to adaptive immune cells, thereby orchestrating a more targeted and specific immune response (Bell et al., 1999). In the pursuit of developmental vaccines targeting cancer, DCs have emerged as a focal point for numerous researchers, attributed to their recognized potential for robust antitumor activity (Murri et al., 2008). In their immature state, DCs are primarily situated within tissues, intermittently traversing the bloodstream and lymphatic vessels. These cells prominently express MHC molecules, albeit with limited expression of costimulatory molecules, notably CD80 or CD86. During their journey through the body, DCs encounter various antigens, which they promptly internalize through a repertoire of mechanisms, including receptor-mediated endocytosis, phagocytosis, or micropinocytosis. Following antigen uptake, DCs migrate towards the afferent lymphoid organs, where they undergo a process of maturation. This maturation entails a series of phenotypic and functional alterations characterized by upregulation of MHC expression and augmented levels of costimulatory molecules such as CD80 and CD86 (Inaba et al., 1994). Along with DC maturation, there is a concomitant increase in cytokine production, notably IL-6, IL-12, IL-13, and TNF-α, alongside heightened secretion of chemokines, exemplified by CCL18. Collectively, these factors facilitate the recruitment of naïve T cells to the vicinity of activated DCs. Upon encounter, DCs and T cells engage in interactions mediated by complementary adhesion molecules, culminating in the formation of immunological synapses. This intricate process results in effective antigen presentation by DCs to T cells, ultimately driving the activation of T cells and eliciting antigen-specific immune responses (Murri et al., 2008). The graphical representation of this process is shown in **Figure 3**.

The employment of DCs in cancer vaccination strategies necessitates a substantial quantity of cells for their generation. Established protocols have been devised to facilitate the *in vitro* production of these large quantities. It has been demonstrated that DCs can be derived from CD34-positive precursors sourced from bone marrow or blood through incubation with cytokine cocktails comprising granulocyte-macrophage colony-stimulating factor (GM-CSF), IL-4, or TNF-α (Caux et al., 1992; Inaba et al., 1994; Caux et al., 1997). An alternative methodology involves the utilization of CD14-positive monocytes from the blood along with cytokines GM-CSF and IL-4, or CD40 ligand, to generate myeloid DCs (Peters et al., 1993; Romani et al., 1994; Sallusto and Lanzavecchia 1994). These myeloid DCs exhibit an immature phenotype characterized by limited expression of costimulatory molecules on their surface. However, they can be induced to mature cells through exposure to various inflammatory stimuli such as TLR ligands, TNF-α, or a combination of compounds containing prostaglandin E2 (PGE2), TNF-α, IL-1β, and IL-6 (Lee et al., 2002).

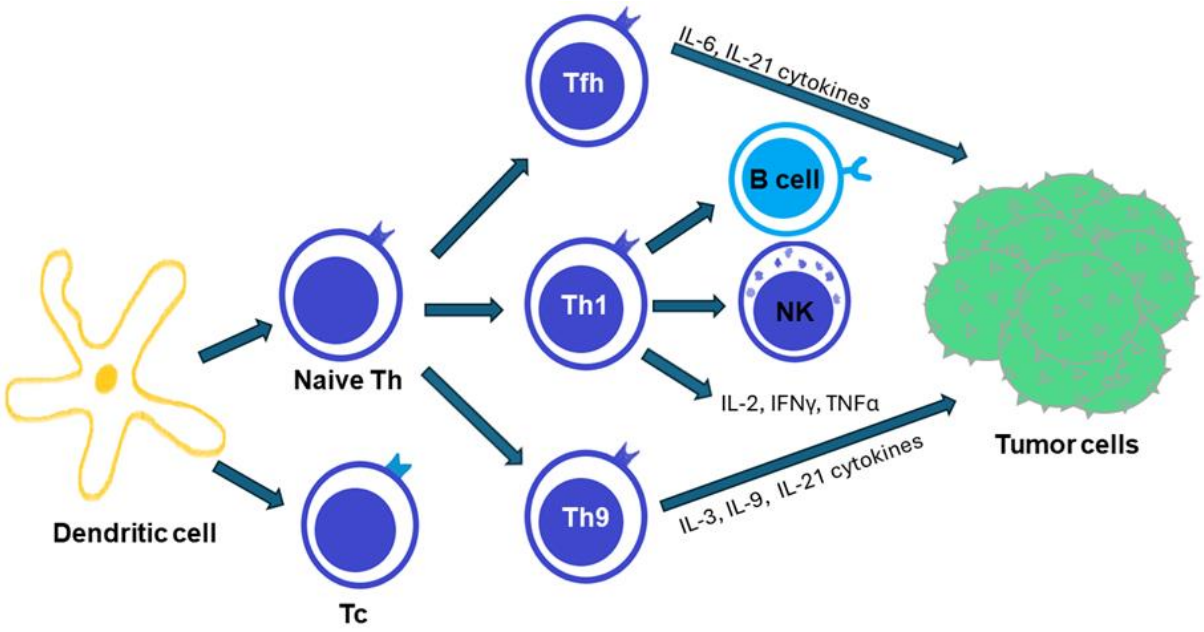

Figure 3: *Dendritic cell-induced CD4+ T-cell (Th) formation and functions and cytotoxic T-cell (Tc) activation in tumor cell killing (based on Basu et al., 2021) Tfh: follicular T cells, function of B cells, activation of natural killer (NK) cells, stimulation of macrophage migration; Th1: enhancement of cellular immune response; Th9: enhance macrophage proliferation, activate natural killer (NK) cells, maintain inflammation.*

1.2.5. Effector T cells (Teff), regulatory T cells (Treg), and natural killer (NK) cells

Stimulation of DCs leads to the upregulation of numerous membrane-bound costimulatory molecules, notably CD80, CD86, and CD40, in addition to the cytokine IL-12, which plays a pivotal role in the optimal activation of T cells, including both $CD4^+$ and $CD8^+$ subsets (Iwasaki and Medzhitov 2004; Boudreau et al., 2011). It has been well-established that TLR agonists play a fundamental role in orchestrating the activation of both innate and adaptive immune responses. The selection of TLR agonists was guided by their capacity to activate antigen-presenting cells, notably DCs. However, recent investigations have revealed that TLRs also exert modulatory effects on various T cell subsets, thus presenting a promising avenue for augmenting the efficacy of cancer immunotherapies (Kaczanowska et al., 2013). In murine experimental models, treatment with TLR agonists has demonstrated efficacy in diminishing tumor size.

Furthermore, in select instances, the adjunctive administration of combination therapeutic modalities, such as chemotherapy agents, monoclonal antibodies, and/or tumor antigen vaccination utilizing proteins, peptides, or plasma DNA, has yielded enhanced outcomes, including notable regression of established tumors (Stone et al., 2009; Davis et al., 2011; Rudilla et al., 2012). $FOXP3^+CD25^+CD4^+$ regulatory T cells play a pivotal role in innate and

adaptive immunity. Primarily recognized for their role in averting autoimmunity, these immunosuppressive entities have also been implicated in fostering tumor progression (Wang et al., 2017). The correlation between Treg abundance and cancer advancement is striking, as evidenced by their enrichment within tumor microenvironments, ascitic fluid, and peripheral blood of cancer patients, which correlates with unfavorable prognostic outcomes. Accumulating evidence suggests that Tregs serve to shield tumors from effective immune surveillance.

Consequently, interventions targeting Tregs represent a key objective in contemporary oncological therapeutic endeavors (Nizar et al., 2009). Additional lymphocytes wielding significant influence in impeding tumor proliferation are NK cells. Following activation, these cells exhibit cytotoxicity and cytokine-producing effector capabilities, culminating in the discharge of cytotoxic molecules that induce apoptosis in cancerous cells. Investigative endeavors into the mechanistic underpinnings of NK cells have furnished compelling evidence elucidating their ability to discern target cells from host healthy cells (Mansell and Jenkins 2013).

1.3. Tumor Immunotherapies

Advanced-stage malignant tumors frequently exhibit resistance to conventional chemotherapy and/or radiation therapy, resulting in dismal survival rates despite aggressive intervention. To substantially enhance clinical outcomes, there is an imperative need to devise therapeutic strategies that are more efficacious and capable of circumventing the intricate defense mechanisms deployed by the tumor (Vinay et al., 2015; Fouad and Aanei 2017). The pivotal involvement of the immune system in the etiology and management of these malignancies is underscored by a plethora of compelling evidence. Noteworthy examples include instances of spontaneous remission observed in cancer patients devoid of therapeutic interventions, the presence of tumor-specific cytotoxic T cells within the tumor microenvironment or adjacent lymphoid tissues, as well as the infiltration of monocytes and lymphocytes amidst aggressively proliferating cell populations. Furthermore, an augmented incidence of certain malignancies has been documented in immunocompromised individuals, thereby reinforcing the intricate interplay between immune function and tumor development (Rosenthal 2001; Baxevanis et al., 2009). An intact and finely tuned immune system exerts active surveillance against the emergence and progression of indolent tumors, a phenomenon termed “cancer immunosurveillance”. Notably, interferon-gamma (IFNγ) has been demonstrated to impede tumor growth in immunocompetent murine models, whereas genetically engineered mice lacking the IFNγ receptor exhibit heightened susceptibility to spontaneous tumor development. Analogously, ablation of crucial constituents of the adaptive

immune response, namely T and B cells, predisposes mice to tumor development (Smyth et al., 2001; Wallace and Smyth 2005; Itoh et al., 2009; Schmiedt et al., 2009). Recent investigations spanning the past two decades have shed light on the nuanced and multifaceted role of the innate immune response in orchestrating antitumor immunity, eclipsing the traditionally emphasized role of adaptive immunity. Although tumor-infiltrating T cells recognizing tumor antigens are discernible within the tumor microenvironment, the established tumor engenders an immunosuppressive milieu typified by augmented expression of cytokines such as transforming growth factor-beta (TGF-β) and IL-10 (Hurwitz and Watkins 2012). These immunosuppressive cues orchestrate an inhibitory effect on T cell activity, further fostering tumor progression (see **Figure 4**) (Staveley-O'Carroll et al., 1998; Sotomayor et al., 1999).

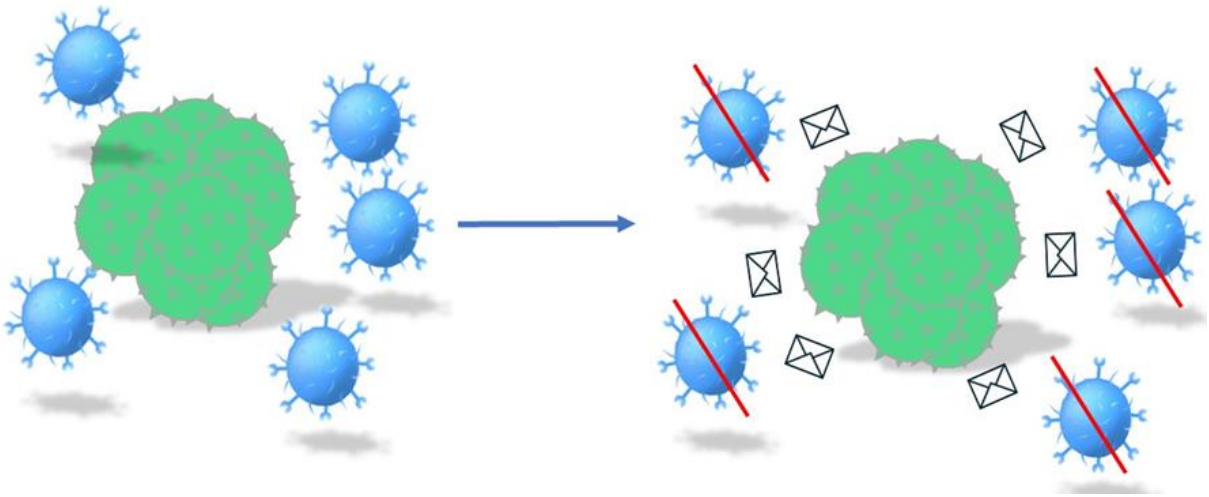

Figure 4: *Immunosuppressive Impact of Tumors: Tumor cells (green) secrete cytokines (envelope) which impede the immune response of tumor antigen-specific T cells (blue).*

Given these insights, immunotherapeutic modalities herald a paradigm shift in the management of malignant tumors, owing to their unparalleled specificity and efficacy (Geering and Fussenegger 2015). These innovative therapeutic approaches can remodel the tumor microenvironment by selectively engaging with immunosuppressive proteins expressed on tumor cells, activated T and B cells, macrophages, and regulatory T cells. They facilitate the generation of local and systemic antitumor immune responses, culminating in the eradication of cancer cells (Farkona et al., 2016; Gong et al., 2018; Kruger et al., 2019). Recently, various approaches to antitumor immunotherapy have garnered significant attention. These encompass therapies predicated on monoclonal antibodies, interventions centered on immune cell manipulation, *in situ* vaccination strategies, checkpoint inhibitor therapies, and diverse combinations with conventional treatment modalities (Gorbet and Ranjan 2020). Furthermore, immune cell activity can be augmented by bolstering cell numbers via *ex vivo* proliferation followed by adoptive cell transfer, often necessitating supplementation with homeostatic or activating cytokines.

Consequently, the manipulated immune cells acquire enhanced functionality or exhibit antigen-specific responses (Lesch and Gill 2021). Antibody-based immunotherapy is a preeminent and dependable strategy in the armamentarium against oncological afflictions. The therapeutic mechanism of action may encompass diverse modalities such as indirect effects such as antibody-dependent cellular cytotoxicity (ADCC) or direct induction of cell death, including apoptosis (Lesch and Gill 2021). However, it is noteworthy that monoclonal antibodies often demonstrate limited efficacy when administered as monotherapy (Coiffier et al., 1998; Coiffier et al., 2002). As with human populations, the prevalence of cancer among animals, particularly companion animals, presents a growing concern from a veterinary standpoint. The Swiss Canine Cancer Registry has meticulously documented the incidence of prevalent tumor types based on data over five decades. Analysis of data encompassing more than one hundred and twenty thousand animals reveals that adenoma/adenocarcinoma (18.1%), mastadenoma/mastocytoma (6.5%), lymphoma (4.3%), melanoma (3.6%), fibroma/fibrosarcoma (3.4%), hemangioma/hemangiosarcoma (2.8%), squamous cell carcinoma (1.9%), and osteoma/osteosarcoma (1.2%) rank among the most prevalent tumor types afflicting canines (Grüntzig et al., 2016). Of particular note, lymphomas emerge as one of the most commonly treated cancers (Schiffman and Breen 2015), alongside B cell neoplasias, which constitute the predominant hematopoietic malignancies in both human and canine populations (Seelig et al., 2016). According to research findings, genetic background plays a pivotal role in both the incidence and progression of cancer. Certain dog breeds exhibit a significantly elevated risk of developing the disease, including dachshunds, Pomeranians, cairn terriers, and bichon frise dogs, comprising ten small and two medium or large breeds. Observations have indicated that tumors may manifest in English bulldogs at an earlier age than in other breeds (Bromberek et al., 2016). Literature reports suggest that the incidence of breast tumors in female dogs can be mitigated through early ovariohysterectomy (Beauvais et al., 2012). Presently, only a limited array of approved FDA (U.S. Food and Drug Administration) or USDA (United States Department of Agriculture) licensed veterinary oncology therapies are accessible to practitioners. The findings underscore the pressing need to develop tailored treatment modalities explicitly catering to the unique requirements of canine and feline patients (Mochel et al., 2019). The landscape of cancer immunotherapy research is prominently characterized by two overarching and complementary strategies: the utilization of immune checkpoint inhibitors, a groundbreaking advancement recently honored with the Nobel Prize in Medicine (Kaiser and Couzin-Frankel 2018), and the engineering of chimeric antigen receptor (CAR) T cells. The former approach is centered on potentiating T cell activation, while the latter endeavors to elicit the generation of T cells equipped to target antigens harbored by distinct cancer cell populations (Kenderian et al., 2014). In both therapeutic paradigms, the attenuation of regulatory T cell formation and function assumes paramount significance.

1.3.1. Therapeutic procedures using immune checkpoint inhibitors (ICIs)

T cell activation represents a finely orchestrated process contingent upon signals emanating from the T cell receptor (TCR) complex and its interplay with associated regulatory proteins. The dynamic interaction between inhibitory and stimulatory proteins dictates the extent of T cell activation, facilitating tolerance towards self-antigens (via inhibitory pathways) while concurrently eliciting an adaptive immune response against foreign antigens (through stimulatory pathways). Immune checkpoints play a pivotal role in orchestrating inhibitory cues that transiently curtail T cell activity under physiological conditions, thereby ensuring the maintenance of immune responsiveness within the requisite physiological confines (Lesch and Gill 2021). Through the utilization of therapies directed at immune checkpoint inhibitors, which modulate key checkpoints within the immune system, the activation of T cells within the tumor microenvironment can be effectively orchestrated, thereby instigating an anti-tumor immune response (Khalil et al., 2016). Immune checkpoint inhibitors encompass specific proteins or monoclonal antibodies designed to target critical regulatory molecules such as CTLA-4 (cytotoxic T-lymphocyte associated protein 4) or PD-1/PD-L1 (programmed cell death protein-1/programmed cell death ligand-1), which serve to regulate the immune system's response to tumor cells. Among the foremost immune checkpoint inhibitors are anti-CTLA-4 (ipilimumab) and anti-PD-1/PD-L1 (nivolumab) (Gorbet and Ranjan 2020). PD-1, a cell surface protein predominantly expressed on activated T cells and B cells, interacts with the transmembrane protein PD-L1 (B7-H1), which is ubiquitously present in both healthy and tumor cells (Zheng and Zhou 2015). This interaction is pivotal in mitigating autoimmune complications and preserving immune system homeostasis. Primarily, PD-1/PD-L1 signaling attenuates the apoptosis of regulatory T cells while concurrently fostering the activation of antigen-specific lymphocytes within the lymph nodes. Consequently, this signaling axis dampens immune responsiveness under physiological conditions, fostering a milieu conducive to immune tolerance. Certain malignancies, including metastatic melanoma, non-small cell lung cancer, and renal cell carcinoma, exploit this regulatory mechanism by modulating the expression of PD-1/PD-L1, thereby subverting an effective immune response (Hargadon et al., 2018). An extensive analysis encompassing a large cohort of breast cancer (n=3647), non-small cell lung cancer (n=4549), and stage III malignant melanoma (n=37) patients revealed a positive correlation between elevated tumor PD-L1 expression and treatment efficacy (for further elucidation, see **Figure 5 A**) (Jacquelot et al., 2017; Kowanetz et al., 2018). CTLA-4, a homolog of CD28 on T cells, engages with CD80 (B7-1) or CD86 (B7-2) molecules expressed on APCs, notably dendritic cells, to modulate immune responses. Unlike CD28, which augments immune activation, CTLA-4 exerts an inhibitory role and exhibits a heightened

affinity for APC MHC co-receptors compared to CD28. Clinically, anti-CTLA-4 agents have emerged as immunostimulatory therapeutics for cancer treatment (see **Figure 5 B**).

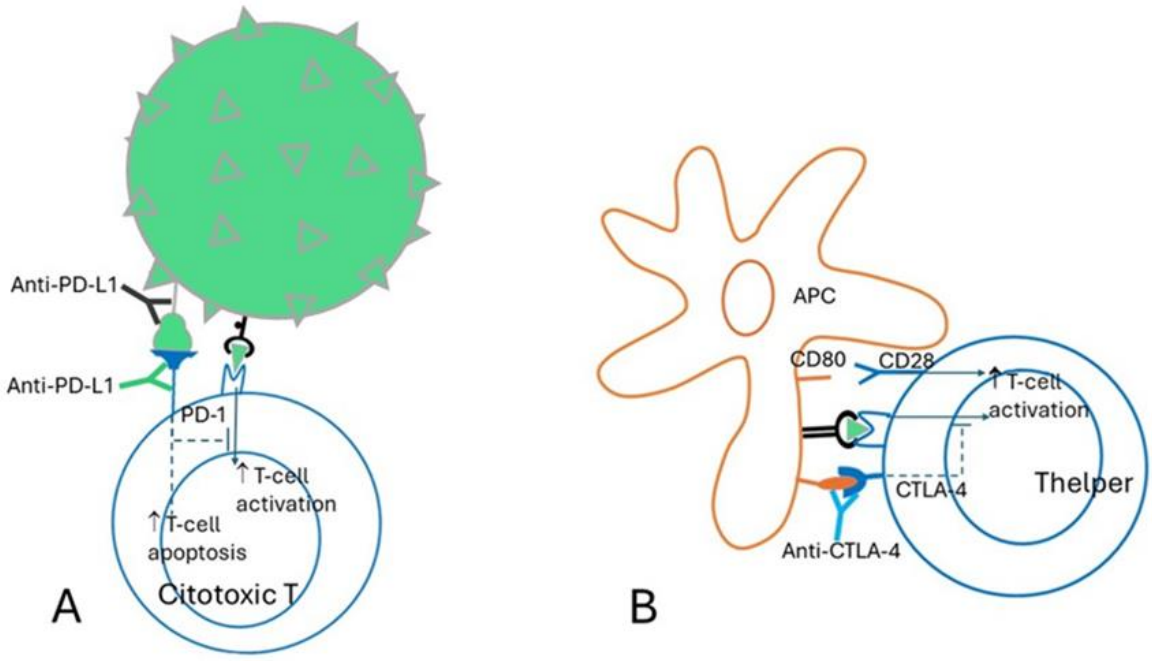

Figure 5: A) *Monoclonal Antibodies Targeting PD-1 and PD-L1: PD-L1, ubiquitously expressed on both healthy and neoplastic cells, engages with PD-1 receptors present on cytotoxic T cells, thereby attenuating immune responses. While this interaction serves to prevent autoimmunity, tumor cells exploit it to evade immune surveillance by inducing T cell apoptosis. Blockade of PD-1 and PD-L1 axes enhances cytotoxic T cell-mediated tumor cell clearance.*
B) *Monoclonal Antibodies Against CTLA-4: Upon antigen presentation, the MHCII on antigen-presenting cells engages with the T cell receptor, necessitating concurrent CD28 binding to CD80. As a CD28 antagonist, CTLA-4 diminishes T helper cell activation. Therefore, monoclonal antibodies against CTLA-4 fortify the CD28-CD80 interaction, promoting sustained T helper cell activation.*

Notably, particular malignancies, including non-small cell lung cancer, small cell lung cancer, gastric adenocarcinoma, and hepatocellular carcinoma, harness mechanisms to impede immune activation (Walker and Sansom 2015), thereby rendering therapy efficacy in such cases. Combinatorial therapy involving both CTLA-4 and PD-1/PD-L1 inhibitors has demonstrated enhanced patient survival in select cancer types, including human metastatic melanoma, advanced renal cell carcinoma, and colon cancer (Rotte 2019). Clinical trials in human subjects have explored anti-PD-1/PD-L1 antibodies in conjunction with standard chemotherapy or radiotherapy (Sato et al., 2020; Zhang et al., 2020). In a clinical study involving canine patients, PD-1 inhibition exhibited favorable safety profiles and demonstrated antitumor efficacy in oral malignant melanoma (OMM) cases with lung metastases. Although the therapeutic outcomes, such as a measurable response in 26.7% of stage IV OMM cases (4/15), did not mirror those observed in advanced melanoma cases in humans, the therapeutic potential of PD-1 inhibition in canine melanoma is discernible (Lin et al., 2016).

1.3.2. Chimeric antigen receptor (CAR) T cell therapy

The fundamental premise of this procedure involves the *ex vivo* generation of T cells equipped with antigen-specific tumor recognition capabilities mediated by the T cell receptor. Following genetic modification, these engineered cells are reintroduced into the host organism, whereupon they exhibit potent tumor eradication capabilities (see **Figure 6**) (Mochel et al., 2019). CAR T cell therapies hold significant promise, particularly in hematologic malignancies (Neelapu et al., 2017; Maude et al., 2018).

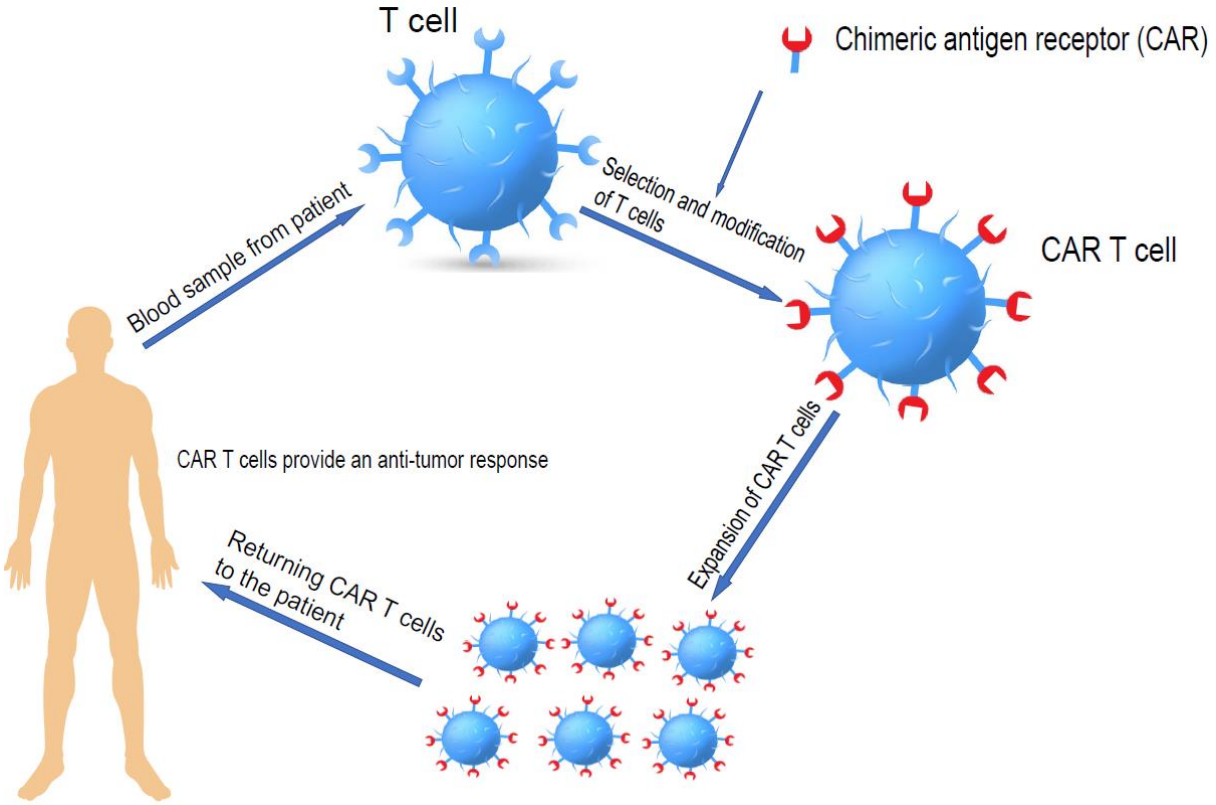

Figure 6: *Illustration of T Cell Modification Using Chimeric Antigen Receptors.*

In the realm of canine medicine, one of the inaugural clinical investigations was conducted by *Panjwani et al.,* (Panjwani et al., 2016), paving the way for subsequent protocol refinements aimed at generating CAR T cells (Mata et al., 2014; Yin et al., 2018). Dogs have emerged as invaluable candidates for preclinical evaluation of human cell-based therapies, owing to their biological similarities and shared environmental exposures with the human populace. Consequently, the manifestation of diseases in dogs parallels that observed in humans (Gardner et al., 2016), rendering them promising models for spontaneous disease studies and innovative CAR T cell investigations. Conversely, insights gleaned from human clinical trials concerning the efficacy and safety of CAR T cells hold potential relevance for developing future cell-based therapies in veterinary oncology, aligning with the overarching goals of the One Health initiative (Schneider et al., 2018).

1.3.3. Dendritic cell-based therapies

Over the past two decades, there has been escalating interest in leveraging DCs and other APCs for potential immunomodulation therapy targeting solid tumors. Activation of dendritic cells was achieved through liposomal delivery of the metastatic murine melanoma antigen B16F10-OVA along with a DC maturation signal, such as IFNγ or GM-CSF, demonstrating robust antitumor efficacy both *in vitro* and *in vivo*. Notably, experimental murine models exhibited a reduction in lung metastases following treatment with activated dendritic cells (van Broekhoven et al., 2004). *Waeckerleman et al.,* (2005) employed poly[lactic-co-glycolic acid] (PLGA) microspheres for targeted delivery of antigens to human monocyte-derived dendritic cells (hMoDCs). PLGA effectively extended antigen presentation by dendritic cells while preserving T cell migration, cytokine secretion, survival, and allostimulation capabilities (Waeckerle-Men and Groettrup 2005).

Moreover, using GM-CSF-stimulated dendritic cells yielded promising outcomes in a murine fibrosarcoma model (Ebrahimi-Nik et al., 2018). In separate investigations, a synergistic approach combining photodynamic therapy, involving the application of a photosensitizer followed by exposure to sunlight or an artificial light source for reactive oxygen radical release, alongside dendritic cell vaccination demonstrated efficacy in inducing an immune response against squamous cell carcinoma (H. Zhang et al., 2018). Additionally, the adenoviral vector (chimeric Ad5/3 vector) holds the potential for selective activation of dendritic cells, offering further avenues for therapeutic exploration (Chondronasiou et al., 2022).

1.3.4. Cytokine therapies

The incidence of spontaneously occurring osteosarcoma (OSA) in dogs markedly exceeds that in the human population, estimated to be approximately 30-50 times higher, with around 45,000 cases reported annually in the United States of America (Anfinsen et al., 2011). In veterinary oncology, the conventional treatment modality for OSA involves surgical resection followed by 4-6 cycles of chemotherapy employing carboplatin and/or doxorubicin (Kent et al., 2004). This therapeutic regimen has demonstrated efficacy in significantly enhancing survival outcomes (Chun et al., 2005). Notably, dogs undergoing solely surgical intervention, typically amputation, face a staggering incidence of metastases in the lungs, bones, or soft tissues, reaching as high as 90% within 14 weeks post-surgery. However, the incorporation of chemotherapy has shown promise in reducing this rate to 25%. Nonetheless, the average overall survival time post-diagnosis ranges from 8 to 12 months (Withrow et al., 1991; Mason 2020). A potential alternative therapeutic approach involves cytokine therapy, particularly IL-2. By augmenting T cell activation, IL-2 administration insert can enhance anti-tumor immunity

and delay the progression of lung metastases, with the potential for promoting their regression through the differentiation and activation of NK and T cells (Mitchell et al., 1991).

In canine subjects, IL-2 therapy administration elicited discernible cytokine expression within lung tissues, concomitant with systemic immune activation characterized by transient fever and reductions in lymphocyte and platelet counts. Furthermore, heightened expression of costimulatory molecules and MHCII on monocytes was observed, alongside augmented cytotoxicity of NK cells. Notably, treated dogs exhibited markedly enhanced overall survival rates compared to control counterparts matched for disease stage (Dow et al., 2005).

1.3.5. mRNA vaccines

In immuno-oncology, significant attention has been directed toward mRNA vaccines in recent years, yielding promising outcomes (Van Hoecke et al., 2021). mRNA as an efficient vehicle for delivering therapeutic proteins to patients, a capacity further enhanced through molecular modifications (Tusup et al., 2019). Extensive investigation has been dedicated to leveraging mRNA-encoding tumor antigens to develop efficacious cancer vaccines. The versatility of mRNA vectors extends to facilitating the introduction of tumor-specific or immune checkpoint-blocking monoclonal antibodies into patients. Moreover, mRNA vectors have been explored for their potential in delivering recombinant monoclonal antibodies – complete or fragmented – targeting tumor antigens, immune cells, or immune activation pathways (Lecocq et al., 2019; Suurs et al., 2019).

Furthermore, mRNA vaccines hold promise in compelling cancerous transformed cells to synthesize intracellular toxic proteins, instigating self-destructive mechanisms within the cells. They also exhibit the potential to modulate the tumor microenvironment to mitigate immunosuppression. Moreover, mRNA vaccines have demonstrated utility in developing CARs (Van Hoecke et al., 2021). These non-tumor antigen mRNA-based immunotherapy strategies have succeeded in preclinical studies (Van Hoecke et al., 2021).

1.3.6. *In situ* vaccination

A burgeoning alternative for the eliciting immune response against tumors is *in situ* vaccination, a novel approach entailing the local administration of immune-activating agents into the tumor microenvironment. The mechanism underlying *in situ* vaccination entails optimal immune activation without mandating biopsy in all patients (Hammerich et al., 2016). However, its efficacy may exhibit variability at an individual level (Hammerich et al., 2019). *In situ* vaccination instills immune reactions and fosters local inflammation by utilizing aspecific, low-molecular-weight molecules that engage the innate immune system. These agents are

delivered directly into the tumor or its microenvironment, harnessing its intrinsic reservoir of antigens to spur a tailored immune response (Hammerich et al., 2015; Lizotte et al., 2016). Consequently, a targeted anti-tumor cellular immune response is locally initiated and propagated systemically throughout the organism, potentially eradicating metastases (Marabelle et al., 2014; Hammerich et al., 2016; Sagiv-Barfi et al., 2018). TLRs discern diverse ligands based on their foreign molecular properties. Human TLR1, 2, 4, 6, and 10 (as well as their analogs in other species) recognize specific lipids, predominantly of bacterial origin. Conversely, TLR5 and 11 identify foreign proteins, whereas TLR3, 7, 8, and 9 detect nucleic acids unique to non-vertebrates (Seledtsov et al., 2015). Furthermore, TLR2 identifies Gram-positive bacteria, and TLR4 discerns lipopolysaccharides from Gram-negative bacteria. In contrast, viruses are identified by TLR3 (double-stranded ribonucleic acid, dsRNA), TLR7 (ssRNA), and TLR9 (unmethylated cytosine and guanine separated by a phosphate group, abbreviated as CpG-DNA). Numerous TLR agonists are promising potential immunomodulators, with CpG-DNA notably employed in several studies as a TLR9 agonist (Sagiv-Barfi et al., 2018). Recognition of the unmethylated CpG motif by TLR9 effectively engenders protection against tumors by instigating cellular immune responses (Li et al., 2007; Houot and Levy 2009; Marabelle et al., 2013; Sagiv-Barfi et al., 2015; Sagiv-Barfi et al., 2018; Tsukamoto et al., 2019). Stimulation of APCs by TLR9 agonists augments antigen uptake and presentation, fostering activation of Th2 cells and cytotoxic T cells (Sagiv-Barfi et al., 2015). Additionally, TLR9 agonists induce OX40 expression on effector T cells within the tumor microenvironment. OX40, a costimulatory molecule belonging to the TNFR superfamily (Vosskuhl et al., 2010; Kursunel and Esendagli 2016), facilitates overcoming the activation threshold of effector T cells that are already antigen-bound via TCR but remain inactive. Stimulation of the OX40 molecule also curtails the function of regulatory T cells. Consequently, combined therapy involving anti-OX40 and CpG has demonstrated favorable outcomes across various tumor types, including lymphoma (A20), melanoma (B16-F10), colon cancer (CT26), and breast cancer (4T1) (Sagiv-Barfi et al., 2018).

1.4. Low molecular weight substances and treatment combinations

Low molecular weight substances are capable of modulating the immune response. In our experiments, we focused on three types of low molecular weight substances: 1) Substances that act as DAMPs or PAMPs, thereby activating DCs and steering the immune response towards a cellular direction; 2) Substances with previously proven antitumor effects that primarily drive the immune response towards a humoral direction and possess strong pro-inflammatory properties; 3) Preparations capable of inhibiting Tregs. These substances were

used individually and/or in various combinations. Additionally, we hypothesized multiple effects for certain molecules (see **Figure 7**), which will be discussed in detail below.

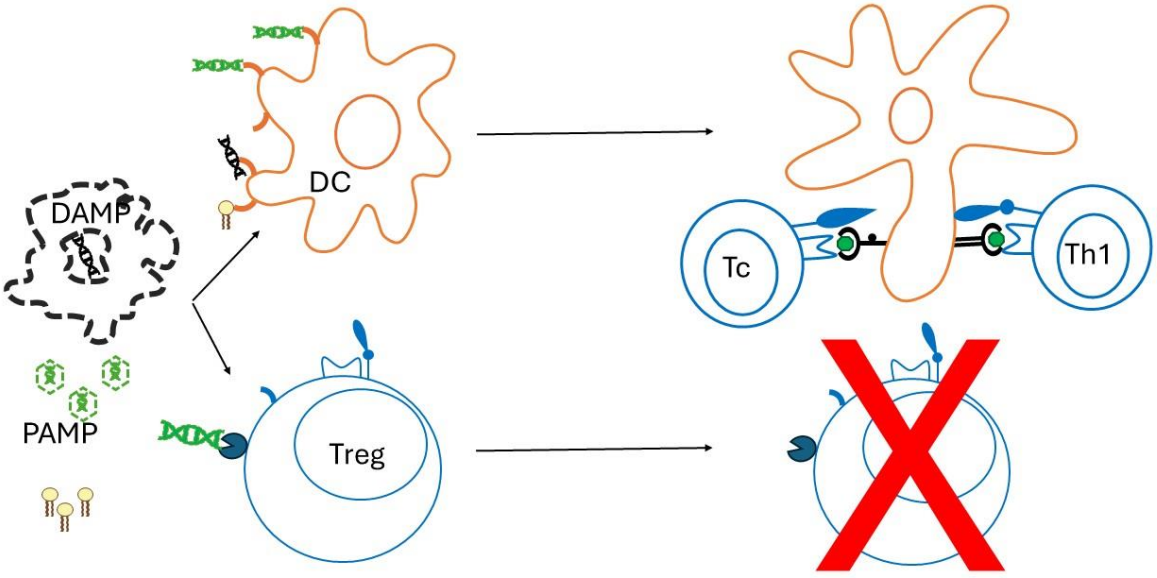

Figure 7: *The three distinct mechanisms of action of the low molecular weight compounds we employed may potentially facilitate the induction of anti-tumor immune responses. Nucleic acids (DNA and RNA) act on CD4⁺ and CD8⁺ T cells through the Toll-like receptors of antigen-presenting cells. Thus, acting on lymphocytes, they enhance the anti-tumor immune response. On the other hand, these molecules inhibit the function of regulatory T cells via RIG-I receptors. Lipopolysaccharides also affect T cells, but they induce inflammation.*

1.4.1. OX40 and Anti-OX40 (Treg inhibitor)

A pivotal strategy in overcoming intratumoral immunosuppression involves regulating the adverse effects of Tregs within the microenvironment. Anti-OX40 represents an agonistic antibody targeting OX40, a costimulatory molecule expressed on both effector T cells and Tregs (Smyth et al., 2014; Sagiv-Barfi et al., 2018). The OX40 possesses a cytoplasmic tail capable of binding OX40 ligands present on numerous molecules within the immune signaling cascade. This engagement induces the expression of proteins that prolong Teffs survival (Survivin, Bcl-2, Bcl-xl, Bfl-1), as delineated in **Figure 8** (Jensen et al., 2010; Mascarelli et al., 2021). Augmenting with anti-OX40 enhances the proliferation of $CD4^+$ and $CD8^+$ T cells and amplifies their response to tumor-associated antigens (TAAs). In a particular investigation, OX40 delineated a subset of high-affinity $CD8^+$ T cells that exhibited heightened IFNγ production *in situ*, with the count of $CD8^+$ T cells doubling upon combination therapy with anti-OX40 and anti-CTLA-4 (Moran et al., 2016; Deng et al., 2019). Moreover, the synergy between anti-OX40 and anti-CTLA-4 demonstrated promising outcomes in a 2014 study conducted in

Oregon, where the combined administration led to observable tumor regression. Notably, this combination induced the generation of Th1 $CD4^+$ T cells, known for IFNγ expression, and Th2 CD4+ T cells, which produce IL-4, IL-5, and IL-13. These latter cytokines are implicated in B cell differentiation (Constant and Bottomly 1997; Redmond et al., 2014).

Moreover, a study by *Zhang et al.,* in 2018 elucidated that heightened OX40 expression orchestrates the suppression of FOXP3 manifestation. OX40 augments the activity of basic leucine zipper ATF-like transcription factor (BATF) and BATF3, pivotal protein-coding transcription factors, thereby instigating the repression of FOXP3 synthesis within a conformationally constrained chromatin milieu (X. Zhang et al., 2018). Essentially, OX40 signaling hinders the transcription of FOXP3 mRNA, thereby impeding the differentiation of naïve $CD4^+$ T cells into Tregs, thus furnishing a strategy to attenuate Tregs functionality without perturbing effector T cells (So and Croft 2007). This orchestrated response proves advantageous in cancer pathology by recalibrating the tumor microenvironment and circumventing Treg-mediated immune evasion. Given the direct impact of OX40 and anti-OX40 interventions on T cell populations, they present as versatile therapeutic modalities across a spectrum of malignancies, obviating the necessity for exhaustive comprehension of tumor-associated antigenic structures and potentially surmounting issues of primary or acquired resistance inherent to immune checkpoint blockade therapy (Aspeslagh et al., 2016; Alves Costa Silva et al., 2020).

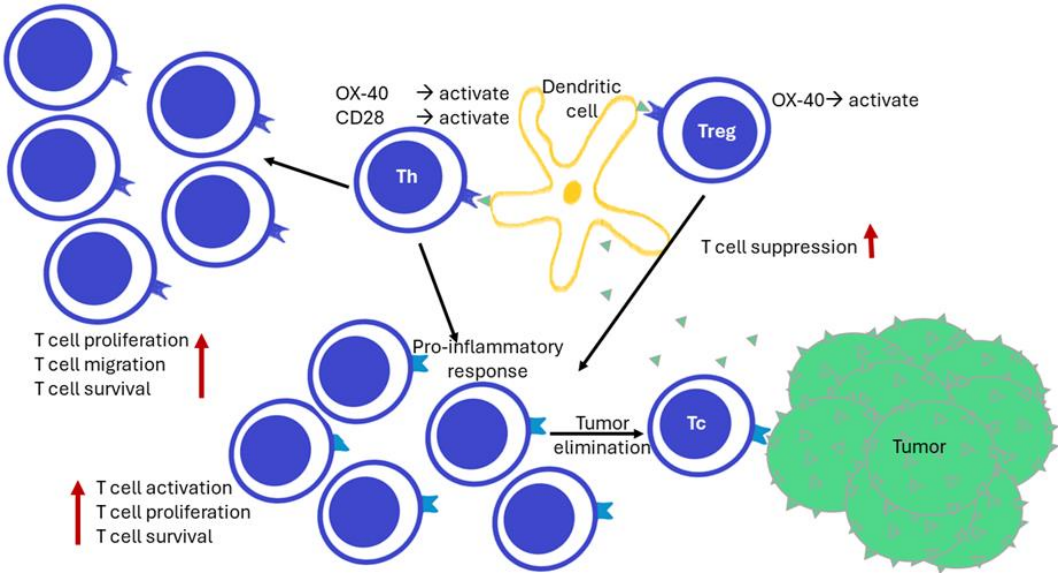

Figure 8: *The binding of OX40 receptor and their ligands initiates a signaling cascade that leads to $CD4^+$ T (Th), regulatory T (Treg) activation, and $CD8^+$ T (Tc) expansion. Although the OX40 connection strengthens the antitumor effect, the activation of Th impairs Treg function, reducing tumor immunosuppression and enhancing the antitumor immune response. Other signaling pathways on Th cells enhance the cellular immune response, increasing the activation, survival, proliferation, and cytotoxicity of T cells. Although the pro-inflammatory cytokines produced by Th also help B cell proliferation, this is less pronounced. (based on Mascarelli et al., 2021).*

1.4.2. Cytosine-Phosphorothioate-Guanine (CpG) (PAMP/DAMP)

Cytosine-phosphorothioate-guanine, abbreviated as CpG, represents an oligodeoxynucleotide (ODN) ligand that engages TLR9, a transmembrane PRR, assumes a pivotal role in recognition of PAMPs expressed across a diverse array of infectious agents, orchestrating subsequent cytokine responses through selective activation of NF-κB and other transcription factors (Offermanns and Rosenthal 2008; Fagerberg et al., 2014). TLR9 encompasses a DNA binding domain specifically tailored for CpG, a motif ubiquitously encountered in bacterial and viral genomes (Sun and Reddy 2013; Matz et al., 2019). Upon localized engagement by CpG, TLR9 catalyzes DC maturation, thereby enhancing TAA presentation (Jensen et al., 2010; Zhou et al., 2021), among other cascading effects. Mature DCs exhibit augmented antigen presentation, notably of OX40 ligand (OX40L) (Jensen et al., 2010). CpG ODNs manifest into three categories contingent upon their structural and functional attributes: CpG-A, CpG-B, and CpG-C. CpG-A ODNs stimulate plasmacytoid dendritic cells to elicit robust production of IFNα and TNFα, thereby fostering the activity of $CD8^+$ T cells and NK cells reliant on these cytokines. NK cells, lacking TLR9, necessitate an intermediary role facilitated by APCs (Marshall et al., 2006; Li et al., 2020). However, they exhibit diminished NF-κB signaling capacity, producing subdued pro-inflammatory cytokines, such as IL-6. Conversely, CpG-B ODNs escalate CD40, CD80, and CD86 expression on APCs, thereby instigating the maturation of diverse immune cell populations, notably B cells. This phenomenon concomitants a conspicuous elevation in IL-6 and TNFα expression compared to CpG-A counterparts (Krieg 2002; Li et al., 2020). CpG-C, exhibiting a hybrid profile of its predecessors, engenders robust cytokine expression, including IFNα, TNFα, and IL-6. Additionally, CpG-C potently stimulates B cell activation akin to CpG-B, thus affording a more comprehensive and efficacious immunostimulatory profile relative to CpG-A and CpG-B variants (Krieg 2002; Li et al., 2020). These attributes position CpG-C as an optimal candidate for immunotherapeutic applications, particularly in synergy with anti-OX40 interventions.

1.4.3. CpG and Anti-OX40

The synergy between CpG and anti-OX40 has been extensively investigated and delineated in numerous studies (Sagiv Barfi et al., 2018; Sagiv-Barfi et al., 2018; Zhou et al., 2021; Pieper et al., 2023), highlighting that CpG-mediated engagement of TLR9 potentiates OX40 expression specifically on $CD4^+$ T cells, predominantly among effector T cells. A comprehensive investigation conducted by Stanford University in 2018 tested this combination for the first time. It was elucidated the specificity of this phenomenon to OX40, excluding the immune checkpoint inhibitors CTLA-4 and PD-1. Furthermore, this study revealed that in the absence of intervention, T cells fail to continually express OX40 following the depletion of

dendritic cells and macrophages *in vitro*, even in the presence of CpG. The conclusion proposed by the investigators is that CpG instigates myeloid cells to secrete cytokines, notably IL-12, IFNγ, and TNFα, thereby fostering OX40 expression in T cells. This mode of action necessitates an intermediary step for efficacy, both *in vitro* and *in vivo*. Intriguingly, intratumoral administration of CpG was found to upregulate OX40 expression, culminating in significant tumor regression locally; however, this effect was notably absent in distant, untreated tumors within the same host. Anti-OX40 monotherapy demonstrated modest efficacy, resulting in marginal delays in tumor progression at local and distant sites. In stark contrast, the combination of anti-OX40 and CpG exhibited remarkable efficacy, precipitating complete regression of treated and untreated A20 lymphomas (Sagiv-Barfi et al., 2018). Notably, this combined regimen sustained an efficient immune response without inducing exhaustion of requisite antibodies necessary for counteracting tumor proliferation, thereby facilitating substantial, if not complete, targeted tumor regression.

Further investigations have corroborated the synergistic efficacy of co-administering CpG and anti-OX40, elucidating their therapeutic potential across a spectrum of malignancies including A20 B cell lymphomas (Sagiv Barfi et al., 2018; Sagiv-Barfi et al., 2018; Proskurina et al., 2023), hepatocellular carcinomas (Zhou et al., 2021), Krebs-2 carcinomas, and Lewis lung carcinomas (Proskurina et al., 2023). Notably, the latter two malignancies exhibited comparatively diminished responsiveness to CpG and anti-OX40 therapy, attributed to the subdued immunogenicity of their tumor-associated antigens (Proskurina et al., 2023). Nevertheless, the combined regimen of anti-OX40 and CpG retains considerable promise as immunotherapeutic modalities across diverse cancer phenotypes. Indeed, compelling evidence underscores the beneficial outcomes of this synergistic approach even in managing metastatic cancers (Hong et al., 2022).

1.4.4. Retinoic Acid-Inducible Gene I (RIG-I) agonists (PAMP/DAMP and Treg inhibitor)

The structural characteristics of the viral-derived nucleic acids we employed allow the host immune system to recognize them as foreign substances. Consequently, TLRs are capable of detecting these nucleic acids. Additionally, their hairpin termini endow them with RLR agonist properties. These nucleic acids also contain CpG motifs. This combination of features enhances their potential to elicit a robust immune response.

1.4.4.1. Influenza A Virus RNA

The innate immune system promptly safeguards against diverse infections through its capacity to recognize and respond to pathogens in a nonspecific manner. The commercially

available 3p-hpRNA is a synthetic preparation based on influenza RNA. Upon encountering influenza A virus (IAV), the innate immune responses are instigated through the recognition of PAMPs by host PRRs, notably including RIG-I (Thoresen et al., 2021) and presumably TLRs. Numerous synthetic RIG-I agonists have been scrutinized for their ability to elicit antiviral defense mechanisms. They are invaluable tools for mechanistic elucidation and potential pharmacological interventions against IAV infection (Lin et al., 2012; Kulkarni et al., 2014; Chiang et al., 2015). Among these, a class of short synthetic stem-loop RNAs (SLRs) bearing triphosphorylated moieties has been engineered to activate the RIG-I pathway, thus precipitating a robust IFN response (Linehan et al., 2018). With a stable RNA tetraloop strategically positioned to occlude the opposing end of the SLR duplex, RIG-I engagement with the triphosphorylated terminus of the SLR duplex is ensured. These synthetic SLRs represent valuable assets for interrogating the intricate mechanisms underlying RIG-I activation. The genome of the influenza A virus consists of eight ssRNA segments in a negative-sense configuration. Remarkably, except for plasmacytoid dendritic cells, the innate immune sensing of IAV is critically reliant on RIG-I (Diebold et al., 2004; Lund et al., 2004). Activation of the RIG-I pathway within infected cells instigates the production of IFNs, thus orchestrating a robust antiviral response against IAV (Kato et al., 2006; Pichlmair et al., 2006; Habjan et al., 2008; Kato et al., 2008: 5; Schmidt et al., 2009; Rehwinkel et al., 2010). Bioinformatics analysis unveils the panhandle structure, a concise dsRNA duplex formed through partial complementarity at the extremities of the viral genome, as the sole conserved RNA secondary structure among negative-strand viruses (Hofacker et al., 2004). Notably, this panhandle configuration also serves as the viral promoter region for viruses harboring a segmented genome (Weber and Weber 2014).

Consequently, it has been postulated that the panhandle structure inherent in the genomic RNA of negative-strand viruses fulfills the dsRNA requisite for RIG-I activation. In alignment with this hypothesis, the association of IAV genomic RNA and defective interfering RNA with RIG-I has been established (Pichlmair et al., 2006; Baum et al., 2010; Rehwinkel et al., 2010). Notably, the panhandle structure of IAV plays a direct role in RIG-I activation and subsequent induction of IFN production (see **Figure 9**) (Liu et al., 2015). Despite its relatively diminutive size compared to analogous structures in other viruses, *in vitro*-transcribed IAV panhandle, RNA demonstrates binding affinity towards RIG-I and elicits IFN production (Liu et al., 2015).

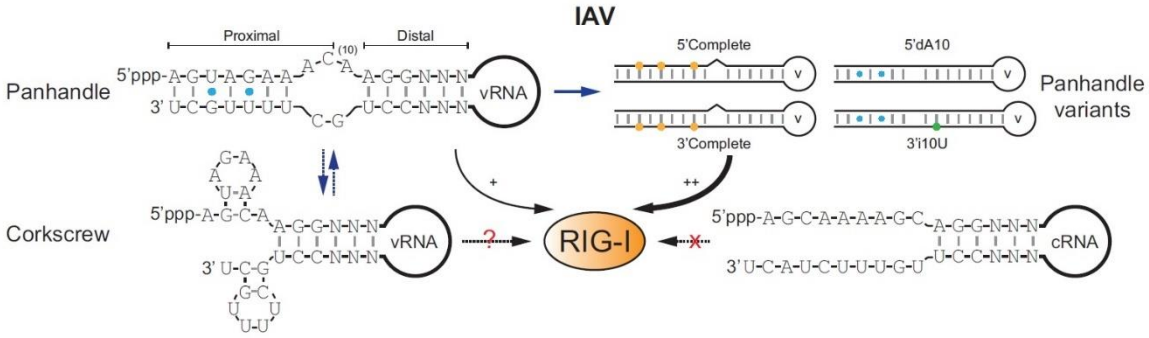

Figure 9: *RIG-I activation by genomic panhandle structures of IAV and other negative-strand RNA viruses.: The IAV genomic promoter region adopts alternate RNA structures, such as the panhandle and corkscrew configurations. The wild-type IAV panhandle directly binds to and activates RIG-I, while panhandle variants with destabilizing elements activate RIG-I more efficiently than the wild type. Whether the IAV promoter region in the corkscrew configuration can activate RIG-I remains unknown (Liu and Zhou 2019).*

During the viral life cycle, the segmented negative-stranded RNA genome is liberated from the endosomal compartment into the cytoplasm before translocation into the nucleus for viral transcription and replication. Throughout this intricate process, IAV infection is discerned by RIG-I, which selectively engages with the panhandle structures intrinsic to viral genomes (Pichlmair et al., 2006; Weber et al., 2013). The 5′-triphosphate segment of RNA, synthesized by viral polymerases, assumes responsibility for mediating the detection of RNA molecules by RIG-I. Notably, 5′-triphosphate RNA directly interacts with RIG-I, thereby serving as a critical determinant for recognition. Consequently, a commercially available, uncapped 5′-triphosphate hairpin RNA, now designated as 3p-hpRNA, emerges as a distinctive molecular signature implicated in detecting viral infection by RIG-I. Remarkably, this signature feature is conspicuous in viruses recognized by RIG-I but conspicuously absent in viruses detected by MDA-5 (Hornung et al., 2006).

1.4.4.2. Porcine Parvovirus Type 1 DNA

The Porcine Parvovirus (PPV) genome consists of a ssDNA molecule with a negative polarity, spanning approximately 4–6 kilobases in length. This genomic entity harbors two distinct open reading frames (ORFs). ORF1 governs the expression of the nonstructural proteins (NSs) like NS1, NS2, and NS3.

Conversely, ORF2 directs the synthesis of three viral capsid proteins (VPs), namely VP1, VP2, and VP3, with the latter arising from the proteolytic cleavage of VP2 (Molitor et al., 1983; Ranz et al., 1989; Bergeron et al., 1996). The terminal regions of the PPV genome feature two palindrome sequences, which collectively form a characteristic stem-loop and hairpin structure spanning approximately 120 to 200 nucleotides. This structural motif is facilitated DNA

replication (Cavalier-Smith 1974; Astell et al., 1985; Cotmore and Tattersall 1987). The hairpin structure of PPV plays a pivotal role in its replication process, with alterations in size, nucleotide composition, and structural conformation potentially modulating the stability of this structure, thereby exerting consequential impacts on viral DNA replication dynamics and possibly influencing the biological attributes of the virus (Hanson and Rhode 1991).

1.4.4.3. Viral RNA and DNA purified in our laboratory

The purified influenza virus RNA from our laboratory contains the complete viral genome of the PR8 strain in segmented form. Due to its hairpin structure, it can act as an agonist for RIG-I and as a ligand for TLR9, being recognized as foreign due to its negative single-stranded RNA nature. It is not stable and therefore prepared freshly each time, yet it is non-cytotoxic.

Similarly, the purified DNA preparation from our own isolate of PPV1 also contains the complete viral genome, with hairpin structures at both ends, and is expected to exhibit similar effects as seen with influenza.

Literature data on these treatment combinations are currently unavailable.

1.5. IL10, IL6, and IFNγ

This section provides a comprehensive overview of the signaling pathways governing the expression of IFNs and ILs, elucidating their intricate roles in modulating inflammatory processes. IFNs are stratified into three distinct categories: types I, II, and III. Type I IFNs are synthesized by monocytes and fibroblasts, primarily in response to viral incursions. Following recognition of viral DNA or RNA by PRRs such as TLR9 or RIG-I, several signal transduction cascades are activated, culminating in the induction of IFN production. Type I IFNs engage with their cognate receptors upon secretion, subsequently triggering the synthesis of effector proteins aimed at curtailing viral biopolymer replication (Levy et al., 2011). Similarly, type III IFNs predominantly instigate antiviral signaling pathways and have demonstrated pronounced efficacy against specific virus families – such as rotaviruses– in contrast to type I IFNs. Despite their divergent functional profiles, both type I and type III IFNs engage in closely intertwined signal transduction pathways (Hermant and Michiels 2014), highlighting the interconnectedness of these essential immune mediators. Type II interferons exclusively encompass IFNγ. IFNγ exerts pleiotropic effects, including stimulating MHC class I and II expression on APCs to augment antigen presentation, activation of innate immune cells, modulation of the Th1/Th2 balance, and mediation of apoptotic pathways. This cytokine is synthesized by NK cells, $CD8^+$ T cells, and $CD4^+$ Th1 cells, rendering it a prime candidate for cytokine enzyme-linked immunosorbent assays (ELISAs). Elevated levels of IFNγ detected

through these assays serve as a reliable indicator of the activation status of these innate immune cell populations. The expression of IFNγ is potentiated notably by IL-12, in addition to IL-15 and IL-18. Specifically, IL-12, secreted by macrophages in response to IFNγ, amplifies the production of IFNγ by activated T cells and NK cells, thereby perpetuating the immune response (Tau and Rothman 1999). In general, cytokines operate through the Janus kinase (JAK)-signal transducer and activator of transcription (STAT) pathway, abbreviated as the JAK-STAT pathway. Lacking intrinsic kinase activity, cytokines rely on this pathway for signal transduction, culminating in the initiation of gene transcription within the cell nucleus. IFNγ conforms to this paradigm. Upon production of IL-12, JAK2 is activated, followed by subsequent phosphorylation of STAT4, thereby instigating target gene expression of IFNγ (Morinobu et al., 2002). IFNγ triggers its own JAK-STAT signal transduction cascade upon activation within the host. This process involves the recruitment of JAK1 and JAK2 to the IFNγ and type II cytokine receptor dimer. Subsequently, JAK1 and JAK2 undergo phosphorylation and, in turn, phosphorylate STAT1, which then dimerizes and facilitates the transcription of interferon-stimulated genes (ISGs). These ISGs encode many IFN-dependent proteins, which orchestrate diverse cellular responses, including the activation of innate immune cells through MHC regulation, stimulation of NK cell activity, and promotion of Th1 cell development and differentiation (Bhat et al., 2018). Interleukin-6 (IL-6) exerts a pleiotropic immunostimulatory influence to such an extent that it was initially construed as comprising at least four distinct molecules. These entities were previously designated as B cell stimulatory factor 2 (BSF-2), hybridoma growth factor (HGF), IFN-β2, and hepatocyte-stimulating factor (HSF). Subsequent identification in 1989 revealed these factors to be functionally identical, prompting their unification under the common appellation of IL-6. Consistent with their former designations, IL-6 exerts direct effects on diverse cellular processes, including B cell maturation into antibody-producing cells, stimulation of B cell fusion with myeloma cells, IFN-like antiviral activities, and induction of protein synthesis in hepatocytes (Kishimoto 1989; Tanaka et al., 2014). The underlying pathway through which IL-6 orchestrates an inflammatory response becomes increasingly elucidated in light of these multifaceted actions. Upon synthesis by T cells or monocytes at the site of inflammation, IL-6 traverses the bloodstream to reach the liver, where hepatocytes represent one of the select cell types expressing the IL-6 receptor (IL-6R). Following binding to IL-6R, a type I cytokine receptor, the resultant complex recruits glycoprotein 130 (gp130), initiating cellular signaling cascades mediated through the JAK-STAT pathway, notably involving JAK1, STAT1, and STAT3. Upon dimerization, this complex translocates into the nucleus, thereby orchestrating the transcription of IL-6 target genes, most of which encode pro- and/or anti-apoptotic proteins (Choy and Rose-John 2017). As previously elucidated, IL-10 assumes a pivotal role in host immunoregulation, primarily through the suppression of Th1 cytokines, MHC antigens, and macrophage costimulatory molecules. The

absence of IL-10 during disease states may precipitate dangerous consequences for the host. While pro-inflammatory molecules may succeed in eliminating the causative agent, unbridled inflammation could give rise to deleterious side effects. Conversely, an excess of IL-10 can lead to the complete suppression of inflammatory cells, thereby impeding disease clearance. The intricate interplay among IL-12, IL-10, and IFNγ is depicted in **Figure 10** (Trinchieri 2007).

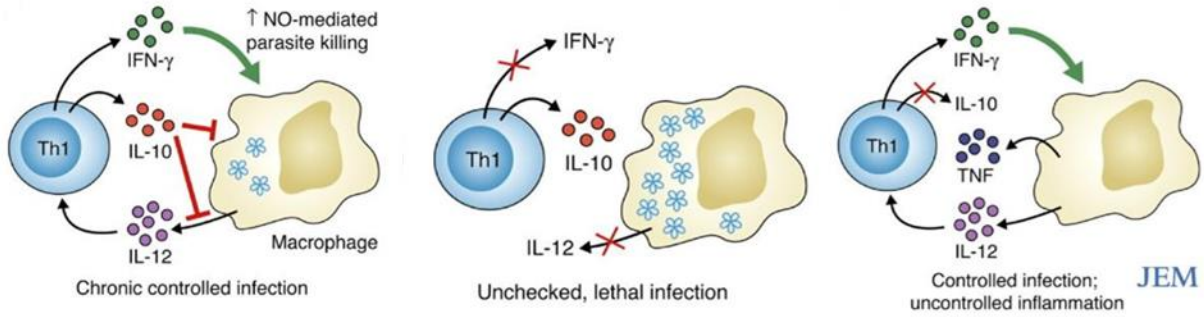

Figure 10: *Three types of interactions between T-helper (Th) 1-mediated release of interleukin-10 (IL-10), interleukin-12 (IL-12), and interferon-gamma (IFNγ) during parasitic (blue marks inside the macrophage) infections (Trinchieri 2007).*

As previously discussed, numerous tumor types exhibit heightened production of IL-10 within their microenvironment, disrupting the delicate equilibrium between IL-10-mediated immunomodulation and the actions of IFNγ and IL-12. This dysregulation facilitates the tumor cells' unchecked proliferation. Consequently, quantifying IL-10 levels emerges as a viable approach for assessing the efficacy of immunostimulatory agents in both untreated and treated tumors.

1.6. Tumor models

We employed two tumor models that have not been previously utilized in immunotherapy treatments according to the literature. In human cases, both types of tumors present numerous challenges in treatment.

1.6.1. The MB49 cell line

Bladder cancer (BC) represents one of the foremost prevalent urogenital malignancies globally, ranking tenth in incidence, with reported cases reaching up to 573,278 in 2021 (Sung et al., 2021). Clinical-pathological categorization delineates bladder urothelial carcinoma as constituting 90–95% of BC instances, with the remaining attributed to bladder adenocarcinomas and squamous cell carcinomas (Kirkali et al., 2005). BC is classified into either muscle-invasive BC (MIBC) or non-muscle-invasive BC (NMIBC). The 5-year overall survival rate for MIBC sans metastasis stands at 36%-48%, whereas MIBC cases exhibiting distant or regional metastasis yield rates of 5% and 36%, respectively (Lenis et al., 2020).

Patient prognoses manifest variability contingent upon diverse clinical profiles and pathological classifications. Presently, standard NMIBC therapy encompasses transurethral resection of the bladder tumor followed by diverse chemotherapeutic modalities. Radical cystectomy is contingent upon MIBC metastasis, wherein subsequent therapeutic interventions comprise chemotherapy, immunotherapy, and targeted therapy (Lenis et al., 2020). Despite notable advancements in BC diagnosis and treatment, metastasis, drug resistance, and tumor recurrence persist at elevated rates, owing to profound genomic instability and marked intratumoral heterogeneity (Witjes et al., 2017; Dy et al., 2017). A suitable orthotopic animal model, characterized by reproducibility, reliability, and simplicity, assumes paramount significance in elucidating BC mechanisms. A murine BC model offers numerous controllable variables within laboratory settings, affording a plethora of experimental parameters (Ratliff 2000). Prior investigations posit the quintessential BC animal model to possess the following attributes: (1) origination within the bladder; (2) tumorigenesis rooted in urothelial cell carcinoma; (3) development within an immunocompetent host; and (4) facile reproducibility in operational terms (Xiao et al., 1999). MB49 cells originate from C57BL mouse bladder epithelial cells that transformed following a singular 24-hour exposure to the chemical carcinogen 7,12-dimethylbenz[a]anthracene (DMBA) during the early stages of an extended primary culture (Summerhayes and Franks 1979). Subsequent transplantation of these transformed cells into syngeneic murine hosts yielded carcinoma development (Summerhayes and Franks 1979). Despite their male provenance, karyotypic analyses have revealed a complete loss of the Y chromosome in 100% of the scrutinized cells (Fabris et al., 2012). This aberration mirrors a common early occurrence observed in human bladder cancer. Recent investigations have underscored the ability of MB49 cells to faithfully recapitulate pivotal aspects of sex-specific disparities in bladder tumor growth dynamics (White-Gilbertson et al., 2016). Notably, MB49 cells display minimal to negligible expression levels of MHC-Class I and II molecules (Lattime et al., 1992). Nevertheless, exposure to interferon-gamma (IFNγ) induces a substantial upregulation in the expression of both MHC Class I and II molecules (Lattime et al., 1992).

1.6.2. The Renca CRL-2947 cell line

Renal carcinomas represent a predominant subset of kidney pathologies, constituting a significant portion of kidney-related malignancies. Renal cell carcinoma, a human malignancy not uncommonly encountered in clinical practice, exhibits a propensity for metastasis, primarily within the pulmonary milieu (Cooley et al., 2021). The Renca CRL-2947 cell line, initially derived from BALB/c mice, stands as a seminal entity among various Renca cell lines employed as models for kidney adenocarcinoma, tailored for murine experimentation. Renca

cell lines, including the renowned CRL-2947 strain, have garnered widespread adoption due to their invasiveness and high proliferative capacity. Although not inherently metastatic, Renca cells have been documented to incite secondary neoplasms. The metastatic potential of Renca cells exhibits variability contingent upon the method of application, with instances of metastasis akin to human disease presentations observed following subcapsular kidney injection and intravenous administration, mainly manifesting in regional lymph nodes, lungs, and liver (Hrushesky and Murphy 1973; Salup and Wiltrout 1986; Salup et al., 1987; Oliver et al., 2019; He et al., 2021).

Conversely, subcutaneous administration tends to yield localized carcinogenic lesions devoid of metastatic potential (Chakrabarty et al., 1994; Sobczuk et al., 2020). Renal neoplasms portend an unfavorable prognosis within the pantheon of oncological pathologies (Renca Syngeneic Murine Model), primarily due to insidious tumor initiation characterized by a paucity of clinical manifestations. Consequently, by the time renal carcinoma manifests clinically, the window for effective intervention may have closed, hindering the prospects of tumor regression and patient remission.

2. Aims

In the course of our inquiries, we investigated the impact of *in situ* vaccination as a therapeutic strategy on tumorigenesis, employing diverse murine models. The therapeutic interventions were conducted on two distinct tumor cell lines: murine bladder carcinoma (MB49) and murine kidney adenocarcinoma (Renca mouse renal adenocarcinoma). Our investigations encompassed the administration of numerous immune agonists and antagonists, inclusive of substances targeting Toll-like receptors 4 and 9, retinoic acid-inducible gene I (RIG-I), and an agonistic monoclonal antibody targeting the OX40 molecule. Throughout our experimentation, we evaluated several commercially available agents alongside those produced within our laboratory.

Our study aimed to identify similarities and differences in treating various tumor types using low molecular weight therapeutic agents. The parameters examined encompassed survival rates, incidence of tumor demarcation, and metastatic progression. To accomplish this, we established the following objectives:

1) Based on the literature, we aimed to evaluate the efficacy of mouse-specific monoclonal anti-OX40 antibody and CpG (TLR-9 ligand) treatment in two previously untested cell lines using an *in vivo* mouse model.
2) We aimed to test lipopolysaccharide (TLR-4 ligand) treatment in an aggressive tumor cell line to confirm or refute previous literature findings.
3) We aimed to conduct the first trial of harpin RNA (3p-hpRNA, RIG-I agonist) treatment as a TLR and RLR ligand.
4) We aimed to conduct the first application of various nucleic acids with hairpin termini (negative single-stranded RNA and single-stranded DNA) as treatments.

Our primary objective was to advance the translational potential of the treatments described subsequently.

3. Materials and methods

3.1. The fundamental framework of the investigations

For our investigations, we initially conducted *in vitro* propagation of the tumor cell lines in tissue culture for our investigation. Subsequently, we subcutaneously implanted the cells into the left or right thigh of mice (following a period of 7 days for the acclimatization of the animals), employing a predetermined cell count established through prior experimentation and/or literature review. Subsequent to this implantation, we randomly allocated the subjects into control and treatment cohorts. Upon attaining a tumor diameter ranging between 5-8 (or 8-12) mm, treatment commenced via intratumoral inoculation of mice. The mice were treated using the *in situ* vaccination method, where the treatment cocktails were injected into the central part of the mice's primary tumors without the use of anesthesia, in accordance with the approved animal experimental protocols (permit number: PE/EA/00922-7/2021). This therapeutic regimen was iterated twice for each experimental group, with mice in the control group receiving no treatment. Our investigation herein sought to scrutinize the efficacy of treatment in eradicating an established neoplasm. Following the prescribed treatments, diligent monitoring of tumor dimensions alongside physiological parameters was conducted for both control and treatment cohorts. The well-being of the murine subjects was assessed daily. Deceased subjects underwent postmortem dissection, and histological analyses of resultant tumors were performed. The efficacy of the treatment modality was appraised by evaluating the presence of tumor progression and distant metastatic dissemination.

3.2. Cancer Cell Lines

In our experimental endeavors, we utilized two distinct cancer cell lineages. Specifically, the 12-dimethylbenzanthracene-induced MB49 murine bladder tumor cell line, MB49-CVCL_7076-Millipore Cat. #SCC148, (Merck, Darmstadt, Germany) was employed. The MB49 carcinoma cell line was adeptly acclimated to C57BL6/N mice (Animalab, Budapest, Hungary), ensuring the establishment of optimal experimental conditions. We utilized 75 cm^2 ventilated tissue culture dishes (Merck, Darmstadt, Germany) for culturing tumor cells. Initially, cells were seeded onto the culture plates at a density of $5x10^5$ cells. Cultivation of tumor cells occurred in RPMI-1640 medium (Merck, Darmstadt, Germany) supplemented with 10% inactivated fetal bovine serum (FBS, Merck, Darmstadt, Germany), 2 mM glutamic acid (Merck, Darmstadt, Germany), penicillin (100 U/ml), and streptomycin (100 µg/ml) (in combination, Merck, Darmstadt, Germany), within an incubator set at 37°C under conditions of 95% humidity and a 5% CO_2 atmosphere. The culture reached confluence after three days. Upon reaching 99% confluency, cell cultures underwent treatment with trypsin-EDTA (Merck, Darmstadt, Germany), subsequently, cells were washed with 10 ml of sterile phosphate-buffered saline

(PBS) and centrifuged at 300 g for 10 minutes at 4°C. Lastly, cells were suspended in RPMI-1640, devoid of FBS and antibiotics. A total of $1x10^7$ MB49 cells (We determined the number of cells for implantation based on the results of earlier (unpublished) experiments by Béla Dénes), comprising a 0.2 ml suspension, were subcutaneously instilled into the left musculus biceps femoris region. Only cell suspensions exhibiting 90% viability, as ascertained via trypan blue (TB, Merck, Darmstadt, Germany) staining, were used for implantation.

The Renca Renal Adenocarcinoma CRL-2947 cell line, acquired from the ATCC (Manassas, Virginia, USA), constituted another focal point of our investigations. These tumor cells underwent cultivation at a controlled temperature of 37°C, under conditions of 95% humidity and a 5% CO_2 concentration, within RPMI-1640 medium (Merck, Darmstadt, Germany). In a manner similar to previous studies, we utilized 75 cm^2 ventilated tissue culture dishes (Corning, New York, USA). Initially, cells were seeded onto the culture plates at a density of $5x10^4$ cells (Hara et al., 2019).This medium was supplemented with 10% inactivated fetal bovine serum (Merck, Darmstadt, Germany), 2 mM glutamic acid, penicillin (100 U/ml), and streptomycin (100 µg/ml). Upon reaching confluency (after four days), the cell cultures underwent treatment with trypsin-EDTA. Subsequently, cells were washed with 10 ml of sterile PBS and centrifuged at 300 x g for 10 minutes at 4°C, followed by suspension and subsequent double washing with RPMI-1640 devoid of serum and antibiotics. A total of $3x10^5$ CRL-2947 cells (as we lacked prior experience with Renca cells, based on previous literature, where values ranged between $5x10^4$ and $5x10^6$, we determined the number of cells to be implanted) (Shvarts et al., 2006; Hara et al., 2019), comprising a 200 µl suspension, were administered subcutaneously into the region of each murine subject's right musculus biceps femoris (BALB/c – Animalab, Budapest, Hungary). Only cell suspensions demonstrating 90% viability were employed for implantation purposes, as determined through TB staining.

3.3. Mice

Throughout the progression of three extensive treatment protocols, we utilized a total of 30 C57BL6/N female mice (Animalab, Budapest, Hungary), aged between 4 and 5 weeks, alongside 102 BALB/c female mice (Animalab, Budapest, Hungary) of the same age cohort, each weighing 17 g. These animals were accommodated within mouse enclosures, with a maximum occupancy of 10 individuals per enclosure, ensuring robust statistical power. Housing conditions maintained a temperature of 20 ± 2°C, humidity levels at 50 ± 10%, and a diurnal rhythm of 12 hours of light followed by 12 hours of darkness, with unrestricted access to food and water ad libitum.

All procedures involving animal subjects strictly adhered to the guidelines outlined in the “Care and Use of Laboratory Animals”, as delineated by the Veterinary Diagnostic Directorate,

National Food Chain Safety Office, Hungary. Tumor implantation was performed following a seven-day acclimatization period.

3.4. Therapeutic Agents

All interventions were administered utilizing a formulation meticulously selected for its presumed efficacy. Mice were subjected to intratumoral treatment regimens involving a variety of concoctions comprising distinct combinations and dosages of commercially available unmethylated CpG oligodeoxynucleotide (TLR9 ligand – InvivoGen, San Diego, California, USA), agonistic rat monoclonal anti-CD134/OX40L receptor antibody (anti-OX40 – Abcam, Cambridge, UK), lipopolysaccharide from *Escherichia coli*, serotype 055:B5 (LPS – InvivoGen, San Diego, California, USA), 3p-hpRNA (5' triphosphate hairpin RNA) – a selective agonist of RIG-I (InvivoGen, San Diego, California, USA), or compounds synthesized within our laboratory, such as influenza virus RNA (IV-RNA), extracted from the mouse-adapted H1N1 influenza A virus strain PR8 (H1N1 strain A/Puerto Rico/8/1934), and parvovirus DNA (porcine parvovirus type 1, PPV1-DNA), sourced from a porcine parvovirus 1 isolate. Prior to administration, all treatment combinations were dissolved in pyrogen-free water. Injection of the treatment cocktails was targeted at the central region of each neoplasm.

3.5. The purification protocol of nucleic acids produced in our own laboratory

We utilized PR8 influenza virus, propagated on Madin-Darby canine kidney cells (ATCC, USA) for this study. Parvovirus was isolated on swine testicular cells (ATCC, USA) by Attila Cságola.

Nucleic acid extraction followed a protocol adapted from Hoelzel AR (1998). Specifically, 200 µl of cell supernatant containing viruses was combined with 75 µl of extraction buffer (50 mM Tris pH 7.5, 1 mM EDTA, 100 mM NaCl, 1% SDS – Merck, Darmstadt, Germany) and 1.5 µl of Proteinase K (20 mg/ml, Merck, Darmstadt, Germany). The mixture was then incubated for 120 minutes at 55ºC with occasional stirring. After incubation, 75 µl of phenol-chloroform-isoamyl alcohol (25:24:1 ratio, Merck, Darmstadt, Germany) was added, mixed thoroughly, and incubated for 5 minutes at room temperature (RT), followed by centrifugation (5 minutes, 7000 x g). The upper aqueous phase was carefully transferred to a fresh Eppendorf tube. Next, 75 µl of chloroform-isoamyl alcohol (24:1 ratio, Merck, Darmstadt, Germany) was added to the aqueous phase, mixed thoroughly, incubated for 5 minutes at RT, and centrifuged (3 minutes, 7000 x g). The resulting upper phase was transferred to a new tube, and 0.1 volume (7-8 µl) of 3 M sodium acetate (Merck, Darmstadt, Germany) and 2-2.5 volumes (approximately 150 µl) of cold (-20ºC) ethanol (96%, Merck, Darmstadt, Germany) were added. The mixture was then incubated overnight at -20ºC, followed by centrifugation (5

minutes, 11000 x g). After discarding the supernatant, the nucleic acids were washed with 150 µl of 70% ethanol (Merck, Darmstadt, Germany), followed by centrifugation (5 minutes, 11000 x g). Finally, the supernatant was removed, and the nucleic acids were dissolved in 100 µl of TE buffer (10 mM Tris pH 8, 1 mM EDTA pH 8; Merck, Darmstadt, Germany) (Hoelzel A. R. (1998) Molecular genetic analysis of populations, a practical approach. Oxford University Press, Oxford, UK).

3.6. Humane endpoints

The animal experimentation conducted herein received explicit approval from the ethics committee of the Veterinary Diagnostic Directorate, National Food Chain Safety Office. Authorization for the animal protocols was duly granted by the Government Office of Pest County Division of Food Chain Safety, Animal Health, Plant Protection Department (permit number: PE/EA/00922-7/2021).

Mice were humanely euthanized via CO_2-induced anoxia upon attainment of a mean tumor diameter (MTD) measuring 20 mm, or in instances where the animal displayed signs of chronic pain or distress, or manifested alterations in health and/or well-being (e.g., compromised mobility, inability to maintain an upright posture, disruption of vital physiological functions). Post-tumor implantation, mice did not receive any form of anesthetic or analgesic treatment, as such interventions were deemed to elicit heightened stress (via animal capture and needle insertion) surpassing the discomfort associated with the condition itself. The expeditious CO_2-mediated sacrifice adhered rigorously to the principles outlined in the Guide for the Care and Use of Laboratory Animals, as delineated by the National Institute for Health (National Research Council, 2011). Daily surveillance of the animals' health status was diligently maintained.

3.7. Pre-Experiments on cell culture

The dosages allocated to each treatment cohort were predicated upon findings from antecedent investigations conducted by the Department of Microbiology and Infectious Diseases. Furthermore, an *in vitro* preliminary assay was performed within the departmental laboratory antecedent to the commencement of the *in vivo* experimentation. This preliminary assessment scrutinized the viability of peripheral blood mononuclear cells (PBMC) after exposure to varying concentrations of the aforementioned therapeutic agents. Diverse experimental groups were delineated to evaluate the cytotoxic impact engendered by distinct dosages and combinations of CpG, anti-OX40, 3p-hpRNA, LPS, IV-RNA, and PPV1-DNA.

On the 7th day post-tumor implantation and 15 days subsequent to the final treatment administration, blood specimens were procured from all mice. After the sample collection, standard cytokine ELISA assays were conducted to quantify the production levels of IFN-γ, IL-6, and IL-10 within each experimental group (our unpublished data).

3.8. Postmortem Data Collection

Throughout the progression of the *in vivo* experimentation, diligent daily surveillance of all murine subjects was undertaken, with deceased specimens promptly subjected to necropsy procedures utilizing stainless steel autopsy scissors and anatomical forceps. Following an initial external inspection, mice underwent an abdominal incision to assess the primary tumor's dimensions, any visible anomalies, and the spatial arrangement of internal organs, along with ascitic fluid presence, if any. The overarching objective of these postmortem evaluations was to identify overt signs of metastasis and secondary pathology. Given the propensity of spontaneously arising bladder cancer and renal adenocarcinomas to metastasize to the lungs and liver, organs including the spleen, liver, kidneys, and lungs were meticulously excised and preserved in an 8% buffered formaldehyde (Merck, Darmstadt, Germany) solution, ensuring optimal tissue fixation pending microscopic examination upon experimentation culmination.

Complete excision of the primary tumor was pursued whenever feasible, with observations recorded regarding consistency, size, shape, as well as the presence of demarcations, necrosis, or inflammatory foci. In instances where complete removal proved unattainable, a substantial sample section, delineating the border between affected and unaffected tissues, was excised instead and likewise preserved in 8% buffered formaldehyde (Merck, Darmstadt, Germany) suspension.

The harvested organ and tumor specimens were meticulously cataloged within labeled containers, detailing the treatment group and the dissection date of each murine subject. Subsequently, these specimens underwent processing within the laboratory facilities of the Directorate of Veterinary Diagnostics, housed within the National Food Chain Safety Office. Organ cross-sections were meticulously prepared, labeled, and subjected to standard hematoxylin-eosin (Merck, Darmstadt, Germany) staining procedures. Following the requisite drying period, microscopic examination ensued, during which any manifestations of metastasis or secondary pathology within the organs were documented alongside the histological characteristics of the primary tumor.

3.9. Statistical analysis

The average survival time for each experimental group was depicted via a Kaplan-Meier survival analysis plot, with the statistical significance of the data points evaluated utilizing the Mantel-Cox (log-rank) test, employing a predetermined significance threshold of $p<0.05$. Additionally, to ascertain the statistical significance of average tumor sizes, comparisons were conducted between each treatment cohort and the PBS control group utilizing the Mann-Whitney test, or One-way ANOVA, F-test. All statistical analysis were made using GraphPad Prism version 10.0.0 for Windows (GraphPad Software, Boston, Massachusetts USA, www.graphpad.com).

3.10. Dosages and Course of Treatment

The selection of primary reagents employed as initial treatments was informed by a meticulous review of pertinent literature, supplemented by insights gleaned from experimental endeavors conducted within the Department of Microbiology and Infectious Diseases. Each substance was procured by the department from diverse suppliers or synthesized within the confines of the department's laboratory facilities. **Table 1** comprehensively delineates the parameters characterizing a series of three experiments, each involving a substantial cohort of murine subjects and encompassing details regarding administered treatments and dosages, murine data, and experimental methodologies. This table provides a comprehensive overview of the investigative framework.

Table 1: *The parameters of the series of experiments.*

Experiment No.	**First experiment**	**Second experiment**	**Third experiment**
Starting date	November 18, 2019	October 5, 2021	February 21, 2023
Ending date	November 9, 2020	November 2, 2021	April 30, 2023
Cell line used	MB49 - CVCL_7076 (Bladder tumor)	Renca CRL-2947 (Renal tumor)	Renca CRL-2947 (Renal tumor)
Number of cells implanted per mouse	$1*10^7$	$3*10^5$	$3*10^5$
Site of implantation	subcutaneously, the left musculus biceps femoris	subcutaneously, the right musculus biceps femoris	subcutaneously, the right musculus biceps femoris
Mouse strain	C57BL6/N, female	BALB/c, female	BALB/c, female

Number of mice utilized	30	30	72 (60 for primary investigation + 12 for pre-experiment cytokine level assessment)
Number of treated mice / group	10	10	10
Number of different treatments	2	2	5
Number of control mice	10	10	10
Treatment group I.	CpG + anti-OX40	CpG + anti-OX40	CpG + anti-OX40
Dosage (per occasion per mouse)	50 µg CpG + 5 µg anti-OX40	50 µg CpG + 5 µg anti-OX40	50 µg CpG + 5 µg anti-OX40
Number of treatments	3	3	3
Treatment days (after tumor implantation)	11, 14, 17	14, 17, 20	10, 14, 17
Treatment group II.	LPS + anti-OX40	CpG + 3p-hpRNA	CpG + 3p-hpRNA
Dosage (per occasion per mouse)	500 ng LPS + 5 µg anti-OX40	50 µg CpG + 3 µg 3p-hpRNA	50 µg CpG + 3 µg 3p-hpRNA
Number of treatments	3	3	3
Treatment days (after tumor implantation)	11, 14, 17	14, 17, 20	10, 14, 17
Treatment group III.	-	-	3p-hpRNA
Dosage (per occasion per mouse)	-	-	3 µg 3p-hpRNA
Number of treatments	-	-	3
Treatment days (after tumor implantation)	-	-	10, 14, 17
Treatment group IV.	-	-	IV-RNA + anti-OX40
Dosage (per occasion per mouse)	-	-	3,2 µg IV-RNA + 5 µg anti-OX40

Number of treatments	-	-	3
Treatment days (after tumor implantation)	-	-	10, 14, 17
Treatment group V.	-	-	PPV1-DNA + anti-OX40
Dosage (per occasion per mouse)	-	-	1,2 µg PPV1-DNA + 5 µg anti-OX40
Number of treatments	-	-	3
Treatment days (after tumor implantation)	-	-	10, 14, 17
Control group treatment	No treatment	No treatment	PBS
Dosage (per occasion per mouse)	-	-	-
Number of treatments	-	-	3
Treatment days (after tumor implantation)	-	-	10, 14, 17
Survival analysis	Yes	Yes	Yes
Primary tumor size analysis	Yes	Yes	Yes
Metastatic progression analysis (histology)	Yes	Yes	Yes
Cytokine level analysis	No	No	Yes
Statistical analysis	Statistical analyses of survival and primary tumor size changes were conducted.	No statistical analyses were conducted.	Statistical analyses of survival and primary tumor size changes were conducted.

4. Results

4.1. First experiment – MB49

The foundation of antitumor immunotherapy lies in the stimulation of the immune system. In this study, we employed two Pathogen-Associated Molecular Patterns (PAMPs): unmethylated CpG oligonucleotide, a ligand of Toll-like receptor 9 (TLR9), and lipopolysaccharide (LPS), acknowledged by TLR4. These were conjoined with an agonistic monoclonal antibody specific to the OX40 receptor (anti-OX40), expressed not only by activated regulatory T cells but also by other activated T cell subsets.

Based on prior investigations into the combination of anti-OX40 and CpG, favorable outcomes have been observed across various malignancies (Sagiv-Barfi et al., 2018). Building upon this foundation, we postulated that administering an agonistic anti-OX40 antibody alongside the TLR9 ligand, unmethylated CpG oligodeoxynucleotide, could evoke antitumor immune responses and eradicate established bladder tumors (MB49) as well as metastases. To assess this conjecture, we subcutaneously implanted mice with MB49 bladder tumors in the left thigh, allowing the tumors to establish until reaching an average diameter of 5-8 mm, subsequently administering the combination of anti-OX40 and CpG or LPS. Post-treatment, we monitored parameters including mouse survival, tumor growth, and regression alongside metastatic events.

4.1.1. Assessment of survival times

The experimental timeline spanned 120 days, equivalent to a decade-long observation period in human analog (The Mouse in Biomedical Research, Volume 3 – 2nd Edition). By day 60, all subjects in control and LPS + anti-OX40 cohorts had succumbed, contrasting with the survival of five individuals in the CpG + anti-OX40 group. Over the subsequent 60 days, two additional mice were either deceased or euthanized due to deteriorating health (both on day 79), exhibiting no discernible tumor lesions. Notably, three members of the CpG + anti-OX40 cohort endured until the experiment's conclusion. Noteworthy, the median survival for the CpG + anti-OX40 group (69.5 days) markedly exceeded that of the control cohort (28.5 days, $p < 0.0042$) and the LPS + anti-OX40 cohort (32 days, $p = 0.0018$). Conversely, no significant variance was discerned between the outcomes of the LPS + anti-OX40 and control groups (see **Figure 11**). Surviving mice from the CpG + anti-OX40 regimen underwent continued monitoring until reaching respective endpoints on days 142, 236, and 357.

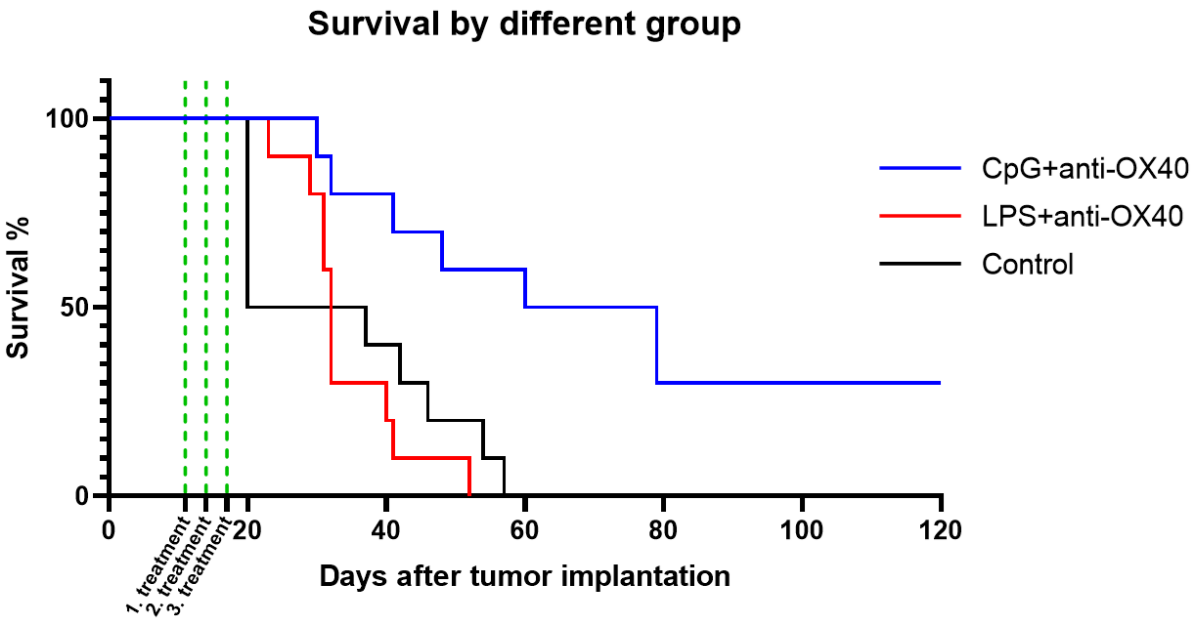

Figure 11: *The experimental timeline encapsulates tumor (MB49 – bladder) implantation, treatment regimens, and survival durations across the various study groups. Our analysis has revealed noteworthy disparities between the CpG + anti-OX40 treatment cohort and both the control and LPS + anti-OX40 treated cohorts. The experimental timeline was previously defined to be 120 days, which is equivalent to a ~ 10 year-long observation period in human analog.*

4.1.2. Primary tumor growth and appearance

Three days after the final treatment, tumor dimensions were assessed across all experimental cohorts and juxtaposed against their pre-treatment sizes (ranging from 5-8 mm). Evident therapeutic effects of the CpG + anti-OX40 intervention were observed, with a marked reduction in tumor size evident in 4 out of 10 subjects (20-50% reduction), complete eradication in 1 subject, and cessation of further tissue proliferation in 2 subjects. Conversely, both the LPS + anti-OX40 and control groups exhibited a significant escalation in mean tumor diameter (refer to **Table 2**). Notably, within the control group, 5 subjects necessitated euthanasia post-assessment due to surpassing a mean tumor diameter threshold of 20 mm.

In instances of tumor-associated mortalities, notable disparities were discerned across the various treatment groups concerning the morphology of primary tumors and the extent of metastatic spread. Among individual subjects within the CpG + anti-OX40 treated cohort where tumor progression persisted despite therapeutic intervention, primary tumors exhibited signs suggestive of early demarcation; nonetheless, two instances manifested local invasiveness. Conversely, within the control group, primary tumors predominantly exhibited a diffuse appearance, often accompanied by central necrosis, with incipient stroma formation observed in three cases. Within the LPS + anti-OX40 treated cohort, primary tumors universally exhibited

local invasiveness, with evidence of necrotic inflammation permeating the entire tumor microenvironment.

Table 2: *Mean tumor diameter (MTD) of primary tumors (measured in millimeters). Assessment was conducted three days post-administration of the final (3rd) treatment across all three groups, noting that the control group received no treatment. Remarkable discrepancies were evident among the three groups (determined via One-way ANOVA, F-test, $p < 0.0001$).*

Mice	Control	LPS + anti-OX40	CpG + anti-OX40
1	22.2 mm	24.8 mm	5.7 mm
2	20.1 mm	22.6 mm	7.2 mm
3	20.9 mm	19.8 mm	8.2 mm
4	13.6 mm	24.4 mm	6.4 mm
5	19.7 mm	16.0 mm	4.1 mm
6	20.2 mm	20.8 mm	0.0 mm
7	13.3 mm	20.1 mm	14.4 mm
8	19.2 mm	22.0 mm	3.8 mm
9	22.1 mm	21.5 mm	3.7 mm
10	21.8 mm	19.6 mm	10.6 mm

4.1.3. Metastatic events

In terms of lung metastases, the most favorable outcomes were observed following CpG + anti-OX40 treatment. Within this cohort, metastatic occurrences were identified in merely five cases (50%), of which three were macroscopically evident, while two were solely detectable via histopathological examination. Conversely, both the LPS + anti-OX40 treated, and control cohorts exhibited macroscopically detectable lung metastases in all twenty subjects (100%) (refer to **Table 3**). Notably, metastases in the LPS + anti-OX40 group displayed a more intricate appearance. Hepatic metastases were identified in two cases (20%) among mice receiving CpG + anti-OX40 treatment, accompanied by hepatomegaly observed in all dissected specimens, featuring an inflammatory backdrop in three instances. Conversely, the highest incidence of liver metastases was observed in the LPS + anti-OX40 treated cohort, occurring in six cases (60%), compared to four cases (40%) in the control group (refer to **Table 3**). Renal metastases were detected in one subject within the CpG + anti-OX40 cohort and in two individuals within the LPS + anti-OX40 group, with no instances noted in the control group (refer to **Table 3**). Notably, neither macroscopic nor histopathological evidence of tumor cell proliferation was observed in the spleen or brain (refer to **Table 3**). Regarding splenic observations, hyperplastic alterations, predominantly lymphoid in nature, were evident in

several cases across both treatment groups. These findings collectively underscore a reduced incidence of metastatic development in the CpG + anti-OX40 treated group relative to the LPS + anti-OX40 and control cohorts.

Table 3: *Histopathological findings revealed a consistent association between tumor-related mortalities and lung metastasis across all instances (n=25). Additionally, a smaller proportion of cases exhibited metastases in the liver (n=12) and kidneys (n=3) beyond the predominant pulmonary metastatic occurrences.*

Treatment	**Metastatic events**				
	Lung	**Liver**	**Kidney**	**Spleen**	**Brain**
CpG + anti-OX40	5	2	1	0	0
LPS + anti-OX40	10	6	2	0	0
Control	10	4	0	0	0

4.2. Second experiment – Renca I.

Building upon our previous findings (described in section *"4.1. First experiment – MB49"*), we posited that concurrent administration of the agonistic anti-OX40 antibody alongside the TLR9 ligand, unmethylated CpG, could elicit an antitumor immune response. Additionally, in conjunction with CpG, we explored the efficacy of a RIG-I ligand (3p-hpRNA), which holds the potential for activating immune responses suppressed by tumor cells through alternative pathways. Our objective encompassed the assessment of inhibiting tumor dissemination and reducing tumor size in the CRL-2947 model. Subcutaneous implantation of Renca CRL-2947 cells into the right thigh of mice facilitated tumor growth, culminating in an average MTD of 8-12 mm. Subsequent inoculation with the combination of CpG and anti-OX40 or 3p-hpRNA ensued. Following treatments, meticulous monitoring encompassed survival durations, tumor dissemination, and tumor dynamics, including growth and regression. Post-sacrifice, comprehensive autopsies were conducted on all subjects. Evaluation encompassed characterization of primary tumor morphology and histological examination of pertinent organs, including lungs, liver, and kidneys.

4.2.1. Assessment of survival times

The experiments were prematurely terminated 28 days following tumor implantation due to progressive tumor growth. Notably, by day 26 post-implantation, the majority of mice (28 out of 30) exhibited primary tumor sizes surpassing the predefined humane endpoint of 20 mm MTD, necessitating intervention. Subsequently, the remaining two mice (one each from the treated groups, respectively) were euthanized two days later. It is hypothesized that the

delayed initiation of treatments, commencing on the 14th day post-tumor implantation, contributed to the irreversible tumor progression. Consequently, any comparison of survival durations was deemed irrelevant in light of these circumstances.

4.2.2. Primary tumor growth and appearance

Primary tumor dimensions were assessed at baseline and six days subsequent to the final treatment across all three experimental cohorts. Notably, none of the administered treatments elicited any statistically significant effect on primary tumor growth. However, intriguing disparities emerged between treated and untreated groups concerning primary tumor morphology and metastatic progression. Notably, primary tumors in the CpG + anti-OX40 and CpG + 3p-hpRNA treated cohorts exhibited signs indicative of incipient demarcation. In stark contrast, primary tumors in the majority of control group subjects displayed a diffuse appearance accompanied by necrotic regions (refer to **Figure 12**).

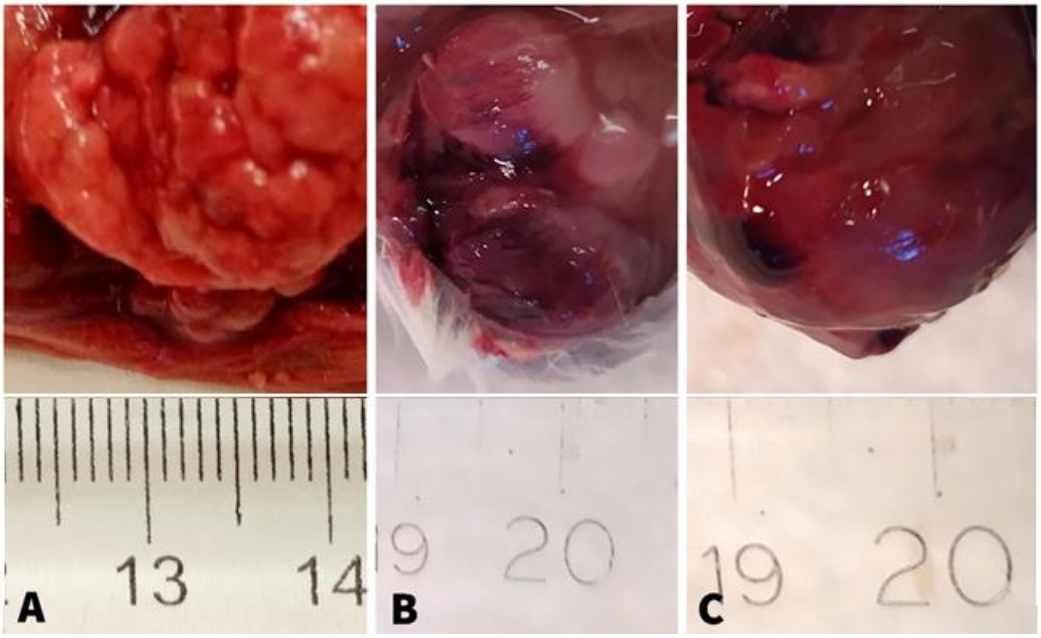

Figure 12: *Primary tumor (Renca – renal) morphology was scrutinized across distinct experimental groups, namely: A) untreated, B) CpG + anti-OX40, and C) CpG + 3p-hpRNA. Noteworthy distinctions emerged, with primary tumors in groups B) and C) manifesting early demarcation, while those in group A) predominantly exhibited a diffuse appearance accompanied by necrosis in the majority of cases.*

4.2.3. Metastatic events

As per existing literature, Renca cell lines traditionally induce metastatic formations exclusively following intravenous or subcapsular kidney injection (see chapter *"1.6.2. The Renca CRL-2947 cell line"*; Hrushesky and Murphy 1973; Salup and Wiltrout 1986; Salup et al., 1987; Chakrabarty et al., 1994; Oliver et al., 2019; Sobczuk et al., 2020; He et al., 2021). However, our investigations revealed metastatic occurrences subsequent to subcutaneous

injection as well. Histological evaluations were conducted across both treated and untreated (control) cohorts, scrutinizing for metastatic presence in the lungs, kidneys, and liver. Remarkably, metastases were exclusively detected in the lungs (refer to **Figure 13**). Specifically, within the control group, lung metastases were identified in 70% of subjects (7 out of 10 mice), while none were evident in any of the treated groups (refer to **Table 4**).

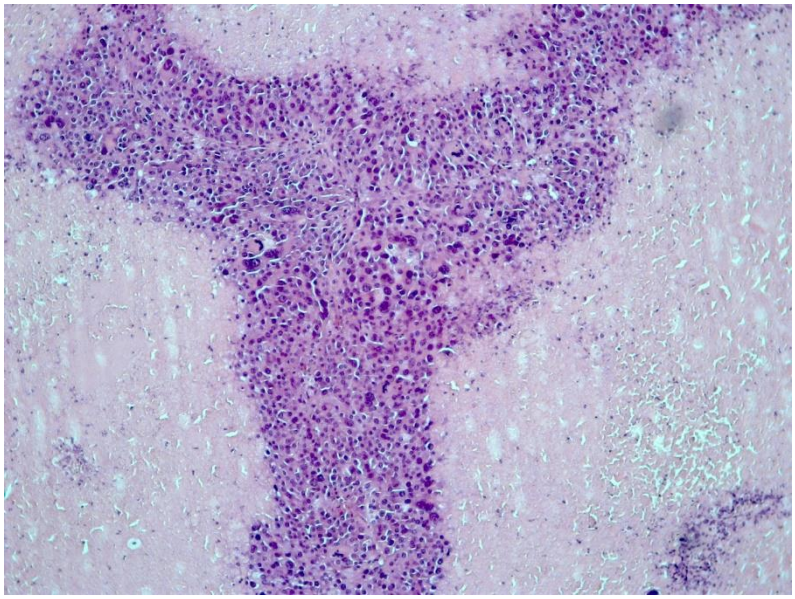

Figure 13: *Histological assessments were systematically undertaken in both experimental cohorts, aimed at discerning the presence of metastatic lesions within the pulmonary, renal, and hepatic tissues. Intriguingly, metastatic occurrences were solely confined to the pulmonary region, with a conspicuous predilection observed within the untreated group, indicative of Renca cell proclivity towards lung metastasis. Sections were meticulously stained utilizing hematoxylin-eosin for comprehensive histopathological evaluation.*

Table 4: *Histopathological outcomes pertaining to intratumoral treatments revealed a notable disparity. Within the control group, lung metastases were identified at a 70% incidence rate, starkly contrasting with the absence of such occurrences in any of the treated groups.*

Treatment	**Mice with metastases (%)**		
	Lung	**Liver**	**Kidney**
CpG + anti-OX40	0	0	0
CpG + 3p-hpRNA	0	0	0
Control	70	0	0

4.3. Third experiment – Renca II.

Upon evaluating the outcomes of our preceding experiment, it became apparent that a modified protocol was warranted. Accordingly, while the mouse strain (BALB/c) and tumor cell line (Renca CRL-2947) remained consistent with the previous iteration, significant alterations

were implemented in treatment regimens. In lieu of the two treatments employed previously (CpG + anti-OX40 and CpG + 3p-hpRNA), a repertoire of five treatment cocktails was introduced (CpG + anti-OX40, CpG + 3p-hpRNA, 3p-hpRNA alone, IV-RNA + anti-OX40, and PPV1-DNA + anti-OX40) – as delineated in **Table 1**. Furthermore, acknowledging the aggressive nature of the Renca CRL-2947 cell line, treatment initiation was expedited relative to the preceding experiment. Technical refinements were also introduced. Prior to embarking on experiments involving a larger cohort of mice, a preliminary study employing two mice per group was conducted. The objective was to assess cytokine levels discernible in untreated, tumor-bearing mice and tumor-free mice subjected to treatment, with a view toward prognosticating treatment efficacy. Cytokines scrutinized included IFN-γ, IL-6, and IL-10. Additionally, a procedural modification entailed the measurement of primary tumor dimensions not only once post-treatment but at four intervals (weekly). This approach facilitated an exploration of temporal dynamics in tumor size alterations alongside delineating the duration of treatment effects, if any. Relative to the preceding experiment employing the Renca CRL-2947 cell line, tangible and favorable outcomes were evidenced across all parameters scrutinized.

4.3.1. Assessment of survival times

Following the preliminary cytokine ELISA results, we commenced a larger-scale experiment comprising 10 mice per group. Any mortality incidents observed during daily surveillance were meticulously recorded on the respective day's chart. The inaugural mortality event occurred on day 21, involving two mice in the untreated PBS group. Subsequent mortalities were diligently documented until the conclusion of the experiment on day 39. The tabulated data are depicted in the Kaplan-Meier survival analysis graph below (**Figure 14**).

On day 38 post-implantation, the surviving mice in each treatment group were compared to the surviving mice in the control group using a Log-rank Mantel-Cox statistical analysis test ($p < 0.05$ threshold). At this juncture, only 20% of the mice from the untreated group remained alive. The survival rates for the various treated groups were as follows: CpG + anti-OX40: 70% (significantly higher than that of the untreated group, $p = 0.0103$), CpG + 3p-hpRNA: 50% (non-significant), 3p-hpRNA: 50% (significant, $p = 0.0467$), IV-RNA + anti-OX40: 60% (also significantly higher than that of the untreated group, $p = 0.0349$), and PPV1-DNA + anti-OX40: 40% (non-significant). Thus, we observed positive outcomes with three out of five treatments in terms of survival rates.

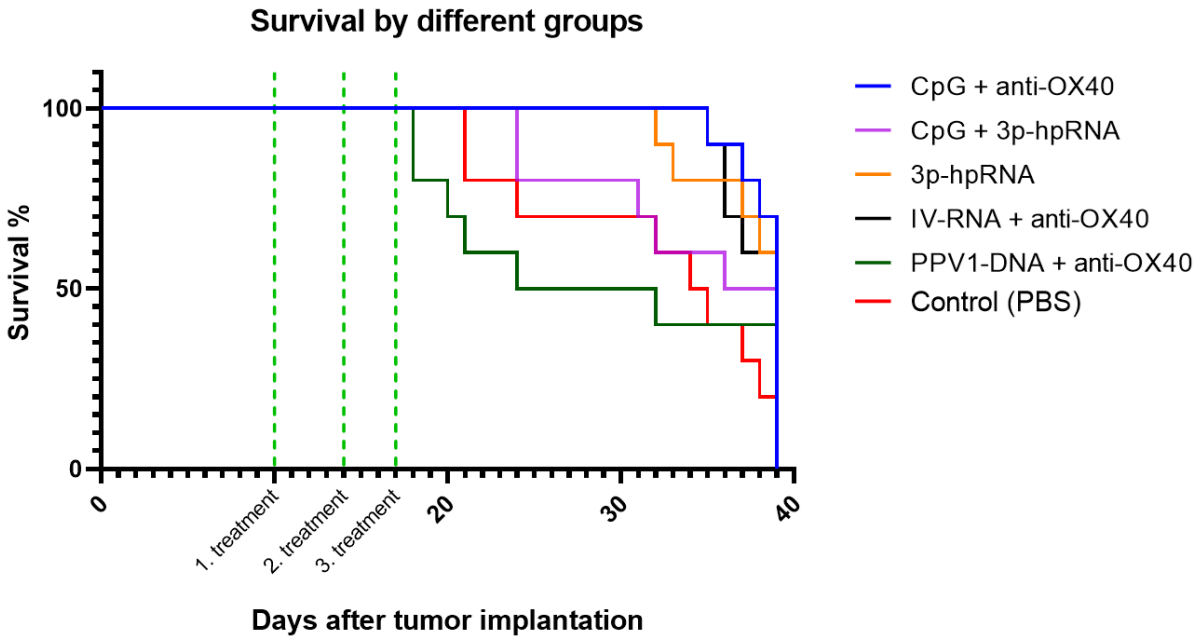

Figure 14: *The experimental timeline encapsulates tumor (Renca – renal) implantation, treatment regimens, and survival durations across the various study groups. Survival times of a total of 60 mice were monitored over a period of 39 days. The percentage of surviving mice is depicted as a function of days since tumor implantation. The CpG + anti-OX40 group is denoted in blue, the CpG + 3p-hpRNA group in orange, the 3p-hpRNA group in purple, the IV-RNA + anti-OX40 group in green, the PPV1-DNA + anti-OX40 group in brown, and the untreated PBS control group in red. Treatments are illustrated by cyan dashed lines administered on days 10, 14, and 17.*

In regard to survival times, both the CpG + anti-OX40, 3p-hpRNA, and IV-RNA + anti-OX40 groups exhibited significantly higher median survival durations compared to the untreated group.

4.3.2. Primary tumor growth and appearance

In addition to median survival time, we investigated the primary tumor growth rate as another variable. Tumor size measurements were conducted in all four groups on days 17, 24, 31, and 38 post-implantation to evaluate disparities between the treated and control group's primary tumors. The findings are illustrated in **Figure 15**, depicting tumor size over time. Each data point represents the median tumor size in the surviving mice within each group.

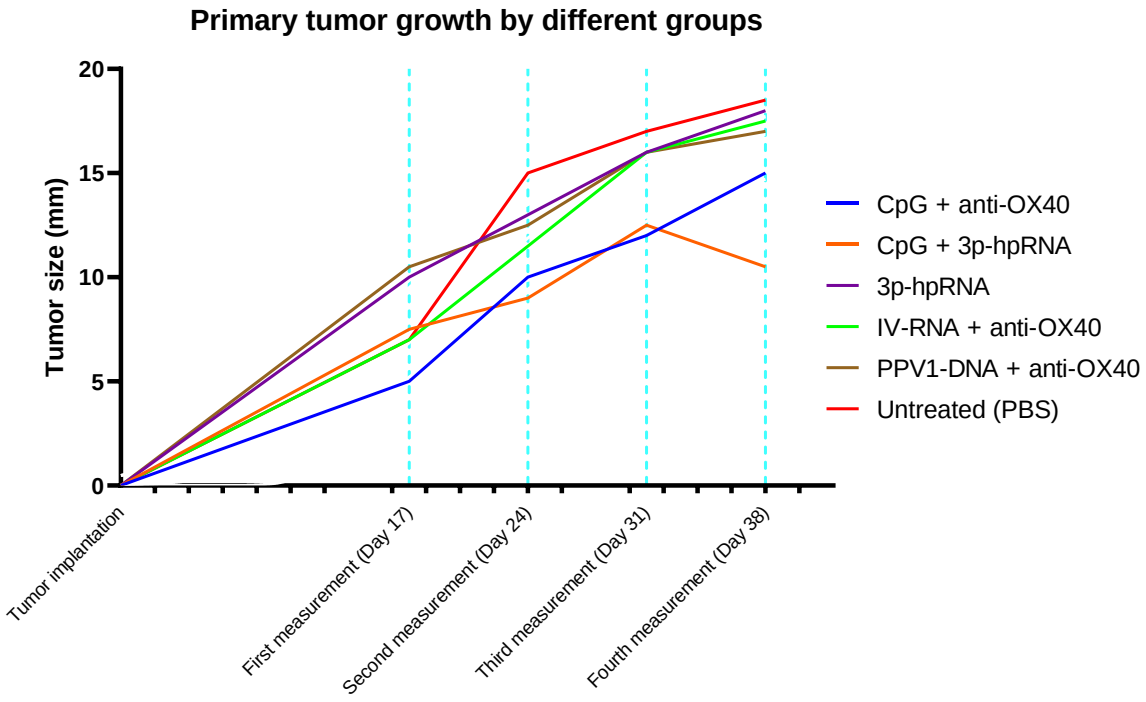

Figure 15: *Primary tumor (Renca – renal) growth is depicted as a function of size over time. The CpG + anti-OX40 group is represented in blue, the CpG + 3p-hpRNA group in orange, the 3p-hp-RNA group in purple, the IV-RNA + anti-OX40 group in green, the PPV1-DNA + anti-OX40 group in brown, and the untreated PBS control group in red. Dotted cyan lines indicate the days on which all tumors were measured, specifically on days 17, 24, 31, and 38.*

Statistical analysis of these values was conducted using a Mann-Whitney test ($p < 0.05$ threshold), comparing each treatment group to the untreated PBS control on each day of measurement. Day 17 showed variable results. The CpG + anti-OX40 ($p = 0.1232$), CpG + 3p-hpRNA ($p = 0.9020$), 3p-hpRNA ($p = 0.0572$), and IV-RNA + anti-OX40 ($p = 0.9587$) groups exhibited non-significant disparities in primary tumor sizes, whereas the PPV1-DNA + anti-OX40 ($p = 0.0014$) group displayed significantly larger tumor sizes compared to the untreated control group. However, by day 24, significant differences in tumor sizes emerged. The CpG + anti-OX40 group ($p = 0.0001$), CpG + 3p-hpRNA group ($p < 0.0001$), IV-RNA + anti-OX40 group ($p = 0.0002$), and notably the PPV1-DNA + anti-OX40 group ($p = 0.0146$) exhibited significantly smaller primary tumor sizes. The 3p-hpRNA group, however, generated a p-value of 0.1591, which was not statistically significant. Day 31 continued along a similar vein but not as positively. The CpG + anti-OX40 and CpG + 3p-hpRNA groups yielded p-values of 0.0007 and 0.0006 respectively. The 3p-hpRNA group continued to show non-significant differences in tumor size compared to the control, with a p-value of 0.8889. Additionally, the IV-RNA + anti-OX40 ($p = 0.1693$) and PPV1-DNA + anti-OX40 ($p = 0.1693$) groups exhibited non-significant differences in primary tumor sizes compared to the untreated control group. By day 38, the

sample sizes of each group needed to be higher to produce significant results. Analyses of the CpG + anti-OX40 (p = 0.0556), CpG + 3p-hpRNA (p = 0.1786), 3p-hpRNA (p = 0.6667), IV-RNA + anti-OX40 (p = 0.6000), and PPV1-DNA + anti-OX40 (p = 0.5238) groups revealed no significant differences in tumor sizes between any of the treatment groups when compared to the control.

In this context, it was observed that all treatments (excluding the 3p-hpRNA group) positively impacted primary tumor growth at least at one juncture. However, it is noteworthy that subsequent to the cessation of treatment effects, primary tumors initiated growth in treated mice as well.

Notable distinctions were observed between the treated and untreated cohorts in terms of primary tumor characteristics. Generally, treated groups exhibited demarcation surrounding primary tumors, whereas untreated mice displayed diffuse primary tumors accompanied by necrosis (**Figure 16**).

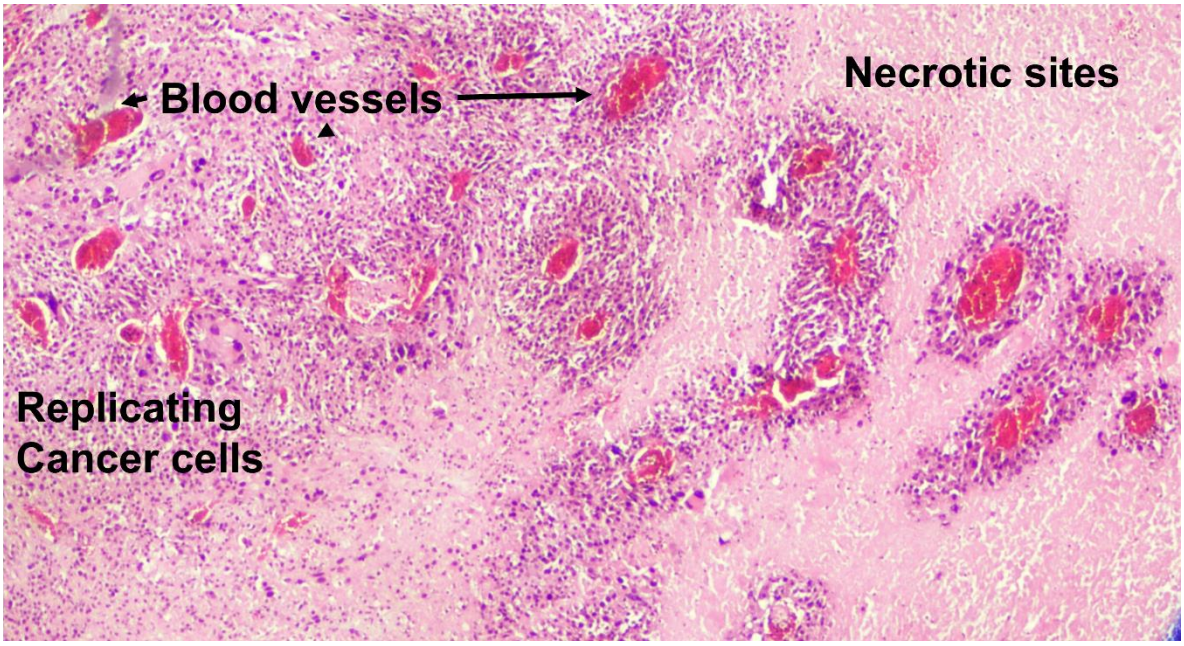

Figure 16: *A histological section depicting a primary tumor (Renca – renal) from an untreated mouse reveals abundant blood vessels, proliferating cancer cells, and areas of necrosis.*

4.3.3. Metastatic events

The ultimate variable assessed encompassed the overall incidence of metastasis across each group, encompassing the untreated (PBS) control. **Table 5** below details the organs impacted by metastasis in each group. Notably, the total number of mice in each group is slightly fewer than 10 due to occasional cannibalistic behavior leading to the loss of organ samples.

In certain instances, we encountered challenges in pinpointing specific metastatic sites, as the primary tumor appeared to disseminate within the abdominal cavity. Although these occurrences may not conform to the conventional definition of metastasis, they nonetheless signify an uncontrolled proliferation of tumor cells. Hence, we included such instances in the tally of the “Abdominal Cavity” column in **Table 5**, denoted by an asterisk (*). Furthermore, within the PPV1-DNA + anti-OX40 group, among the two cases listed in the “Abdominal Cavity” column, we identified ovarian metastasis in one case and pancreatic metastasis in the other, indicated by two asterisks (**).

Table 5: *Metastatic incidences across the investigated groups are delineated. Sites of metastasis are indicated within each column, with the aggregate count of metastatic occurrences in each group provided in the far-right column.*

Treatments	**Mice with metastases (%)**			
	Lung	**Kidney**	**Abdominal cavity***	**Total**
CpG + anti-OX40	25 (2/8)	0	0	**25 (2/8)**
CpG + 3p-hpRNA	11.1 (1/9)	0	22.2 (2/9)	**33.3 (3/9)**
IV-RNA + anti-OX40	12.5 (1/8)	0	0	**12.5 (1/8)**
3p-hpRNA	37.5 (3/8)	0	0	**37.5(3/8)**
PPV1-DNA + anti-OX40	37.5 (3/8)	0	25 (2/8)**	**62.5 (5/8)**
Untreated (PBS)	44.4 (4/9)	0	33.3 (3/9)	**77.7 (7/9)**

** Disseminated tumor cells detected within the abdominal cavity are included in the overall tally of metastatic events, notwithstanding their deviation from the conventional definition of metastasis.*

*** In one instance, ovarian metastasis was identified, while pancreatic metastasis was observed in the other.*

The incidence of metastasis varied among the treatment groups: CpG + anti-OX40, CpG + 3p-hpRNA, IV-RNA + anti-OX40, and 3p-hpRNA groups exhibited metastasis in 25%, 33%, 13%, and 38% of cases, respectively. Conversely, the untreated (PBS) group displayed metastasis in 78% of mice. Notably, the PPV1-DNA + anti-OX40 group demonstrated a reduced occurrence of metastases compared to the untreated group, albeit not when compared to the other treated groups. A histological illustration of lung metastasis is presented in **Figure 17**.

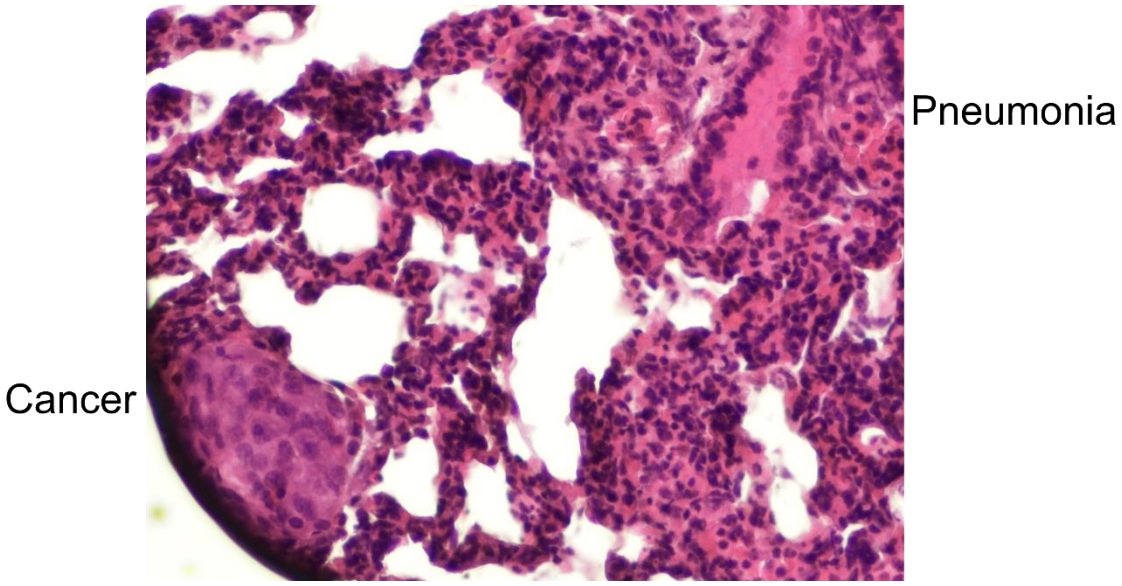

Figure 17: *A histological section of the lung from a mouse in the untreated group reveals the presence of pneumonia alongside lung metastases.*

5. Discussion

Bladder cancer (BC) and renal cell carcinoma (RCC) represent significant concerns within the domain of malignant neoplasms and associated mortalities. BC stands out as a prevalent malignancy within the urogenital sphere globally, holding the tenth position in incidence (Sung et al., 2021). The clinical-pathological classification underscores bladder urothelial carcinoma as the predominant histological subtype, encompassing 90-95% of BC cases, while the residual fraction is apportioned between bladder adenocarcinomas and squamous cell carcinomas (Kirkali et al., 2005). In men and women, kidney cancer accounts for approximately 5% and 3% of all malignancies, respectively. Notably, kidney cancer ranks as the sixth most prevalent cancer among men and the tenth among women (Miller et al., 2018). RCC overwhelmingly constitutes over 90% of all kidney cancers in humans (Hsieh et al., 2017), thereby accentuating its pivotal role within the realm of oncology.

In individuals afflicted with BC or RCC, the advent of metastases is a common occurrence. For RCC, approximately 30-50% of localized tumors transition into metastatic disease, and even post-surgical intervention, nearly 40% of patients with localized RCC manifest distant metastases (Pavlakis et al., 2004). This underscores the aggressive nature inherent in these malignancies and underscores the imperative necessity for the identification of innovative therapeutic modalities.

Accordingly, our experimental endeavors were conducted utilizing tumor cell lines that function as murine counterparts modeling BC and RCC. Within this context, the harnessing of the immune system's anticancer potential emerges as a promising avenue for exploration. Nonetheless, recent apprehensions have arisen concerning the utilization of immune checkpoint inhibitors in advanced human RCC (Pal et al., 2023). A multimodal strategy entailing the integration of a low-mass tyrosine kinase inhibitor alongside a monoclonal antibody targeting programmed cell death ligand was pursued. Noteworthy, both the tyrosine kinase inhibitor monotherapy and the combination regimen elicited adverse effects, with survival metrics exhibiting no discernible ameliorative trends.

However, our strategy towards Treg inhibition deviated via a distinctive methodology. Rather than opting for systemic suppression, we elected for intratumoral injections comprising agents possessing putative Treg antagonistic properties, specifically CpG + anti-OX40 and CpG + 3p-hpRNA, subsequently 3p-hpRNA alone, IV-RNA + anti-OX40, and PPV1-DNA + anti-OX40.

5.1. Investigation on the MB49 cell line

In our endeavor to explore novel avenues for cancer immunotherapy, we have leveraged a promising strategy, namely, *in situ* vaccination, utilizing the combination of CpG and anti-OX40 within the context of the MB49 murine bladder tumor cell line. Subsequently, we adopted this combination as the standard treatment regimen for all ensuing experiments.

Notably, Sagiv-Barfi et al., have demonstrated the efficacy of *in situ* vaccination across various malignancies, including lymphoma (A20), melanoma (B16–F10), colon (CT26), and breast cancer (4T1) cell lines (Sagiv-Barfi et al., 2018). However, to date, the application of this method in the context of bladder cancer remains unexplored within the scientific literature.

Our investigation reveals promising insights into the potential efficacy of *in situ* vaccination utilizing the aforementioned combination in the MB49 bladder cancer cell line within a murine model. Nevertheless, our findings exhibit a less robust response compared to those reported by Sagiv-Barfi et al., (Sagiv-Barfi et al., 2018), potentially attributable to variances in the immune milieu of the experimental animals, due to the random formation of groups among mice, as well as the aggressive type of tumor we used. Additionally, treatment duration, interval between treatments, and concurrent administration of CpG (or LPS) and anti-OX40 may have influenced treatment outcomes (Messenheimer et al., 2017). Overall, encouraging outcomes have been garnered in the context of mouse bladder carcinoma through the utilization of CpG and agonistic anti-OX40 treatment, thus furnishing a framework for subsequent investigations involving TLR agonists and antagonists. These agents possess the capability to orchestrate immune responses towards targeted cellular pathways. *In situ* vaccination presents a promising avenue for tumor therapy, boasting heightened specificity compared to conventional chemotherapeutic agents and offering a more economically viable alternative relative to other immunotherapeutic modalities.

Of particular note, our evaluation of the combination of anti-OX40 and the TLR4 ligand LPS did not demonstrate enhanced therapeutic efficacy, contrary to expectations. Instead, administration of LPS alongside anti-OX40 resulted in pathological changes reminiscent of those described by *Sato et al., in 1987* (Sato et al., 1987), characterized by hemorrhagic necrosis extending into adjacent healthy tissues, thereby potentially exacerbating tumor aggressiveness and metastatic propensity (Pidgeon et al., 1999; Harmey et al., 2002). Furthermore, the detrimental impact of endotoxin on survival outcomes suggests caution in its application. This phenomenon may be attributed to the utilization of an impure lipid-A derivative in our experimental paradigm or the phenomenon of rapidly developing LPS tolerance reported by previous authors, leading to the downregulation of anti-OX40 on regulatory T cells (Rockwell et al., 2010).

Consequently, we discontinued using LPS in our subsequent studies, emphasizing the importance of refining treatment protocols to reduce side effects and increase therapeutic efficacy. As we used an aggressive tumor cell line, this could easily explain the failure of LPS. In a less aggressive case, the increase in inflammation caused by LPS may result in the production of tumor-specific B cells. Therefore, it is easy to imagine that the treatment itself could be effective in such cases. The exact reason for our failure has not been resolved in this thesis, but we can explain it by regularities in immunology and plan to investigate this in the future.

5.2. Investigation on the Renca CRL-2947 cell line I.

In our subsequent experimental endeavor, in conjunction with the previously efficacious CpG + anti-OX40 treatment regimen, we explored an alternative combination aimed at activating the RIG-I pathway, hypothesized to evoke an antitumor response. Although these interventions did not yield tumor eradication or reduction in primary tumor size, notable observations pertaining to anticancer efficacy emerged.

Primarily, both experimental immunomodulatory cocktails elicited discernible alterations in the appearance and structural integrity of the primary tumors, characterized by evident signs of demarcation. In contrast, primary tumors in the control cohort exhibited diffuse morphology coupled with necrotic manifestations. Moreover, both experimental treatments demonstrated a remarkable antimetastatic effect, evidenced by the absence of metastatic lesions in mice treated with the intratumorally administered cocktails, in stark contrast to the 70% incidence of lung metastases observed in the control group.

These preliminary findings suggest that the intratumorally administered cocktails harbor promising antimetastatic potential, thereby laying a foundation for further investigative endeavors aimed at refining therapeutic modalities to convert ostensibly incurable malignancies into treatable entities. Subsequent investigations are warranted to validate the efficacy of these treatments in eradicating primary tumors. Successful validation could potentially facilitate post-treatment surgical excision to preempt recurrence, obviating the need for adjunctive therapeutic interventions such as chemotherapy. The implications of this inquiry are of paramount significance in the context of malignancies, given their proclivity for early metastatic dissemination, underscoring the critical imperative of early detection.

Furthermore, it is imperative to consider the impact of treatment on existing metastatic lesions. Our findings indicate the absence of detectable metastatic growths prior to intervention, suggesting a window of opportunity for localized intervention even in instances of established metastasis. An intriguing avenue for further exploration entails investigating

whether treatment directed at the primary tumor can localize metastatic foci and impede the emergence of new tumors, thereby augmenting therapeutic outcomes in advanced disease states.

5.3. Investigation on the Renca CRL-2947 cell line II.

Building upon the foundational insights gleaned from our initial Renca experiment, it became evident that while the employed treatments and Treg inhibition exerted discernible positive effects, optimization of treatment protocols was imperative to enhance therapeutic outcomes. Consequently, we embarked on a subsequent experimental endeavor characterized by an iterative approach aimed at refining treatment modalities.

In this follow-up investigation utilizing Renca cells, we explored a repertoire of novel treatment combinations, incorporating formulations containing proprietary compounds synthesized within our laboratory. Furthermore, we implemented modifications to experimental parameters to comprehensively assess treatment efficacy. Noteworthy adaptations included an augmented frequency of primary tumor measurements, increasing from a single assessment to four discrete evaluations throughout the experimental timeline. Additionally, we expanded our investigative scope to encompass the analysis of cytokine profiles, specifically interrogating levels of key mediators, such as IFN-γ, IL-6, and IL-10, within the milieu of tumor-bearing mice and treated cohorts devoid of tumor burden. To substantiate the anticipated efficacy of our selected treatment combinations, we conducted a preliminary experiment employing two mice per group to evaluate the impact of implanted tumors and diverse treatments on various cytokine levels. Although drawing definitive conclusions from the preliminary experiment with a small sample size is not feasible, the results are noteworthy. Differences in cytokine concentrations were observed between the control group and the treated animals, underscoring the significance of these findings. The cytokines examined included IFN-γ, pivotal for innate and adaptive immunity against viral infections and anticancer responses; IL-6, implicated in inflammation, immune response modulation, and hematopoiesis; and IL-10, renowned for its potent anti-inflammatory properties and central role in regulating the host immune response. The results obtained from the preliminary experiment were included in the “Appendices” of the doctoral dissertation.

By integrating these refinements, we aimed to elucidate nuanced insights into the interplay between treatment interventions and immune responses, thereby facilitating the optimization of therapeutic strategies for Renca-induced malignancies. These iterative efforts underscore our commitment to advancing the frontier of cancer therapeutics through rigorous scientific inquiry and methodological refinement.

Following the culmination of our latest experimental iteration, we have arrived at a pivotal juncture where the therapeutic interventions under scrutiny exhibit considerable promise. Notably, discernible and sustained treatment effects have been observed, underscored by tangible outcomes, including prolonged survival of murine subjects, reduction in primary tumor dimensions, and attenuation of metastatic dissemination.

In the context of the CpG + anti-OX40 treatment regimen, our expectations were to see an augmented median survival time in comparison to the untreated group, based on previous evidence with similar variables (Sagiv Barfi et al., 2018; Sagiv-Barfi et al., 2018; Zhou et al., 2021; Hong et al., 2022; Pieper et al., 2023; Proskurina et al., 2023). Concurrently, the exploration of the CpG + 3p-hpRNA treatment paradigm sought to delineate the combined stimulatory effects of these agents, with a particular emphasis on assessing whether a commensurate immune-activating response could be elicited upon substitution of anti-OX40. Furthermore, an independent examination of the RIG-I ligand 3p-hpRNA aimed to elucidate its precise immunomodulatory effects, given its relatively understudied status compared to its counterparts. In essence, our investigative thrust revolved around deciphering whether 3p-hpRNA could engender immune pathway activation akin to CpG, notwithstanding the distinct provenance of their respective receptors within the broader family of PRRs.

Additionally, the administration of purified IV-RNA and PPV1-DNA, both synthesized within our laboratory, in conjunction with anti-OX40, was predicated on the hypothesis that these formulations, akin to 3p-hpRNA, might elicit antitumor responses through RIG-I pathway activation. The envisaged outcome encompassed a scenario where the median survival times across all experimental cohorts would, ideally, surpass those of the untreated control group.

While the anticipated outcome was realized within the CpG + anti-OX40, 3p-hpRNA, and IV-RNA + anti-OX40 treatment cohorts, notable deviations were evident in the remaining treatment groups relative to the untreated control, where discernible disparities in median survival times were absent. These findings underscore the intricacies inherent in therapeutic responses within the realm of cancer immunotherapy, emphasizing the dynamic and multifaceted nature of treatment outcomes. Consequently, there exists an imperative for ongoing iterative refinement of therapeutic strategies to maximize efficacy and optimize clinical outcomes.

Given the absence of neoplastic cell interference in treated mice, cytokine assessment entailed baseline evaluation, thereby precluding confounding influences. Detection of augmented levels of pro-inflammatory cytokines in these ostensibly healthy subjects would corroborate the activation of targeted immunostimulatory pathways, substantiating the therapeutic efficacy of our interventions.

The observation of statistical significance in tumor sizes midway through the experimental timeline suggests a potential efficacy of the administered treatment agents in mitigating tumor growth rates. However, caution must be exercised in drawing definitive conclusions due to the limitation imposed by the modest sample size at the 38-day mark.

Furthermore, the observed trends pertaining to metastatic occurrence align with our a priori expectations. It is well-documented that Renca CRL-2947 tumors typically do not manifest early metastatic dissemination; however, once the primary tumor attains a critical, life-threatening size, metastasis becomes an inevitable consequence. Notably, the treatment modalities not only exerted a mitigating effect on tumor growth but also demonstrated efficacy in curtailing metastatic spread. Morphologically, treated tumors exhibited early demarcation, indicative of reactivation of cytotoxic CD8+ T cells and other immune effectors, thereby engendering discernible delineation between tumor and adjacent tissue. Conversely, untreated tumors evinced rapid necrotic progression devoid of well-defined boundaries.

Although complete eradication of metastatic dissemination was not achieved, the significant reduction in its incidence heralds a promising therapeutic outcome. Remarkably, across metrics encompassing primary tumor dimensions and metastatic occurrence, all treatment regimens conferred discernible beneficial effects relative to the untreated control group at various junctures throughout the experimental trajectory.

Despite the promising outcomes observed post-treatment, a discernible decline in the animals' quality of life necessitated the premature termination of the experiment on day 39 post-implantation. Addressing this challenge, we propose several potential avenues for refinement. Firstly, augmenting the number or frequency of treatments could offer a pragmatic approach to enhancing therapeutic efficacy while mitigating adverse effects. Alternatively, employing a slow-absorption carrier during vaccine administration may serve to alleviate the need for frequent treatment administrations, thereby alleviating treatment-associated complications.

Nevertheless, in light of our findings, we contend that these treatment modalities serve as a robust foundation for future exploration in the realm of immunotherapeutic investigations. To the best of our knowledge, as of July 2024, no studies have delved into the combined effects of RIG-I ligands and anti-OX40 as co-stimulants. Furthermore, optimization of treatment concentrations and frequencies holds promise for yielding even more pronounced therapeutic outcomes, contingent upon rigorous assessment of cytotoxicity levels prior to translational endeavors in human or animal trials. The identification of optimal treatment combinations has the potential to address challenges related to both primary and acquired resistance, as well as metastatic progression, particularly when integrated with existing oncotherapeutic modalities.

The exploration of these variables represents a compelling frontier in cancer research, with the potential to yield transformative insights and therapeutic strategies. Thus, continued investigation into these avenues holds immense promise for driving innovation and advancement in the field of oncology.

Table 6 serves as a comprehensive summary of the attained results and a critical evaluation of the treatments employed, delineating both the favorable and unfavorable outcomes stemming from our interventions.

Table 6: *Meticulous evaluation of antitumor interventions deployed across a series of three trials. Drawing upon the outcomes garnered from investigations conducted on the MB49 (a) and Renca CRL-2947 (b) cell lines, key metrics encompassing survival durations, tumor dimensions and the incidence of metastatic dissemination.*

a) MB49 cell line

Treatments	**Findings Across Various Dimensions**		
	Survival time	**Tumor size**	**Metastases**
CpG + anti-OX40	**+**	**+**	**+**
LPS + anti-OX40	-	-	-

b) Renca CRL-2947 cell line

Treatments	**Findings Across Various Dimensions**		
	Survival time	**Tumor size**	**Metastases**
CpG + anti-OX40	**+**	**+**	**+**
CpG + 3p-hpRNA	**-**	**+**	**+**
3p-hpRNA	**+**	**-**	**+**
IV-RNA + anti-OX40	**+**	**+**	**+**
PPV1 + anti-OX40	**-**	**+**	**-**

+: *We successfully elicited an antitumor response with the treatment.*

-: *We were unable to elicit an antitumor response with the treatment.*

5.4. Conclusions

Our investigations have yielded promising outcomes in mouse bladder carcinoma and mouse renal carcinoma, leveraging a repertoire of treatments including CpG + anti-OX40, CpG

+ 3p-hpRNA, 3p-hpRNA, IV-RNA + anti-OX40, and PPV1 + anti-OX40. These findings lay a foundation for future exploration involving TLR and RLR agonists and antagonists, which hold the potential to modulate immune responses along cellular pathways.

Collectively, the series of three experiments conducted herein have yielded a multitude of favorable outcomes, thereby establishing a robust framework for subsequent investigations. Building upon these results, we posit that *in situ* vaccination represents a promising avenue for anti-tumor immunotherapy across diverse malignancies, either as a standalone intervention or in synergy with conventional or targeted therapies. Nonetheless, refinement of our “in-house” treatment combinations, dosing regimens, treatment frequencies, and overall treatment protocols, as delineated in this study and supplemented by our conceptual innovations, is imperative to further enhance therapeutic efficacy and clinical translation.

6. Novel Scientific Findings

The findings elucidated within the series of experiments forming the focal point of this doctoral thesis represent a wealth of novel and invaluable insights in the domain of immuno-oncology.

1. It was the first case to combine anti-OX40 and CpG (TLR-9 ligand) treatment in two *in vivo* murine models: 1) bladder carcinoma derived from MB49 cell line and 2) renal adenocarcinoma derived from the Renca CRL-2947 cell line. In both cases, significant improvements were observed: primary tumor sizes were significantly reduced, survival times were significantly extended, early signs of demarcation were observed, and the incidence of metastasis showed a decreasing trend.
2. Unlike other studies, we obtained negative results with the combination of anti-OX40 treatment and LPS (TLR-4 ligand). The treatments did not yield favorable outcomes in the mouse bladder cancer model, with no significant changes observed in tumor size, demarcation, metastasis incidence, or survival times.
3. This was the first case where 3p-hpRNA (RIG-I agonist) treatment alone and in combination with CpG was investigated in a mouse tumor tissue (renal adenocarcinoma model). Both treatments yielded positive results similar to those observed with the anti-OX40 and CpG treatment, including reductions in primary tumor size and early signs of demarcation (tending), decreased incidence of metastasis (tending), and significantly extended survival times.
4. For the first time, we examined nucleic acids (RNA from PR8 mouse-adapted influenza virus strain and DNA from porcine parvovirus type 1 isolated by the Immunology Research Group) combined with anti-OX40 for treating a mouse renal adenocarcinoma model. Both treatments resulted in a significant reduction in primary tumor size, observable early demarcation, a trend towards decreased metastasis incidence, and extended survival times (significant for RNA, trending for DNA).

7. Reference List

Alfred Witjes J, Lebret T, Compérat EM, Cowan NC, De Santis M, Bruins HM, Hernández V, Espinós EL, Dunn J, Rouanne M, et al., 2017. Updated 2016 EAU Guidelines on Muscle-invasive and Metastatic Bladder Cancer Eur Urol. 71(3):462–475. doi:10.1016/j.eururo.2016.06.020.

Alves Costa Silva C, Facchinetti F, Routy B, Derosa L. 2020. New pathways in immune stimulation: targeting OX40. ESMO Open. 5(1):e000573. doi:10.1136/esmoopen-2019-000573.

Anfinsen KP, Grotmol T, Bruland OS, Jonasdottir TJ. 2011. Breed-specific incidence rates of canine primary bone tumors — A population based survey of dogs in Norway. Can J Vet Res. 75(3):209–215.

Anwar MA, Shah M, Kim J, Choi S. 2019. Recent clinical trends in Toll-like receptor targeting therapeutics. Med Res Rev. 39(3):1053–1090. doi:10.1002/med.21553.

Aspeslagh S, Postel-Vinay S, Rusakiewicz S, Soria J-C, Zitvogel L, Marabelle A. 2016. Rationale for anti-OX40 cancer immunotherapy. Eur J Cancer. 52:50–66. doi:10.1016/j.ejca.2015.08.021.

Astell CR, Chow MB, Ward DC. 1985. Sequence analysis of the termini of virion and replicative forms of minute virus of mice DNA suggests a modified rolling hairpin model for autonomous parvovirus DNA replication. Journal of Virology. 54(1):171–177. doi:10.1128/jvi.54.1.171-177.1985.

Basu A, Ramamoorthi G, Albert G, Gallen C, Beyer A, Snyder C, Koski G, Disis ML, Czerniecki BJ, Kodumudi K. 2021. Differentiation and Regulation of TH Cells: A Balancing Act for Cancer Immunotherapy. Front Immunol. 12:669474. doi:10.3389/fimmu.2021.669474.

Batlle E, Massagué J. 2019. Transforming Growth Factor-β Signaling in Immunity and Cancer. Immunity. 50(4):924–940. doi:10.1016/j.immuni.2019.03.024.

Baum A, Sachidanandam R, García-Sastre A. 2010. Preference of RIG-I for short viral RNA molecules in infected cells revealed by next-generation sequencing. Proceedings of the National Academy of Sciences. 107(37):16303–16308. doi:10.1073/pnas.1005077107.

Baxevanis CN, Perez SA, Papamichail M. 2009. Cancer immunotherapy. Crit Rev Clin Lab Sci. 46(4):167–189. doi:10.1080/10408360902937809.

Bayraktar R, Bertilaccio MTS, Calin GA. 2019. The Interaction Between Two Worlds: MicroRNAs and Toll-Like Receptors. Front Immunol. 10:1053. doi:10.3389/fimmu.2019.01053.

Beauvais W, Cardwell JM, Brodbelt DC. 2012. The effect of neutering on the risk of mammary tumours in dogs – a systematic review. Journal of Small Animal Practice. 53(6):314–322. doi:10.1111/j.1748-5827.2011.01220.x.

Bell D, Young JW, Banchereau J. 1999. Dendritic cells. Adv Immunol. 72:255–324. doi:10.1016/s0065-2776(08)60023-1.

Bergeron J, Hébert B, Tijssen P. 1996. Genome organization of the Kresse strain of porcine parvovirus: identification of the allotropic determinant and comparison with those of NADL-2 and field isolates. Journal of Virology. 70(4):2508–2515. doi:10.1128/jvi.70.4.2508-2515.1996.

Berke IC, Modis Y. 2012. MDA5 cooperatively forms dimers and ATP-sensitive filaments upon binding double-stranded RNA. The EMBO Journal. 31(7):1714–1726. doi:10.1038/emboj.2012.19.

Bhat MY, Solanki HS, Advani J, Khan AA, Keshava Prasad TS, Gowda H, Thiyagarajan S, Chatterjee A. 2018. Comprehensive network map of interferon gamma signaling. J Cell Commun Signal. 12(4):745–751. doi:10.1007/s12079-018-0486-y.

Bloom AC, Bender LH, Tiwary S, Pasquet L, Clark K, Jiang T, Xia Z, Morales-Kastresana A, Jones JC, Walters I, et al., 2019. Intratumorally delivered formulation, INT230-6, containing potent anticancer agents induces protective T cell immunity and memory. Oncoimmunology. 8(10):e1625687. doi:10.1080/2162402X.2019.1625687.

Borg N. 2019. RIG-I like receptors. [[WikiJournal of Science| WikiJournal of Science]]. 2(1):1. doi:10.15347/WJS/2019.001.

Boudreau JE, Bonehill A, Thielemans K, Wan Y. 2011. Engineering dendritic cells to enhance cancer immunotherapy. Mol Ther. 19(5):841–853. doi:10.1038/mt.2011.57.

Bourgeois C, Rocha B, Tanchot C. 2002. A Role for CD40 Expression on CD8+ T Cells in the Generation of CD8+ T Cell Memory. Science. 297(5589):2060–2063. doi:10.1126/science.1072615.

van Broekhoven CL, Parish CR, Demangel C, Britton WJ, Altin JG. 2004. Targeting dendritic cells with antigen-containing liposomes: a highly effective procedure for induction of antitumor immunity and for tumor immunotherapy. Cancer Res. 64(12):4357–4365. doi:10.1158/0008-5472.CAN-04-0138.

Bromberek JL, Rout ED, Agnew MR, Yoshimoto J, Morley PS, Avery AC. 2016. Breed Distribution and Clinical Characteristics of B Cell Chronic Lymphocytic Leukemia in Dogs. J Vet Intern Med. 30(1):215–222. doi:10.1111/jvim.13814.

Caux C, Dezutter-Dambuyant C, Schmitt D, Banchereau J. 1992. GM-CSF and TNF-α cooperate in the generation of dendritic Langerhans cells. Nature. 360(6401):258–261. doi:10.1038/360258a0.

Caux C, Massacrier C, Vanbervliet B, Dubois B, Durand I, Cella M, Lanzavecchia A, Banchereau J. 1997. CD34+ Hematopoietic Progenitors From Human Cord Blood Differentiate Along Two Independent Dendritic Cell Pathways in Response to Granulocyte-Macrophage Colony-Stimulating Factor Plus Tumor Necrosis Factor α: II. Functional Analysis. Blood. 90(4):1458–1470. doi:10.1182/blood.V90.4.1458.

Cavalier-Smith T. 1974. Palindromic base sequences and replication of eukaryote chromosome ends. Nature. 250(5466):467–470. doi:10.1038/250467a0.

Chakrabarty A, Hillman GG, Maughan RL, Visscher DW, Ali E, Pontes JE, Haas GP. 1994. Influence of tumor site on the therapy of murine kidney cancer. Anticancer Res. 14(2A):373–378.

Chang ZL. 2010. Important aspects of Toll-like receptors, ligands and their signaling pathways. Inflamm Res. 59(10):791–808. doi:10.1007/s00011-010-0208-2.

Charles A Janeway J, Travers P, Walport M, Shlomchik MJ. 2001. The production of armed effector T cells. In: Immunobiology: The Immune System in Health and Disease. 5th edition. Garland Science. [accessed 2024 May 2]. https://www.ncbi.nlm.nih.gov/books/NBK27118/.

Chen X, Cheng F, Liu Y, Zhang L, Song L, Cai X, You T, Fan X, Wang D, Gong A, et al., 2019. Toll-like receptor 2 and Toll-like receptor 4 exhibit distinct regulation of cancer cell stemness mediated by cell death-induced high-mobility group box 1. EBioMedicine. 40:135–150. doi:10.1016/j.ebiom.2018.12.016.

Chiang C, Beljanski V, Yin K, Olagnier D, Ben Yebdri F, Steel C, Goulet M-L, DeFilippis VR, Streblow DN, Haddad EK, et al., 2015. Sequence-Specific Modifications Enhance the Broad-Spectrum Antiviral Response Activated by RIG-I Agonists. J Virol. 89(15):8011–8025. doi:10.1128/JVI.00845-15.

Chondronasiou D, Gill D, Mosteiro L, Urdinguio RG, Berenguer-Llergo A, Aguilera M, Durand S, Aprahamian F, Nirmalathasan N, Abad M, et al., 2022. Multi-omic rejuvenation of naturally aged tissues by a single cycle of transient reprogramming. Aging Cell. 21(3):e13578. doi:10.1111/acel.13578.

Choy E, Rose-John S. 2017. Interleukin-6 as a Multifunctional Regulator: Inflammation, Immune Response, and Fibrosis. Journal of Scleroderma and Related Disorders. 2(2_suppl):S1–S5. doi:10.5301/jsrd.5000265.

Chun R, Garrett LD, Henry C, Wall M, Smith A, Azene NM. 2005. Toxicity and efficacy of cisplatin and doxorubicin combination chemotherapy for the treatment of canine osteosarcoma. J Am Anim Hosp Assoc. 41(6):382–387. doi:10.5326/0410382.

Coiffier B, Haioun C, Ketterer N, Engert A, Tilly H, Ma D, Johnson P, Lister A, Feuring-Buske M, Radford JA, et al., 1998. Rituximab (anti-CD20 monoclonal antibody) for the treatment of patients with relapsing or refractory aggressive lymphoma: a multicenter phase II study. Blood. 92(6):1927–1932.

Coiffier B, Lepage E, Briere J, Herbrecht R, Tilly H, Bouabdallah R, Morel P, Van Den Neste E, Salles G, Gaulard P, et al., 2002. CHOP chemotherapy plus rituximab compared with CHOP alone in elderly patients with diffuse large-B-cell lymphoma. N Engl J Med. 346(4):235–242. doi:10.1056/NEJMoa011795.

Constant SL, Bottomly K. 1997. INDUCTION OF TH1 AND TH2 CD4+ T CELL RESPONSES:The Alternative Approaches. Annual Review of Immunology. 15:297–322. doi:10.1146/annurev.immunol.15.1.297.

Cooley LS, Rudewicz J, Souleyreau W, Emanuelli A, Alvarez-Arenas A, Clarke K, Falciani F, Dufies M, Lambrechts D, Modave E, et al., 2021. Experimental and computational modeling for signature and biomarker discovery of renal cell carcinoma progression. Molecular Cancer. 20(1):136. doi:10.1186/s12943-021-01416-5.

Cotmore SF, Tattersall P. 1987. The Autonomously Replicating Parvoviruses of Vertebrates. In: Maramorosch K, Murphy FA, Shatkin AJ, editors. Advances in Virus Research. 33:91–174.

Davis MB, Vasquez-Dunddel D, Fu J, Albesiano E, Pardoll D, Kim YJ. 2011. Intratumoral administration of TLR4 agonist absorbed into a cellular vector improves antitumor responses. Clin Cancer Res. 17(12):3984–3992. doi:10.1158/1078-0432.CCR-10-3262.

DeNardo DG, Ruffell B. 2019. Macrophages as regulators of tumour immunity and immunotherapy. Nat Rev Immunol. 19(6):369–382. doi:10.1038/s41577-019-0127-6.

Deng J, Zhao S, Zhang X, Jia K, Wang H, Zhou C, He Y. 2019. OX40 (CD134) and OX40 ligand, important immune checkpoints in cancer. Onco Targets Ther. 12:7347–7353. doi:10.2147/OTT.S214211.

Dennis KL, Blatner NR, Gounari F, Khazaie K. 2013. Current status of interleukin-10 and regulatory T-cells in cancer. Current Opinion in Oncology. 25(6):637. doi:10.1097/CCO.0000000000000006.

Diebold SS, Kaisho T, Hemmi H, Akira S, Reis e Sousa C. 2004. Innate Antiviral Responses by Means of TLR7-Mediated Recognition of Single-Stranded RNA. Science. 303(5663):1529–1531. doi:10.1126/science.1093616.

Dow S, Elmslie R, Kurzman I, Macewen G, Pericle F, Liggitt D. 2005. Phase I Study of Liposome–DNA Complexes Encoding the Interleukin-2 Gene in Dogs with Osteosarcoma Lung Metastases. Human Gene Therapy. 16(8):937–946. doi:10.1089/hum.2005.16.937.

Dy GW, Gore JL, Forouzanfar MH, Naghavi M, Fitzmaurice C. 2017. Global Burden of Urologic Cancers, 1990-2013. Eur Urol. 71(3):437–446. doi:10.1016/j.eururo.2016.10.008.

Ebrahimi-Nik H, Corwin WL, Shcheglova T, Das Mohapatra A, Mandoiu II, Srivastava PK. 2018. CD11c+ MHCIIlo GM-CSF-bone marrow-derived dendritic cells act as antigen donor cells and as antigen presenting cells in neoepitope-elicited tumor immunity against a mouse fibrosarcoma. Cancer Immunol Immunother. 67(9):1449–1459. doi:10.1007/s00262-018-2202-4.

Emens LA, Middleton G. 2015. The interplay of immunotherapy and chemotherapy: harnessing potential synergies. Cancer Immunol Res. 3(5):436–443. doi:10.1158/2326-6066.CIR-15-0064.

Fabris VT, Lodillinsky C, Pampena MB, Belgorosky D, Lanari C, Eiján AM. 2012. Cytogenetic characterization of the murine bladder cancer model MB49 and the derived invasive line MB49-I. Cancer Genet. 205(4):168–176. doi:10.1016/j.cancergen.2012.02.002.

Fagerberg L, Hallström BM, Oksvold P, Kampf C, Djureinovic D, Odeberg J, Habuka M, Tahmasebpoor S, Danielsson A, Edlund K, Asplund A, Sjöstedt E, Lundberg E, Szigyarto CA, Skogs M, Takanen JO, Berling H, Tegel H, Mulder J, Nilsson P, Schwenk JM, Lindskog C, Danielsson F, Mardinoglu F., Sivertsson A, von Feilitzen K, Forsberg M, Zwahlen M, Olsson IM, Navani S, Huss M, Nielsen J, Ponten F, Uhlén, M. (2014). Analysis of the human tissue-specific expression by genome-wide integration of transcriptomics and antibody-based proteomics. Molecular & cellular proteomics : MCP, 13(2), 397–406. https://doi.org/10.1074/mcp.M113.035600

Farkona S, Diamandis EP, Blasutig IM. 2016. Cancer immunotherapy: the beginning of the end of cancer? BMC Med. 14:73. doi:10.1186/s12916-016-0623-5.

Fouad YA, Aanei C. 2017. Revisiting the hallmarks of cancer. Am J Cancer Res. 7(5):1016–1036.

Gardner HL, Fenger JM, London CA. 2016. Dogs as a Model for Cancer. Annu Rev Anim Biosci. 4:199–222. doi:10.1146/annurev-animal-022114-110911.

Geering B, Fussenegger M. 2015. Synthetic immunology: modulating the human immune system. Trends Biotechnol. 33(2):65–79. doi:10.1016/j.tibtech.2014.10.006.

Gong J, Chehrazi-Raffle A, Reddi S, Salgia R. 2018. Development of PD-1 and PD-L1 inhibitors as a form of cancer immunotherapy: a comprehensive review of registration trials and future considerations. J Immunother Cancer. 6(1):8. doi:10.1186/s40425-018-0316-z.

Gonzalez-Garza MT, Cruz-Vega DE, Maldonado-Bernal C. 2020. IL10 as Cancer Biomarker. In: Translational Research in Cancer. IntechOpen. [accessed 2024 May 2]. https://www.intechopen.com/chapters/70795.

Gorbet M-J, Ranjan A. 2020. Cancer immunotherapy with immunoadjuvants, nanoparticles, and checkpoint inhibitors: Recent progress and challenges in treatment and tracking response to immunotherapy. Pharmacol Ther. 207:107456. doi:10.1016/j.pharmthera.2019.107456.

Grüntzig K, Graf R, Boo G, Guscetti F, Hässig M, Axhausen KW, Fabrikant S, Welle M, Meier D, Folkers G, et al., 2016. Swiss Canine Cancer Registry 1955–2008: Occurrence of the Most Common Tumour Diagnoses and Influence of Age, Breed, Body Size, Sex and Neutering Status on Tumour Development. Journal of Comparative Pathology. 155(2):156–170. doi:10.1016/j.jcpa.2016.05.011.

Habjan M, Andersson I, Klingström J, Schümann M, Martin A, Zimmermann P, Wagner V, Pichlmair A, Schneider U, Mühlberger E, et al., 2008. Processing of Genome 5′ Termini as a Strategy of Negative-Strand RNA Viruses to Avoid RIG-I-Dependent Interferon Induction. PLOS ONE. 3(4):e2032. doi:10.1371/journal.pone.0002032.

Hammerich L, Bhardwaj N, Kohrt HE, Brody JD. 2016. In situ vaccination for the treatment of cancer. Immunotherapy. 8(3):315–330. doi:10.2217/imt.15.120.

Hammerich L, Binder A, Brody JD. 2015. In situ vaccination: Cancer immunotherapy both personalized and off-the-shelf. Molecular Oncology. 9(10):1966–1981. doi:10.1016/j.molonc.2015.10.016.

Hammerich L, Marron TU, Upadhyay R, Svensson-Arvelund J, Dhainaut M, Hussein S, Zhan Y, Ostrowski D, Yellin M, Marsh H, et al., 2019. Systemic clinical tumor regressions and potentiation of PD1 blockade with in situ vaccination. Nat Med. 25(5):814–824. doi:10.1038/s41591-019-0410-x.

Hanson ND, Rhode SL. 1991. Parvovirus NS1 stimulates P4 expression by interaction with the terminal repeats and through DNA amplification. Journal of Virology. 65(8):4325–4333. doi:10.1128/jvi.65.8.4325-4333.1991.

Hara T, Miyake H, Hinata N, Fujisawa M. 2019. Inhibition of Tumor Growth and Sensitization to Sunitinib by RNA Interference Targeting Programmed Death-ligand 1 in Mouse Renal Cell Carcinoma RenCa Model. Anticancer Research. 39(9):4737–4742. doi:10.21873/anticanres.13656.

Hargadon KM, Johnson CE, Williams CJ. 2018. Immune checkpoint blockade therapy for cancer: An overview of FDA-approved immune checkpoint inhibitors. Int Immunopharmacol. 62:29–39. doi:10.1016/j.intimp.2018.06.001.

Harmey J, Bucana C, Lu W, Anne-Marie B, Mcdonnell S, Lynch C, Bouchier-Hayes D, Dong Z. 2002. Harmey JH, Bucana CD, Lu W, Byrne AM, McDonnell S, Lynch C, Bouchier-Hayes D, Dong Z. 2002. Lipopolysaccharide-induced metastatic growth is associated with increased angiogenesis, vascular permeability and tumor cell invasion. Int J Cancer 101: 415-422. International journal of cancer Journal international du cancer. 101:415–22. doi:10.1002/ijc.10632.

He X, Zhou S, Dolan M, Shi Y, Wang J, Quinn B, Jahagirdar D, Huang W-C, Tsuji M, Pili R, et al., 2021. Immunization with short peptide particles reveals a functional CD8+ T-cell neoepitope in a murine renal carcinoma model. J Immunother Cancer. 9(12):e003101. doi:10.1136/jitc-2021-003101.

Hermant P, Michiels T. 2014. Interferon-λ in the Context of Viral Infections: Production, Response and Therapeutic Implications. Journal of Innate Immunity. 6(5):563–574. doi:10.1159/000360084.

Hernandez C, Huebener P, Schwabe RF. 2016. Damage-associated molecular patterns in cancer: a double-edged sword. Oncogene. 35(46):5931–5941. doi:10.1038/onc.2016.104.

Hodi FS, O'Day SJ, McDermott DF, Weber RW, Sosman JA, Haanen JB, Gonzalez R, Robert C, Schadendorf D, Hassel JC, et al., 2010. Improved survival with ipilimumab in patients with metastatic melanoma. N Engl J Med. 363(8):711–723. doi:10.1056/NEJMoa1003466.

Hoelzel, A R (ed.), Molecular Genetic Analysis of Populations: A Practical Approach (Oxford, 1998; online edn, Oxford Academic, 31 Oct. 2023), https://doi.org/10.1093/oso/9780199636341.001.0001, accessed 25 July 2024.

Hofacker IL, Stadler PF, Stocsits RR. 2004. Conserved RNA secondary structures in viral genomes: a survey. Bioinformatics. 20(10):1495–1499. doi:10.1093/bioinformatics/bth108.

Hong WX, Sagiv-Barfi I, Czerwinski DK, Sallets A, Levy R. 2022. Neoadjuvant Intratumoral Immunotherapy with TLR9 Activation and Anti-OX40 Antibody Eradicates Metastatic Cancer. Cancer Research. 82(7):1396–1408. doi:10.1158/0008-5472.CAN-21-1382.

Hornung V, Ellegast J, Kim S, Brzózka K, Jung A, Kato H, Poeck H, Akira S, Conzelmann K-K, Schlee M, et al., 2006. 5'-Triphosphate RNA Is the Ligand for RIG-I. Science. 314(5801):994–997. doi:10.1126/science.1132505.

Houot R, Levy R. 2009. T-cell modulation combined with intratumoral CpG cures lymphoma in a mouse model without the need for chemotherapy. Blood. 113(15):3546–3552. doi:10.1182/blood-2008-07-170274.

Hrushesky WJ, Murphy GP. 1973. Investigation of a new renal tumor model. J Surg Res. 15(5):327–336. doi:10.1016/0022-4804(73)90096-6.

Hsieh JJ, Purdue MP, Signoretti S, Swanton C, Albiges L, Schmidinger M, Heng DY, Larkin J, Ficarra V. 2017. Renal cell carcinoma. Nat Rev Dis Primers. 3:17009. doi:10.1038/nrdp.2017.9.

Hurwitz AA, Watkins SK. 2012. Immune suppression in the tumor microenvironment: a role for dendritic cell-mediated tolerization of T cells. Cancer Immunol Immunother. 61(2):289–293. doi:10.1007/s00262-011-1181-5.

Inaba K, Witmer-Pack M, Inaba M, Hathcock KS, Sakuta H, Azuma M, Yagita H, Okumura K, Linsley PS, Ikehara S, et al., 1994. The tissue distribution of the B7-2 costimulator in mice: abundant expression on dendritic cells in situ and during maturation in vitro. J Exp Med. 180(5):1849–1860. doi:10.1084/jem.180.5.1849.

Itoh H, Horiuchi Y, Nagasaki T, Sakonju I, Kakuta T, Fukushima U, Uchide T, Yamashita M, Kuwabara M, Yusa S-I, et al., 2009. Evaluation of immunological status in tumor-bearing dogs. Vet Immunol Immunopathol. 132(2–4):85–90. doi:10.1016/j.vetimm.2009.04.020.

Iwasaki A, Medzhitov R. 2004. Toll-like receptor control of the adaptive immune responses. Nat Immunol. 5(10):987–995. doi:10.1038/ni1112.

Jacquelot N, Roberti MP, Enot DP, Rusakiewicz S, Ternès N, Jegou S, Woods DM, Sodré AL, Hansen M, Meirow Y, et al., 2017. Predictors of responses to immune checkpoint blockade in advanced melanoma. Nat Commun. 8(1):592. doi:10.1038/s41467-017-00608-2.

Janssen EM, Lemmens EE, Wolfe T, Christen U, von Herrath MG, Schoenberger SP. 2003. CD4+ T cells are required for secondary expansion and memory in CD8+ T lymphocytes. Nature. 421(6925):852–856. doi:10.1038/nature01441.

Jensen SM, Maston LD, Gough MJ, Ruby CE, Redmond WL, Crittenden M, Li Y, Puri S, Poehlein CH, Morris N, et al., 2010. Signaling Through OX40 Enhances Antitumor Immunity. Seminars in Oncology. 37(5):524–532. doi:10.1053/j.seminoncol.2010.09.013.

Jiang T, Shi T, Zhang H, Hu J, Song Y, Wei J, Ren S, Zhou C. 2019. Tumor neoantigens: from basic research to clinical applications. Journal of Hematology & Oncology. 12(1):93. doi:10.1186/s13045-019-0787-5.

Kaczanowska S, Joseph AM, Davila E. 2013. TLR agonists: our best frenemy in cancer immunotherapy. J Leukoc Biol. 93(6):847–863. doi:10.1189/jlb.1012501.

Kaiser J, Couzin-Frankel J. 2018. Cancer immunotherapy sweeps Nobel for medicine. Science. 362(6410):13. doi:10.1126/science.362.6410.13.

Kanzler H, Barrat FJ, Hessel EM, Coffman RL. 2007. Therapeutic targeting of innate immunity with Toll-like receptor agonists and antagonists. Nat Med. 13(5):552–559. doi:10.1038/nm1589.

Kato H, Takeuchi O, Mikamo-Satoh E, Hirai R, Kawai T, Matsushita K, Hiiragi A, Dermody TS, Fujita T, Akira S. 2008. Length-dependent recognition of double-stranded ribonucleic acids by retinoic acid–inducible gene-I and melanoma differentiation–associated gene 5. Journal of Experimental Medicine. 205(7):1601–1610. doi:10.1084/jem.20080091.

Kato H, Takeuchi O, Sato S, Yoneyama M, Yamamoto M, Matsui K, Uematsu S, Jung A, Kawai T, Ishii KJ, et al., 2006. Differential roles of MDA5 and RIG-I helicases in the recognition of RNA viruses. Nature. 441(7089):101–105. doi:10.1038/nature04734.

Kaur A, Baldwin J, Brar D, Salunke DB, Petrovsky N. 2022. Toll-like receptor (TLR) agonists as a driving force behind next-generation vaccine adjuvants and cancer therapeutics. Current Opinion in Chemical Biology. 70:102172. doi:10.1016/j.cbpa.2022.102172.

Kawai T, Akira S. 2010. The role of pattern-recognition receptors in innate immunity: update on Toll-like receptors. Nat Immunol. 11(5):373–384. doi:10.1038/ni.1863.

Kenderian SS, Ruella M, Gill S, Kalos M. 2014. Chimeric antigen receptor T-cell therapy to target hematologic malignancies. Cancer Res. 74(22):6383–6389. doi:10.1158/0008-5472.CAN-14-1530.

Kent MS, Strom A, London CA, Seguin B. 2004. Alternating carboplatin and doxorubicin as adjunctive chemotherapy to amputation or limb-sparing surgery in the treatment of appendicular osteosarcoma in dogs. J Vet Intern Med. 18(4):540–544. doi:10.1892/0891-6640(2004)18<540:acadaa>2.0.co;2.

Khajeh Alizadeh Attar M, Anwar MA, Eskian M, Keshavarz-Fathi M, Choi S, Rezaei N. 2018. Basic understanding and therapeutic approaches to target toll-like receptors in cancerous microenvironment and metastasis. Med Res Rev. 38(5):1469–1484. doi:10.1002/med.21480.

Khalil DN, Smith EL, Brentjens RJ, Wolchok JD. 2016. The future of cancer treatment: immunomodulation, CARs and combination immunotherapy. Nat Rev Clin Oncol. 13(5):273–290. doi:10.1038/nrclinonc.2016.25.

Khan AA, Khan Z, Warnakulasuriya S. 2016. Cancer-associated toll-like receptor modulation and insinuation in infection susceptibility: association or coincidence? Ann Oncol. 27(6):984–997. doi:10.1093/annonc/mdw053.

Kirkali Z, Chan T, Manoharan M, Algaba F, Busch C, Cheng L, Kiemeney L, Kriegmair M, Montironi R, Murphy WM, et al., 2005. Bladder cancer: epidemiology, staging and grading, and diagnosis. Urology. 66(1):4–34. doi:10.1016/j.urology.2005.07.062.

Kishimoto T. 1989. The biology of interleukin-6. Blood. 74(1):1–10.

Kowanetz M, Zou W, Gettinger SN, Koeppen H, Kockx M, Schmid P, Kadel EE, Wistuba I, Chaft J, Rizvi NA, et al., 2018. Differential regulation of PD-L1 expression by immune and tumor cells in NSCLC and the response to treatment with atezolizumab (anti–PD-L1). Proceedings of the National Academy of Sciences. 115(43):E10119–E10126. doi:10.1073/pnas.1802166115.

Krieg AM. 2002. CpG Motifs in Bacterial DNA and Their Immune Effects*. Annual Review of Immunology. 20(20):709–760. doi:10.1146/annurev.immunol.20.100301.064842.

Kruger S, Ilmer M, Kobold S, Cadilha BL, Endres S, Ormanns S, Schuebbe G, Renz BW, D'Haese JG, Schloesser H, et al., 2019. Advances in cancer immunotherapy 2019 – latest trends. Journal of Experimental & Clinical Cancer Research. 38(1):268. doi:10.1186/s13046-019-1266-0.

Kulkarni RR, Rasheed MAU, Bhaumik SK, Ranjan P, Cao W, Davis C, Marisetti K, Thomas S, Gangappa S, Sambhara S, et al., 2014. Activation of the RIG-I pathway during influenza vaccination enhances the germinal center reaction, promotes T follicular helper cell induction, and provides a dose-sparing effect and protective immunity. J Virol. 88(24):13990–14001. doi:10.1128/JVI.02273-14.

Kursunel MA, Esendagli G. 2016. The untold story of IFN-γ in cancer biology. Cytokine & Growth Factor Reviews. 31:73–81. doi:10.1016/j.cytogfr.2016.07.005.

Kyi C, Postow MA. 2016. Immune checkpoint inhibitor combinations in solid tumors: opportunities and challenges. Immunotherapy. 8(7):821–837. doi:10.2217/imt-2016-0002.

Laidlaw BJ, Craft JE, Kaech SM. 2016. The multifaceted role of CD4+ T cells in CD8+ T cell memory. Nat Rev Immunol. 16(2):102–111. doi:10.1038/nri.2015.10.

Lattime EC, Gomella LG, McCue PA. 1992. Murine bladder carcinoma cells present antigen to BCG-specific CD4+ T-cells. Cancer Res. 52(15):4286–4290.

Lecocq Q, De Vlaeminck Y, Hanssens H, D'Huyvetter M, Raes G, Goyvaerts C, Keyaerts M, Devoogdt N, Breckpot K. 2019. Theranostics in immuno-oncology using nanobody derivatives. Theranostics. 9(25):7772–7791. doi:10.7150/thno.34941.

Lee AW, Truong T, Bickham K, Fonteneau J-F, Larsson M, Da Silva I, Somersan S, Thomas EK, Bhardwaj N. 2002. A clinical grade cocktail of cytokines and PGE2 results in uniform maturation of human monocyte-derived dendritic cells: implications for immunotherapy. Vaccine. 20(4):A8–A22. doi:10.1016/s0264-410x(02)00382-1.

Lenis AT, Lec PM, Chamie K, Mshs MD. 2020. Bladder Cancer: A Review. JAMA. 324(19):1980–1991. doi:10.1001/jama.2020.17598.

Lesch S, Gill S. 2021. The promise and perils of immunotherapy. Blood Advances. 5(18):3709–3725. doi:10.1182/bloodadvances.2021004453.

Levy DE, Marié IJ, Durbin JE. 2011. Induction and function of type I and III interferon in response to viral infection. Current Opinion in Virology. 1(6):476–486. doi:10.1016/j.coviro.2011.11.001.

Li J, Song W, Czerwinski DK, Varghese B, Uematsu S, Akira S, Krieg AM, Levy R. 2007. Lymphoma immunotherapy with CpG oligodeoxynucleotides requires TLR9 either in the host or in the tumor itself. J Immunol. 179(4):2493–2500. doi:10.4049/jimmunol.179.4.2493.

Li MO, Flavell RA. 2008. Contextual Regulation of Inflammation: A Duet by Transforming Growth Factor-β and Interleukin-10. Immunity. 28(4):468–476. doi:10.1016/j.immuni.2008.03.003.

Li T, Wu J, Zhu S, Zang G, Li S, Lv X, Yue W, Qiao Y, Cui J, Shao Y, et al., 2020. A Novel C Type CpG Oligodeoxynucleotide Exhibits Immunostimulatory Activity In Vitro and Enhances Antitumor Effect In Vivo. Front Pharmacol. 11:8. doi:10.3389/fphar.2020.00008.

Lin L, Liu Q, Berube N, Detmer S, Zhou Y. 2012. 5′-Triphosphate-Short Interfering RNA: Potent Inhibition of Influenza A Virus Infection by Gene Silencing and RIG-I Activation. J Virol. 86(19):10359–10369. doi:10.1128/JVI.00665-12.

Lin Z, Chen X, Li Z, Luo Y, Fang Z, Xu B, Han M. 2016. PD-1 Antibody Monotherapy for Malignant Melanoma: A Systematic Review and Meta-Analysis. PLoS One. 11(8):e0160485. doi:10.1371/journal.pone.0160485.

Linehan MM, Dickey TH, Molinari ES, Fitzgerald ME, Potapova O, Iwasaki A, Pyle AM. 2018. A minimal RNA ligand for potent RIG-I activation in living mice. Sci Adv. 4(2):e1701854. doi:10.1126/sciadv.1701854.

Linsley PS, Ledbetter JA. 1993. The Role of the CD28 Receptor During T Cell Responses to Antigen. Annual Review of Immunology. 11(11):191–212. doi:10.1146/annurev.iy.11.040193.001203.

Liu G, Park H-S, Pyo H-M, Liu Q, Zhou Y. 2015. Influenza A Virus Panhandle Structure Is Directly Involved in RIG-I Activation and Interferon Induction. Journal of Virology. 89(11):6067–6079. doi:10.1128/jvi.00232-15.

Liu G, Zhou Y. 2019. Cytoplasm and Beyond: Dynamic Innate Immune Sensing of Influenza A Virus by RIG-I. Journal of Virology. 93(8):10.1128/jvi.02299-18. doi:10.1128/jvi.02299-18.

Lizotte PH, Wen AM, Sheen MR, Fields J, Rojanasopondist P, Steinmetz NF, Fiering S. 2016. In situ vaccination with cowpea mosaic virus nanoparticles suppresses metastatic cancer. Nat Nanotechnol. 11(3):295–303. doi:10.1038/nnano.2015.292.

Loiarro M, Ruggiero V, Sette C. 2010. Targeting TLR/IL-1R Signalling in Human Diseases. Mediators Inflamm. 2010:674363. doi:10.1155/2010/674363.

Lund JM, Alexopoulou L, Sato A, Karow M, Adams NC, Gale NW, Iwasaki A, Flavell RA. 2004. Recognition of single-stranded RNA viruses by Toll-like receptor 7. Proceedings of the National Academy of Sciences. 101(15):5598–5603. doi:10.1073/pnas.0400937101.

Luo Q, Zhang L, Luo C, Jiang M. 2019. Emerging strategies in cancer therapy combining chemotherapy with immunotherapy. Cancer Lett. 454:191–203. doi:10.1016/j.canlet.2019.04.017.

Mansell A, Jenkins BJ. 2013. Dangerous liaisons between interleukin-6 cytokine and toll-like receptor families: a potent combination in inflammation and cancer. Cytokine Growth Factor Rev. 24(3):249–256. doi:10.1016/j.cytogfr.2013.03.007.

Marabelle A, Kohrt H, Caux C, Levy R. 2014. Intratumoral immunization: a new paradigm for cancer therapy. Clin Cancer Res. 20(7):1747–1756. doi:10.1158/1078-0432.CCR-13-2116.

Marabelle A, Kohrt H, Sagiv-Barfi I, Ajami B, Axtell RC, Zhou G, Rajapaksa R, Green MR, Torchia J, Brody J, et al., 2013. Depleting tumor-specific Tregs at a single site eradicates disseminated tumors. J Clin Invest. 123(6):2447–2463. doi:10.1172/JCI64859.

Marshall JD, Heeke DS, Abbate C, Yee P, Van Nest G. 2006. Induction of interferon-γ from natural killer cells by immunostimulatory CpG DNA is mediated through plasmacytoid-dendritic-cell-produced interferon-α and tumour necrosis factor-α. Immunology. 117(1):38–46. doi:10.1111/j.1365-2567.2005.02261.x.

Mascarelli DE, Rosa RSM, Toscaro JM, Semionatto IF, Ruas LP, Fogagnolo CT, Lima GC, Bajgelman MC. 2021. Boosting Antitumor Response by Costimulatory Strategies Driven to 4-1BB and OX40 T-cell Receptors. Front Cell Dev Biol. 2021 Jun 30;9:692982. doi: 10.3389/fcell.2021.692982.

Mason NJ. 2020. Comparative Immunology and Immunotherapy of Canine Osteosarcoma. Adv Exp Med Biol. 1258:199–221. doi:10.1007/978-3-030-43085-6_14.

Mata M, Vera JF, Gerken C, Rooney CM, Miller T, Pfent C, Wang LL, Wilson-Robles HM, Gottschalk S. 2014. Toward immunotherapy with redirected T cells in a large animal model: ex vivo activation, expansion, and genetic modification of canine T cells. J Immunother. 37(8):407–415. doi:10.1097/CJI.0000000000000052.

Matz KM, Guzman RM, Goodman AG. 2019. The Role of Nucleic Acid Sensing in Controlling Microbial and Autoimmune Disorders. Int Rev Cell Mol Biol. 345:35–136. doi:10.1016/bs.ircmb.2018.08.002.

Maude SL, Laetsch TW, Buechner J, Rives S, Boyer M, Bittencourt H, Bader P, Verneris MR, Stefanski HE, Myers GD, et al., 2018. Tisagenlecleucel in Children and Young Adults with B-Cell Lymphoblastic Leukemia. N Engl J Med. 378(5):439–448. doi:10.1056/NEJMoa1709866.

Messenheimer DJ, Jensen SM, Afentoulis ME, Wegmann KW, Feng Z, Friedman DJ, Gough MJ, Urba WJ, Fox BA. 2017. Timing of PD-1 Blockade Is Critical to Effective Combination Immunotherapy with Anti-OX40. Clin Cancer Res. 23(20):6165–6177. doi:10.1158/1078-0432.CCR-16-2677.

Miller KD, Goding Sauer A, Ortiz AP, Fedewa SA, Pinheiro PS, Tortolero-Luna G, Martinez-Tyson D, Jemal A, Siegel RL. 2018. Cancer Statistics for Hispanics/Latinos, 2018. CA Cancer J Clin. 68(6):425–445. doi:10.3322/caac.21494.

Mitchell DH, Withrow SJ, Johnston MR, Kruse CA. 1991. Cytotoxicity against autologous, allogeneic, and xenogeneic tumor targets by human recombinant interleukin-2-activated lymphocytes from healthy dogs and dogs with lung tumors. Am J Vet Res. 52(7):1132–1136.

Mochel JP, Ekker SC, Johannes CM, Jergens AE, Allenspach K, Bourgois-Mochel A, Knouse M, Benzekry S, Wierson W, LeBlanc AK, et al., 2019. CAR T Cell Immunotherapy in Human and Veterinary Oncology: Changing the Odds Against Hematological Malignancies. AAPS J. 21(3):50. doi:10.1208/s12248-019-0322-1.

Molitor TW, Joo HS, Collett MS. 1983. Porcine parvovirus: virus purification and structural and antigenic properties of virion polypeptides. Journal of Virology. 45(2):842–854. doi:10.1128/jvi.45.2.842-854.1983.

Moran AE, Polesso F, Weinberg AD. 2016. Immunotherapy Expands and Maintains the Function of High-Affinity Tumor-Infiltrating CD8 T Cells In Situ. The Journal of Immunology. 197(6):2509–2521. doi:10.4049/jimmunol.1502659.

Morinobu A, Gadina M, Strober W, Visconti R, Fornace A, Montagna C, Feldman GM, Nishikomori R, O'Shea JJ. 2002. STAT4 serine phosphorylation is critical for IL-12-induced IFN-γ production but not for cell proliferation. Proceedings of the National Academy of Sciences. 99(19):12281–12286. doi:10.1073/pnas.182618999.

Murri AA, Hilmy M, Bell J, Wilson C, McNicol A-M, Lannigan A, Doughty JC, McMillan DC. 2008. The relationship between the systemic inflammatory response, tumour proliferative activity, T-lymphocytic and macrophage infiltration, microvessel density and survival in patients with primary operable breast cancer. Br J Cancer. 99(7):1013–1019. doi:10.1038/sj.bjc.6604667.

Neelapu SS, Locke FL, Bartlett NL, Lekakis LJ, Miklos DB, Jacobson CA, Braunschweig I, Oluwole OO, Siddiqi T, Lin Y, et al., 2017. Axicabtagene Ciloleucel CAR T-Cell Therapy in Refractory Large B-Cell Lymphoma. N Engl J Med. 377(26):2531–2544. doi:10.1056/NEJMoa1707447.

Nizar S, Copier J, Meyer B, Bodman-Smith M, Galustian C, Kumar D, Dalgleish A. 2009. T-regulatory cell modulation: the future of cancer immunotherapy? Br J Cancer. 100(11):1697–1703. doi:10.1038/sj.bjc.6605040.

Offermanns S, Rosenthal W. 2008. Encyclopedia of Molecular Pharmacology. Springer Science & Business Media.

Oliver AJ, Davey AS, Keam SP, Mardiana S, Chan JD, von Scheidt B, Beavis PA, House IG, Van Audernaerde JR, Darcy PK, et al., 2019. Tissue-specific tumor microenvironments influence responses to immunotherapies. Clin Transl Immunology. 8(11):e1094. doi:10.1002/cti2.1094.

O'Neill RE, Cao X. 2019. Co-stimulatory and co-inhibitory pathways in cancer immunotherapy. Adv Cancer Res. 143:145–194. doi:10.1016/bs.acr.2019.03.003.

Pal SK, Albiges L, Tomczak P, Suárez C, Voss MH, de Velasco G, Chahoud J, Mochalova A, Procopio G, Mahammedi H, et al., 2023. Atezolizumab plus cabozantinib versus cabozantinib monotherapy for patients with renal cell carcinoma after progression with previous immune checkpoint inhibitor treatment (CONTACT-03): a multicentre, randomised, open-label, phase 3 trial. Lancet. 402(10397):185–195. doi:10.1016/S0140-6736(23)00922-4.

Palumbo MO, Kavan P, Miller WH, Panasci L, Assouline S, Johnson N, Cohen V, Patenaude F, Pollak M, Jagoe RT, et al., 2013. Systemic cancer therapy: achievements and challenges that lie ahead. Front Pharmacol. 4:57. doi:10.3389/fphar.2013.00057.

Panjwani MK, Smith JB, Schutsky K, Gnanandarajah J, O'Connor CM, Powell DJ, Mason NJ. 2016. Feasibility and Safety of RNA-transfected CD20-specific Chimeric Antigen Receptor T Cells in Dogs with Spontaneous B Cell Lymphoma. Mol Ther. 24(9):1602–1614. doi:10.1038/mt.2016.146.

Patidar A, Selvaraj S, Sarode A, Chauhan P, Chattopadhyay D, Saha B. 2018. DAMP-TLR-cytokine axis dictates the fate of tumor. Cytokine. 104:114–123. doi:10.1016/j.cyto.2017.10.004.

Pavlakis GM, Sakorafas GH, Anagnostopoulos GK. 2004. Intestinal metastases from renal cell carcinoma: a rare cause of intestinal obstruction and bleeding. Mt Sinai J Med. 71(2):127–130.

Pearlman AH, Hwang MS, Konig MF, Hsiue EH-C, Douglass J, DiNapoli SR, Mog BJ, Bettegowda C, Pardoll DM, Gabelli SB, et al., 2021. Targeting public neoantigens for cancer immunotherapy. Nat Cancer. 2(5):487–497. doi:10.1038/s43018-021-00210-y.

Peters JH, Xu H, Ruppert J, Ostermeier D, Friedrichs D, Gieseler RK. 1993. Signals required for differentiating dendritic cells from human monocytes in vitro. Adv Exp Med Biol. 329:275–280. doi:10.1007/978-1-4615-2930-9_46.

Pichlmair A, Schulz O, Tan CP, Näslund TI, Liljeström P, Weber F, Reis e Sousa C. 2006. RIG-I-Mediated Antiviral Responses to Single-Stranded RNA Bearing 5'-Phosphates. Science. 314(5801):997–1001. doi:10.1126/science.1132998.

Pidgeon GP, Harmey JH, Kay E, Costa MD, Redmond HP, Bouchier-Hayes DJ. 1999. The role of endotoxin/lipopolysaccharide in surgically induced tumour growth in a murine model of metastatic disease. British Journal of Cancer. 81(8):1311–1317. doi:10.1038/sj.bjc.6694369.

Pieper AA, Spiegelman DV, Felder MAR, Feils AS, Tsarovsky NW, Zaborek J, Morris ZS, Erbe AK, Rakhmilevich AL, Sondel PM. 2023. Factors impacting the efficacy of the in-situ vaccine with CpG and OX40 agonist. Cancer Immunol Immunother. 72(7):2459–2471. doi:10.1007/s00262-023-03433-3.

Proskurina AS, Ruzanova VS, Ritter GS, Efremov YR, Mustafin ZS, Lashin SA, Burakova EA, Fokina AA, Zatsepin TS, Stetsenko DA, et al., 2023. Antitumor efficacy of multi-target *in situ* vaccinations with CpG oligodeoxynucleotides, anti-OX40, anti-PD1 antibodies, and aptamers. J Biomed Res. 37(3):194–212. doi:10.7555/JBR.36.20220052.

Rakoff-Nahoum S, Medzhitov R. 2009. Toll-like receptors and cancer. Nat Rev Cancer. 9(1):57–63. doi:10.1038/nrc2541.

Ranz AI, Manclús JJ, Díaz-Aroca E, Casal JI. 1989. Porcine Parvovirus: DNA Sequence and Genome Organization. Journal of General Virology. 70(10):2541–2553. doi:10.1099/0022-1317-70-10-2541.

Ratliff TL. 2000. Role of animal models in understanding intravesical therapy with bacille Calmette-Guérin. Clin Infect Dis. 31(3):S106-108. doi:10.1086/314065.

Redmond WL, Linch SN, Kasiewicz MJ. 2014. Combined Targeting of Costimulatory (OX40) and Coinhibitory (CTLA-4) Pathways Elicits Potent Effector T Cells Capable of Driving Robust Antitumor Immunity. Cancer Immunology Research. 2(2):142–153. doi:10.1158/2326-6066.CIR-13-0031-T.

Rehwinkel J, Gack MU. 2020. RIG-I-like receptors: their regulation and roles in RNA sensing. Nat Rev Immunol. 20(9):537–551. doi:10.1038/s41577-020-0288-3.

Rehwinkel J, Tan CP, Goubau D, Schulz O, Pichlmair A, Bier K, Robb N, Vreede F, Barclay W, Fodor E, et al., 2010. RIG-I Detects Viral Genomic RNA during Negative-Strand RNA Virus Infection. Cell. 140(3):397–408. doi:10.1016/j.cell.2010.01.020.

Renca Syngeneic Murine Model. Altogen Labs. [accessed 2024 May 2]. https://altogenlabs.com/xenograft-models/kidney-cancer-xenograft/renca-xenograft-model/.

Rockwell CE, Morrison David C, Qureshi N. 2010. Lipid A-Mediated Tolerance and Cancer Therapy. In: Jeannin J-F, editor. Lipid A in Cancer Therapy. New York, NY: Springer. (Advances in Experimental Medicine and Biology). p. 81–99. [accessed 2020 Dec 3]. https://doi.org/10.1007/978-1-4419-1603-7_8.

Romagnani S. 1999. Th1/Th2 Cells. Inflammatory Bowel Diseases. 5(4):285–294. doi:10.1097/00054725-199911000-00009.

Romani N, Gruner S, Brang D, Kämpgen E, Lenz A, Trockenbacher B, Konwalinka G, Fritsch PO, Steinman RM, Schuler G. 1994. Proliferating dendritic cell progenitors in human blood. J Exp Med. 180(1):83–93. doi:10.1084/jem.180.1.83.

Rosenthal RC. 2001. Veterinary Oncology Secrets. Hanley & Belfus.

Rotte A. 2019. Combination of CTLA-4 and PD-1 blockers for treatment of cancer. Journal of Experimental & Clinical Cancer Research. 38(1):255. doi:10.1186/s13046-019-1259-z.

Rudilla F, Fayolle C, Casares N, Durantez M, Arribillaga L, Lozano T, Villanueva L, Pio R, Sarobe P, Leclerc C, et al., 2012. Combination of a TLR4 ligand and anaphylatoxin C5a for the induction of antigen-specific cytotoxic T cell responses. Vaccine. 30(18):2848–2858. doi:10.1016/j.vaccine.2012.02.052.

Sagiv Barfi I, Czerwinski DK, Shree T, Levy R. 2018. In Situ Vaccination with Cpg and Anti-OX40 Antibody: Preclinical Optimization for Clinical Translation. Blood. 132(1):2943. doi:10.1182/blood-2018-99-117872.

Sagiv-Barfi I, Czerwinski DK, Levy S, Alam IS, Mayer AT, Gambhir SS, Levy R. 2018. Eradication of spontaneous malignancy by local immunotherapy. Sci Transl Med. 10(426):eaan4488. doi:10.1126/scitranslmed.aan4488.

Sagiv-Barfi I, Kohrt HE, Burckhardt L, Czerwinski DK, Levy R. 2015. Ibrutinib enhances the antitumor immune response induced by intratumoral injection of a TLR9 ligand in mouse lymphoma. Blood. 125(13):2079–2086. doi:10.1182/blood-2014-08-593137.

Said EA, Dupuy FP, Trautmann L, Zhang Y, Shi Y, El-Far M, Hill BJ, Noto A, Ancuta P, Peretz Y, et al., 2010. Programmed death-1–induced interleukin-10 production by monocytes impairs CD4+ T cell activation during HIV infection. Nat Med. 16(4):452–459. doi:10.1038/nm.2106.

Saito T, Hirai R, Loo Y-M, Owen D, Johnson CL, Sinha SC, Akira S, Fujita T, Gale M. 2007. Regulation of innate antiviral defenses through a shared repressor domain in RIG-I and LGP2. Proceedings of the National Academy of Sciences. 104(2):582–587. doi:10.1073/pnas.0606699104.

Sallusto F, Lanzavecchia A. 1994. Efficient presentation of soluble antigen by cultured human dendritic cells is maintained by granulocyte/macrophage colony-stimulating factor plus interleukin 4 and downregulated by tumor necrosis factor alpha. J Exp Med. 179(4):1109–1118. doi:10.1084/jem.179.4.1109.

Salup RR, Back TC, Wiltrout RH. 1987. Successful treatment of advanced murine renal cell cancer by bicompartmental adoptive chemoimmunotherapy. J Immunol. 138(2):641–647.

Salup RR, Wiltrout RH. 1986. Adjuvant immunotherapy of established murine renal cancer by interleukin 2-stimulated cytotoxic lymphocytes. Cancer Res. 46(7):3358–3363.

Sato H, Ito M, Abe T, Kumano N, Motomiya M, Konno K. 1987. Antitumor Activity of Cyclophosphamide and Lipopolysaccharide in Tumor-Bearing Mice Pretreated with BCG. The Tohoku Journal of Experimental Medicine. 153(2):151–160. doi:10.1620/tjem.153.151.

Sato H, Okonogi N, Nakano T. 2020. Rationale of combination of anti-PD-1/PD-L1 antibody therapy and radiotherapy for cancer treatment. Int J Clin Oncol. 25(5):801–809. doi:10.1007/s10147-020-01666-1.

Satoh T, Akira S. 2016. Toll-Like Receptor Signaling and Its Inducible Proteins. Microbiol Spectr. 4(6). doi:10.1128/microbiolspec.MCHD-0040-2016.

Schiffman JD, Breen M. 2015. Comparative oncology: what dogs and other species can teach us about humans with cancer. Philos Trans R Soc Lond B Biol Sci. 370(1673):20140231. doi:10.1098/rstb.2014.0231.

Schmidt A, Schwerd T, Hamm W, Hellmuth JC, Cui S, Wenzel M, Hoffmann FS, Michallet M-C, Besch R, Hopfner K-P, et al., 2009. 5′-triphosphate RNA requires base-paired structures to activate antiviral signaling via RIG-I. Proceedings of the National Academy of Sciences. 106(29):12067–12072. doi:10.1073/pnas.0900971106.

Schmiedt CW, Grimes JA, Holzman G, McAnulty JF. 2009. Incidence and risk factors for development of malignant neoplasia after feline renal transplantation and cyclosporine-based immunosuppression. Vet Comp Oncol. 7(1):45–53. doi:10.1111/j.1476-5829.2008.00172.x.

Schneider B, Balbas-Martinez V, Jergens AE, Troconiz IF, Allenspach K, Mochel JP. 2018. Model-Based Reverse Translation Between Veterinary and Human Medicine: The One Health Initiative. CPT Pharmacometrics Syst Pharmacol. 7(2):65–68. doi:10.1002/psp4.12262.

Schumacher TN, Scheper W, Kvistborg P. 2019. Cancer Neoantigens. Annu Rev Immunol. 37:173–200. doi:10.1146/annurev-immunol-042617-053402.

Seelig DM, Avery AC, Ehrhart EJ, Linden MA. 2016. The Comparative Diagnostic Features of Canine and Human Lymphoma. Vet Sci. 3(2):11. doi:10.3390/vetsci3020011.

Seledtsov VI, Goncharov AG, Seledtsova GV. 2015. Multiple-purpose immunotherapy for cancer. Biomed Pharmacother. 76:24–29. doi:10.1016/j.biopha.2015.10.020.

Shvarts O, Janzen N, Lam JS, Leppert JT, Caliliw R, Figlin RA, Belldegrun AS, Zeng G. 2006. RENCA/carbonic anhydrase-IX: A murine model of a carbonic anhydrase-IX-expressing renal cell carcinoma. Urology. 68(5):1132–1138. doi:10.1016/j.urology.2006.08.1073.

Smyth MJ, Godfrey DI, Trapani JA. 2001. A fresh look at tumor immunosurveillance and immunotherapy. Nat Immunol. 2(4):293–299. doi:10.1038/86297.

Smyth MJ, Ngiow SF, Teng MW. 2014. Targeting regulatory T cells in tumor immunotherapy. Immunology & Cell Biology. 92(6):473–474. doi:10.1038/icb.2014.33.

So T, Croft M. 2007. Cutting Edge: OX40 Inhibits TGF-β- and Antigen-Driven Conversion of Naive CD4 T Cells into CD25+Foxp3+ T cells1. The Journal of Immunology. 179(3):1427–1430. doi:10.4049/jimmunol.179.3.1427.

Sobczuk P, Brodziak A, Khan MI, Chhabra S, Fiedorowicz M, Wełniak-Kamińska M, Synoradzki K, Bartnik E, Cudnoch-Jędrzejewska A, Czarnecka AM. 2020. Choosing The Right Animal Model for Renal Cancer Research. Transl Oncol. 13(3):100745. doi:10.1016/j.tranon.2020.100745.

Sotomayor EM, Borrello I, Tubb E, Rattis FM, Bien H, Lu Z, Fein S, Schoenberger S, Levitsky HI. 1999. Conversion of tumor-specific CD4+ T-cell tolerance to T-cell priming through in vivo ligation of CD40. Nat Med. 5(7):780–787. doi:10.1038/10503.

Spranger S. 2016. Mechanisms of tumor escape in the context of the T-cell-inflamed and the non-T-cell-inflamed tumor microenvironment. Int Immunol. 28(8):383–391. doi:10.1093/intimm/dxw014.

Staveley-O'Carroll K, Sotomayor E, Montgomery J, Borrello I, Hwang L, Fein S, Pardoll D, Levitsky H. 1998. Induction of antigen-specific T cell anergy: An early event in the course of tumor progression. Proc Natl Acad Sci U S A. 95(3):1178–1183. doi:10.1073/pnas.95.3.1178.

Stone GW, Barzee S, Snarsky V, Santucci C, Tran B, Langer R, Zugates GT, Anderson DG, Kornbluth RS. 2009. Nanoparticle-Delivered Multimeric Soluble CD40L DNA Combined with Toll-Like Receptor Agonists as a Treatment for Melanoma. PLoS One. 4(10):e7334. doi:10.1371/journal.pone.0007334.

Summerhayes IC, Franks LM. 1979. Effects of donor age on neoplastic transformation of adult mouse bladder epithelium in vitro. J Natl Cancer Inst. 62(4):1017–1023.

Sun Y, Reddy P. 2013. Intracellular Sensors of Immunity and Allogeneic Hematopoietic Stem Cell Transplantation. In: Immune Biology of Allogeneic Hematopoietic Stem Cell Transplantation. p. 425–447.

Sung H, Ferlay J, Siegel RL, Laversanne M, Soerjomataram I, Jemal A, Bray F. 2021. Global Cancer Statistics 2020: GLOBOCAN Estimates of Incidence and Mortality Worldwide for 36 Cancers in 185 Countries. CA Cancer J Clin. 71(3):209–249. doi:10.3322/caac.21660.

Suurs FV, Lub-de Hooge MN, de Vries EGE, de Groot DJA. 2019. A review of bispecific antibodies and antibody constructs in oncology and clinical challenges. Pharmacol Ther. 201:103–119. doi:10.1016/j.pharmthera.2019.04.006.

Takeda K, Akira S. 2004. TLR signaling pathways. Semin Immunol. 16(1):3–9. doi:10.1016/j.smim.2003.10.003.

Takeuchi O, Akira S. 2010. Pattern recognition receptors and inflammation. Cell. 140(6):805–820. doi:10.1016/j.cell.2010.01.022.

Tanaka T, Narazaki M, Kishimoto T. 2014. IL-6 in Inflammation, Immunity, and Disease. Cold Spring Harb Perspect Biol. 6(10):a016295. doi:10.1101/cshperspect.a016295.

Tau G, Rothman P. 1999. Biologic functions of the IFN-γ receptors. Allergy. 54(12):1233–1251. doi:10.1034/j.1398-9995.1999.00099.x.

Tauriello DVF, Sancho E, Batlle E. 2022. Overcoming TGFβ-mediated immune evasion in cancer. Nat Rev Cancer. 22(1):25–44. doi:10.1038/s41568-021-00413-6.

Thaiss CA, Semmling V, Franken L, Wagner H, Kurts C. 2011. Chemokines: A New Dendritic Cell Signal for T Cell Activation. Front Immunol. 2:31. doi:10.3389/fimmu.2011.00031.

The Mouse in Biomedical Research, Volume 3 - 2nd Edition | Elsevier Shop. [accessed 2024 May 2]. https://shop.elsevier.com/books/the-mouse-in-biomedical-research/fox/978-0-12-369457-7.

Thoresen D, Wang W, Galls D, Guo R, Xu L, Pyle AM. 2021. The molecular mechanism of RIG-I activation and signaling. Immunol Rev. 304(1):154–168. doi:10.1111/imr.13022.

Topalian Suzanne L., Hodi F. Stephen, Brahmer Julie R., Gettinger Scott N., Smith David C., McDermott David F., Powderly John D., Carvajal Richard D., Sosman Jeffrey A., Atkins Michael B., et al., 2012. Safety, Activity, and Immune Correlates of Anti–PD-1 Antibody in Cancer. New England Journal of Medicine. 366(26):2443–2454. doi:10.1056/NEJMoa1200690.

Trinchieri G. 2007. Interleukin-10 production by effector T cells: Th1 cells show self control. Journal of Experimental Medicine. 204(2):239–243. doi:10.1084/jem.20070104.

Tsukamoto H, Kubota K, Shichiku A, Maekawa M, Mano N, Yagita H, Ohta S, Tomioka Y. 2019. An agonistic anti-Toll-like receptor 4 monoclonal antibody as an effective adjuvant for cancer immunotherapy. Immunology. 158(2):136–149. doi:10.1111/imm.13095.

Tusup M, French LE, De Matos M, Gatfield D, Kundig T, Pascolo S. 2019. Design of in vitro Transcribed mRNA Vectors for Research and Therapy. Chimia (Aarau). 73(6):391–394. doi:10.2533/chimia.2019.391.

Urban-Wojciuk Z, Khan MM, Oyler BL, Fåhraeus R, Marek-Trzonkowska N, Nita-Lazar A, Hupp TR, Goodlett DR. 2019. The Role of TLRs in Anti-cancer Immunity and Tumor Rejection. Front Immunol. 10:2388. doi:10.3389/fimmu.2019.02388.

Van Hoecke L, Verbeke R, Dewitte H, Lentacker I, Vermaelen K, Breckpot K, Van Lint S. 2021. mRNA in cancer immunotherapy: beyond a source of antigen. Molecular Cancer. 20(1):48. doi:10.1186/s12943-021-01329-3.

Vinay DS, Ryan EP, Pawelec G, Talib WH, Stagg J, Elkord E, Lichtor T, Decker WK, Whelan RL, Kumara HMCS, et al., 2015. Immune evasion in cancer: Mechanistic basis and therapeutic strategies. Semin Cancer Biol. 35:S185–S198. doi:10.1016/j.semcancer.2015.03.004.

Vosskuhl K, Greten TF, Manns MP, Korangy F, Wedemeyer J. 2010. Lipopolysaccharide-Mediated Mast Cell Activation Induces IFN-γ Secretion by NK Cells. JI. 185(1):119–125. doi:10.4049/jimmunol.0902406.

Waeckerle-Men Y, Groettrup M. 2005. PLGA microspheres for improved antigen delivery to dendritic cells as cellular vaccines. Adv Drug Deliv Rev. 57(3):475–482. doi:10.1016/j.addr.2004.09.007.

Wages NA, Chiuzan C, Panageas KS. 2018. Design considerations for early-phase clinical trials of immune-oncology agents. J Immunother Cancer. 6(1):81. doi:10.1186/s40425-018-0389-8.

Wajant H, Pfizenmaier K, Scheurich P. 2003. Tumor necrosis factor signaling. Cell Death Differ. 10(1):45–65. doi:10.1038/sj.cdd.4401189.

Walker LSK, Sansom DM. 2015. Confusing signals: recent progress in CTLA-4 biology. Trends Immunol. 36(2):63–70. doi:10.1016/j.it.2014.12.001.

Wallace ME, Smyth MJ. 2005. The role of natural killer cells in tumor control—effectors and regulators of adaptive immunity. Springer Semin Immun. 27(1):49–64. doi:10.1007/s00281-004-0195-x.

Wang H, Franco F, Ho P-C. 2017. Metabolic Regulation of Tregs in Cancer: Opportunities for Immunotherapy. Trends Cancer. 3(8):583–592. doi:10.1016/j.trecan.2017.06.005.

Weber M, Gawanbacht A, Habjan M, Rang A, Borner C, Schmidt AM, Veitinger S, Jacob R, Devignot S, Kochs G, et al., 2013. Incoming RNA virus nucleocapsids containing a 5'-triphosphorylated genome activate RIG-I and antiviral signaling. Cell Host Microbe. 13(3):336–346. doi:10.1016/j.chom.2013.01.012.

Weber M, Weber F. 2014. Segmented negative-strand RNA viruses and RIG-I: divide (your genome) and rule. Current Opinion in Microbiology. 20:96–102. doi:10.1016/j.mib.2014.05.002.

White-Gilbertson S, Davis M, Voelkel-Johnson C, Kasman LM. 2016. Sex differences in the MB49 syngeneic, murine model of bladder cancer. Bladder (San Franc). 3(1):e22. doi:10.14440/bladder.2016.73.

Withrow SJ, Powers BE, Straw RC, Wilkins RM. 1991. Comparative aspects of osteosarcoma. Dog versus man. Clin Orthop Relat Res.(270):159–168.

Xiao Z, McCallum TJ, Brown KM, Miller GG, Halls SB, Parney I, Moore RB. 1999. Characterization of a novel transplantable orthotopic rat bladder transitional cell tumour model. Br J Cancer. 81(4):638–646. doi:10.1038/sj.bjc.6690741.

Yang Y, Li H, Fotopoulou C, Cunnea P, Zhao X. 2022. Toll-like receptor-targeted anti-tumor therapies: Advances and challenges. Front Immunol. 13:1049340. doi:10.3389/fimmu.2022.1049340.

Yin Y, Boesteanu AC, Binder ZA, Xu C, Reid RA, Rodriguez JL, Cook DR, Thokala R, Blouch K, McGettigan-Croce B, et al., 2018. Checkpoint Blockade Reverses Anergy in IL-13Rα2 Humanized scFv-Based CAR T Cells to Treat Murine and Canine Gliomas. Mol Ther Oncolytics. 11:20–38. doi:10.1016/j.omto.2018.08.002.

Zeng W, Sun L, Jiang X, Chen X, Hou F, Adhikari A, Xu M, Chen ZJ. 2010. Reconstitution of the RIG-I Pathway Reveals a Signaling Role of Unanchored Polyubiquitin Chains in Innate Immunity. Cell. 141(2):315–330. doi:10.1016/j.cell.2010.03.029.

Zhang H, Wang P, Wang Xiaojie, Shi L, Fan Z, Zhang G, Yang D, Bahavar CF, Zhou F, Chen WR, et al., 2018. Antitumor Effects of DC Vaccine With ALA-PDT-Induced Immunogenic Apoptotic Cells for Skin Squamous Cell Carcinoma in Mice. Technol Cancer Res Treat. 17:1533033818785275. doi:10.1177/1533033818785275.

Zhang J, Yan Y, Li J, Adhikari R, Fu L. 2020. PD-1/PD-L1 Based Combinational Cancer Therapy: Icing on the Cake. Frontiers in Pharmacology. 11:722.

Zhang X, Xiao X, Lan P, Li J, Dou Y, Chen W, Ishii N, Chen S, Xia B, Chen K, et al., 2018. OX40 Costimulation Inhibits Foxp3 Expression and Treg Induction via BATF3-Dependent and Independent Mechanisms. Cell Reports. 24(3):607–618. doi:10.1016/j.celrep.2018.06.052.

Zheng P, Zhou Z. 2015. Human Cancer Immunotherapy with PD-1/PD-L1 Blockade. Biomark Cancer. 7(2):15–18. doi:10.4137/BIC.S29325.

Zhou Z, Lin L, An Y, Zhan M, Chen Y, Cai M, Zhu X, Lu L, Zhu K. 2021. The Combination Immunotherapy of TLR9 Agonist and OX40 Agonist via Intratumoural Injection for Hepatocellular Carcinoma. J Hepatocell Carcinoma. 8:529–543. doi:10.2147/JHC.S301375.

Zloza A, Kohlhapp FJ, Lyons GE, Schenkel JM, Moore TV, Lacek AT, O'Sullivan JA, Varanasi V, Williams JW, Jagoda MC, et al., 2012. NKG2D signaling on CD8+ T cells represses T-bet and rescues CD4-unhelped CD8+ T cell memory recall but not effector responses. Nat Med. 18(3):422–428. doi:10.1038/nm.2683.

8. Scientific publications

8.1. Original Full-Length Publications in Peer-Reviewed Journals with Assigned Impact Factors

Gulyás D., Kovács G., Jankovics I., Hidvégi M., Dénes B., Kálfalvy-Molnár L., Nagypál R., Lőrincz M.: **Antimetastatic effect of intratumoral Treg antagonists in mice with renal cancer.** Acta Vet Hung. 2024 Jun 18. doi: 10.1556/004.2024.01037. PMID: 38888963. – **IF: 0.70 (Q3)**

Gulyás D., Földi D., Kovács G, Dénes B., Lőrincz M.: **A különböző immunológiai alapú terápiák alkalmazása a daganatok elleni küzdelemben (Irodalmi összefoglaló), (Utilization of various immunotherapies against cancer).** Magyar Állatorvosok Lapja, 146 (3). pp. 167-180. ISSN 0025-004X. (2024.03). doi: 10.56385/magyallorv.2024.03.167-180 – **IF: 0.30 (Q4)**

Gulyás D., Kovács G., Jankovics I., Mészáros L., Lőrincz M., Dénes B.: **Effects of the combination of a monoclonal agonistic mouse anti-OX40 antibody and toll-like receptor agonists: Unmethylated CpG and LPS on an MB49 bladder cancer cell line in a mouse model.** PLoS One. 2022 Jul 8;17(7):e0270802. doi: 10.1371/journal.pone.0270802. PMID: 35802726; PMCID: PMC9269874. – **IF: 3.70 (Q1)**

8.2. Oral Conference Presentations

Gulyás D., Jankovics I., Dénes B., Földi D., Rodgers R., Commins K., Andócs G., Lőrincz M.: **Különböző RIG-I agonisták daganatellenes hatása vese adenocarcinoma egérmodellen.** MTA Állatorvos-tudományi Bizottsága, ÁTE Állatorvostudományi Doktori Iskola – Akadémiai Beszámolók, Budapest, Hungary (2024)

Gulyás D., Jankovics I., Dénes B., Földi D., Rodgers R., Commins K., Andócs G., Kovács G., Lőrincz M.: **Antitumor activities of different RIG-I agonists in a murine model of kidney adenocarcinoma.** Updates in Cancer Novel Immunotherapies, Rochester, MN, USA (2023)

Gulyás D., Mészáros L., Lőrincz M., Jankovics I., Kovács G., Dénes B..: **A veleszületett immunválasz módosításának hatása az állatok daganataira.** MTA Állatorvos-tudományi Bizottsága, ÁTE Állatorvostudományi Doktori Iskola – Akadémiai Beszámolók, Budapest, Hungary (2021)

Gulyás D., Mészáros L., Lőrincz M., Dénes B.: **Effect of the modulation of the innate immune responses on bladder cancer in mouse model.** 9th Interdisciplinary Doctoral Conference, Pécs, Hungary (2020)

8.3. Poster Conference Presentations

Gulyás D., Jankovics I., Dénes B., Földi D., Rodgers R., Commins K., Andócs G., Kovács G., Lőrincz M.: **Antitumor activities of different RIG-I agonists in a murine model of kidney adenocarcinoma.** AACR Special Conference in Cancer Research: Tumor Immunology and Immunotherapy in Toronto, ON, Canada (2023)

9. Appendices

Preliminary results – Cytokine ELISA tests – Third experiment – Renca II.

Table 8: *A total of twelve mice were subjected to analysis to quantify the production of three cytokines (IFN-γ, IL-6, and IL-10). Mice implanted with Renca CRL-2947 are denoted in the table as "Tumor +", whereas those not subjected to implantation are designated as "Tumor -".*

	IFN-γ (pg/ml)	**IL-6 (pg/ml)**	**IL-10 (pg/ml)**
Tumor +, no treatment I.	Neg.	Neg.	350
Tumor +, no treatment II.	13,125	Neg.	190
Tumor -, CpG + anti-OX40 I.	Neg.	Neg.	Neg.
Tumor -, CpG + anti-OX40 II.	72,5	Neg.	Neg.
Tumor -, CpG + 3p-hpRNA I.	13	34	Neg.
Tumor -, CpG + 3p-hpRNA II.	6,5	Neg.	Neg.
Tumor -, IV-RNA + anti-OX40 I.	Neg.	Neg.	Neg.
Tumor -, IV-RNA + anti-OX40 II.	20,5	Neg.	Neg.
Tumor -, 3p-hpRNA I.	12,5	Neg.	Neg.
Tumor -, 3p-hpRNA II.	37,5	Neg.	Neg.
Tumor -, PPV1-DNA + anti-OX40 I.	42,5	56	1666
Tumor -, PPV1-DNA + anti-OX40 II.	Neg.	12	Neg.

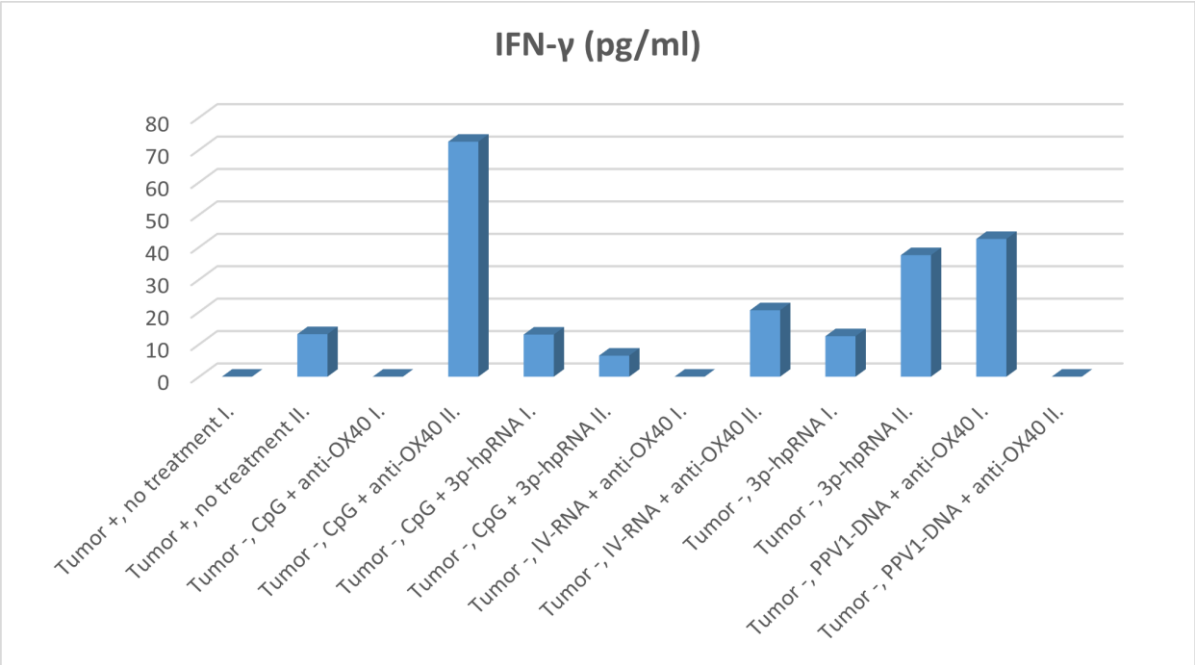

Figure 18: *Levels of IFN-γ in tumor-bearing mice (untreated) and treated mice. Elevated IFN-γ levels were observed following four out of the five treatments (CpG + anti-OX40, IV-RNA + anti-OX40, 3p-hpRNA, and PPV1-DNA + anti-OX40) relative to untreated tumor-bearing mice.*

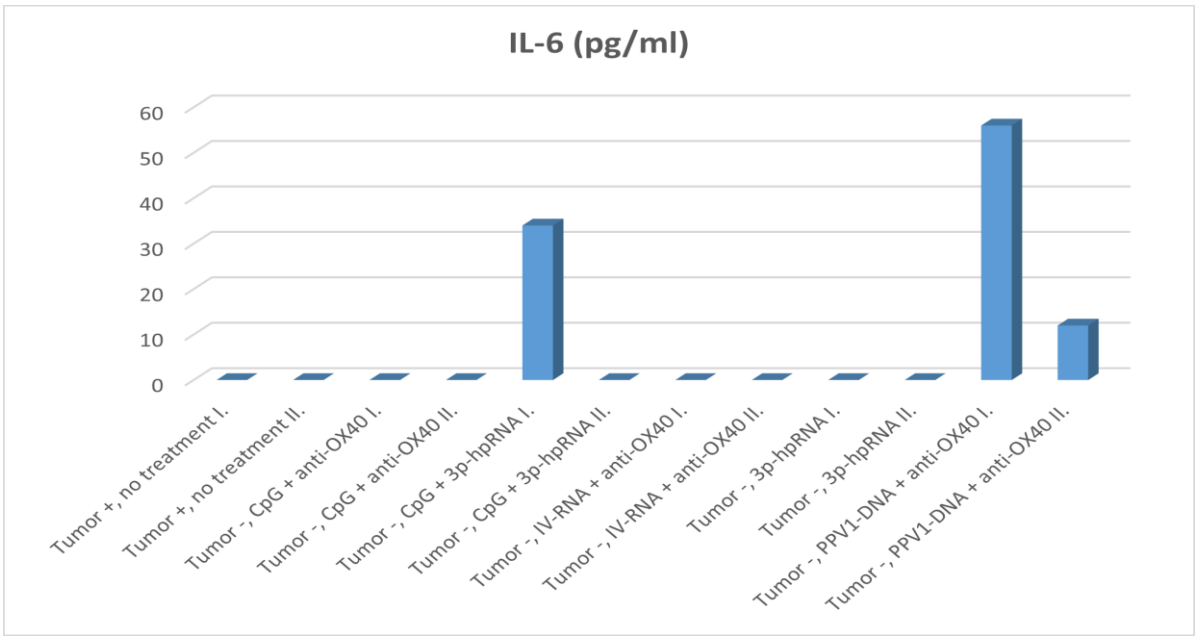

Figure 19: *Levels of IL-6 in tumor-bearing mice (untreated) and treated mice. Elevated IL-6 levels were observed in two out of five treatments (CpG + 3p-hpRNA and PPV1-DNA + anti-OX40), relative to tumor-positive mice.*

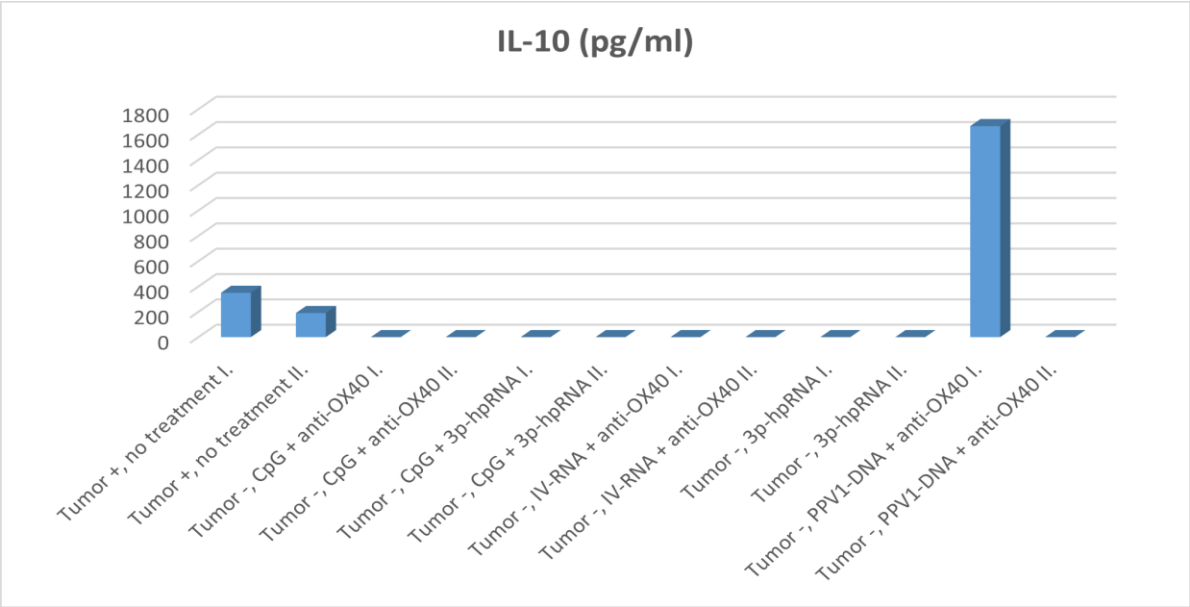

Figure 20: *Levels of IL-10 in tumor-bearing mice (untreated) and treated mice. All two untreated, tumor-positive mice exhibited positive results for IL-10. Conversely, mice subjected to any of the treatments tested displayed negative results (with the exception of one potential outlier in the PPV1-DNA + anti-OX40 group). In this instance, the outcome is deemed positive, as all treatments demonstrated the capability to downregulate IL-10 and consequently modulate regulatory T cell activity. Furthermore, our findings suggest that implanted tumors have the capacity to upregulate Treg activity in tumor-positive mice.*

With respect to cytokine profiles, noteworthy observations emerged whereby all administered treatments elicited elevation in either IFN-γ or IL-6 levels within the murine bloodstream. Equally significant is the collective finding that each of the five treatment modalities concomitantly attenuated IL-10 levels as well. This reduction in IL-10 levels holds profound significance, as it correlates with the suppression of Treg activity, thereby underscoring the immunomodulatory efficacy of the therapeutic interventions employed. Although drawing definitive conclusions from the preliminary experiment with a small sample size is not feasible, the results obtained are noteworthy.

10. Acknowledgements

First and foremost, I extend my gratitude to Márta Lőrincz and Béla Dénes, esteemed mentors whose guidance predates the inception of my doctoral studies. Their mentorship has afforded me invaluable opportunities to immerse myself in the profound intricacies of the researcher's vocation. Their astute counsel has significantly influenced the preparation of my publications and dissertation. Moreover, their steadfast support facilitated my attendance at conferences both domestically and abroad.

I seize this occasion to express my appreciation to all members of the Department of Microbiology and Infectious Diseases who have accompanied me on this scholarly journey. Specifically, I extend my thanks to Miklós Tenk, presently at the helm of the department, and László Fodor, former departmental head during my nascent years as a doctoral candidate. Their provision of laboratory facilities for conducting pivotal research and workspace within the Department has been indispensable. I express my gratitude to all colleagues within the Immunology Unit, including Józsefné Herbák, Éva Szűcs-Somlyó, Dóra Földi, and Gábor Andócs, for their invaluable help spanning various facets of my professional undertakings. Also, to László Mészáros, Rebeka Nagypál, Lilla Kálfalvy-Molnár, Rhiannon Rodgers, and Katie Commins for their invaluable contributions to the collective achievements garnered over the years. These esteemed individuals demonstrated active engagement in research endeavors during their tenure as students, culminating in the successful completion of their diploma theses. Furthermore, I am grateful to the University of Veterinary Medicine Budapest for providing an enriching environment conducive to my doctoral studies.

I am indebted to István Jankovics† and Máté Hidvégi for their invaluable assistance in the planning, execution, and evaluation of experiments, which significantly contributed to the realization of the findings delineated in the dissertation. The counsel imparted by Róbert Glávits proved instrumental in evaluating histopathological results. I am also grateful for the assistance rendered by Annamária Gáspárné Stoll, which was immensely beneficial.

My profound appreciation extends to my family for their endorsement and encouragement throughout my collegiate journey. Their unwavering support, understanding, and perpetual motivation have been instrumental in shaping both my personal and academic development. I extend my heartfelt gratitude to my wife and children, namely Vanda, Ella, Dömötör, and Panka, as well as to my parents, Mónika and Zoltán. My appreciation also extends to my brother, Dávid, and his family, comprising Noémi, Olivér, Dániel, and Laura. Furthermore, I express my thanks to my grandparents, Éva, Pál†, Erika, and István, and to my fathers- and mother-in-law, Magdolna, István, and Gábor. Reflecting on my achievements, I recognize the

pivotal role you have played as pillars of strength. I aspire to continually honor your support and make you proud in all my future endeavors.

Financial support for the empirical investigations underlying the doctoral dissertation

The investigations in the present dissertation were supported by the European Union and co-financed by the European Social Fund in the form of a grant (EFOP-3.6.3- VEKOP-16-2017-00005, project title: Strengthening the scientific replacement by supporting the academic workshops and programs of students, developing a mentoring process).

The investigations in the present dissertation were supported by the National Research, Development and Innovation Fund of Hungary under the Tématerületi Kiválósági Program 2020 funding scheme in the form of a grant (2020-4.1.1-TKP2020).

The investigations in the present dissertation were supported by the Project nr. 2019-1.2.1-Egyetemi-Öko-2019-00010 has been implemented with the support provided by the National Research, Development and Innovation Fund of Hungary, financed under the 2019-1.2.1-Egyetemi-Öko funding scheme.

The investigations in the present dissertation were supported by the Project no. RRF-2.3.1-21-2022-00001 has been implemented with the support provided by the Recovery and Resilience Facility (RRF), financed under the National Recovery Fund budget estimate, RRF-2.3.1-21 funding scheme.

The investigations in the present dissertation were supported by The Uro Optika Foundation: Advancing Treatment Conditions for Urinary Tract Disorders (Renca cell line acquisition).